Behavioral and Physiological Significance of PKC-mediated Phosphorylation of the GluN2A C-terminus

by

Deebika Balu
B.Tech. (Anna University) 2005
M.S. (Michigan State University) 2007, 2010

Thesis submitted in partial fulfillment of the requirements
for the degree of Doctor of Philosophy in Biological Sciences
in the Graduate College of the
University of Illinois at Chicago, 2015

Chicago, Illinois

Defense Committee:
Simon T. Alford, Chair
John P. Leonard, Advisor
John R. Larson, Psychiatry
Michael E. Ragozzino, Psychology
Jennifer V. Schmidt

To

my beloved grandmother, Mrs. Sankari Subramanian,

and the cherished memories I have of her.

ACKNOWLEDGMENTS

The generation of *Grin2a*Δ*PKC* mouse used in this dissertation was supported by NIH Small Grant Program of the National Institutes of Health under award number R03NS056321.

I wish to express my heartfelt thanks to my dissertation advisor, Dr. John Leonard, for his excellent guidance, and encouragement. His broad knowledge of electrophysiology has guided me through this work and his suggestions during my practice research presentations enabled me to think from an audience perspective. I wish to thank him for understanding my weird working schedules due to my personal commitments.

I wish to express my gratitude to my dissertation committee chairperson Dr. Simon Alford for his thoughtful comments during the entire period of this research. His commitment to scientific research and knowledge has always been an inspiration for me. His ideas for experiments based on my results during every committee meeting was very helpful.

I wish to thank Dr. Jennifer Schmidt for her patience in guiding me through the intricacies of PCR troubleshooting. I thank her for allowing me to use her lab PCR machine and PCR ingredients when everything stops working in my laboratory! Her thoughtful questions on the behavioral paradigms I used during my research has helped me think about various aspects of my research.

I would also like to thank Dr. John Larson who did all the electrophysiology experiments on the *Grin2a*Δ*PKC* mice. His broad knowledge and expertise in electrophysiological techniques has helped me during the last two years of this work.

ACKNOWLEDGMENTS (Continued)

I am thankful to Dr. Michael Ragozzino for guiding me over the past four years in helping me setup many behavioral experiments. I am grateful to him for offering his probabilistic reversal training apparatus for running light-dark box emergence tests on the *Grin2a*Δ*PKC* mice.

I also wish to thank Drs. David Wirtshafter and Thomas Park for introducing me to the world of Fos immunostaining. Thom's patience while teaching me how to do a transcardial perfusion in a mouse, and his cheerful demeanor has taught me how to handle many things diplomatically. Dave's vast knowledge on everything under the skull has helped me gain a new perspective on neuroanatomy. I will truly miss his neuroscience fables!

I am thankful to Dr. Aixa Alfonso for her assistance in academic issues. My special thanks to fellow neurobiology graduate students in Aixa's lab: Saleel Raut, Liliana Marquez and Lillian Perez for filling boring lunch sessions with lively and interesting conversations. I also wish to acknowledge all the neurobiology graduate students for their comments and suggestions during my journal club presentations.

I wish to thank the administrative staff of Biological Sciences department, especially Margaret Kleist, Beth Brand, and Alma Sias for their excellent assistance.

There may not be anyone who could be happier than my parents Drs. K. Balu and P. S. Meenakshi. Their constant support and advice on my personal and academic life have been helpful several times. I wish to express my deepest gratitude for the love and encouragement I had from my in-laws, L.M. Chandrasekaran and Devi Chandrasekaran. No words can fully express my appreciation of my best friend and husband Dr. Saravan Kumar Chandrasekaran.

ACKNOWLEDGMENTS (Continued)

His unwavering support and desire to stand by me during easy and tough days helped me cruise through PhD despite the physical distance between us.

PREFACE

Early studies on N-methyl-D-aspartate receptors established that the calcium entry through these receptors may underlie some forms of synaptic plasticity implicating these receptors in a number of neurodegenerative diseases (such as huntington's disease, Parkinson's disease) and neurological disorders (such as ischemic stroke, and neuropathic pain). The next set of studies focused on subunit and regional specificity of NMDARs in the brain. Thus, a number of mutant mice have been generated having either over-expressed or deleted specific subunit(s) of the receptor in the whole brain or in a specific region to study questions pertaining to development of synapses and establishment of neuronal circuits. Recent studies were focused on modulation of these receptors by kinases (or phosphatases) by phosphorylating (or de-phosphorylating) specific amino acids in its intracellular C-terminal domain. My dissertation work has focused on a relatively less studied NMDAR subunit, the GluN2A and its modulation by Protein Kinase C.

This dissertation is based on the experimental data collected from various behavioral, electrophysiological and immunostaining experiments done using *Grin2a*Δ*PKC* mice. These mice were generated using the support from a NIH grant (R03NS056321) in collaboration with the University of Illinois at Chicago Transgenic Production Service by Dr. Jennifer Schmidt, and Dr. Aleksey Yevtodiyenko. I have been in-charge of genotyping the animal colony and designing and setting up the experiments since the time I had joined the Leonard lab. Most of the behavioral experiment protocols were based on Dr. Michael Ragozzino's recommendations, and

the light dark emergence test was performed by modifying his probabilistic reversal training apparatus. All the behavioral experiments were performed and analyzed in a blind-fashion with the help from undergraduate students who worked in our lab either for their independent projects or capstone projects. Erin Budris, Eric Zhuang helped in the Plus/Y/T maze alteration experiments. Lusine Gomtsian and Nina Kaur helped in the anxiety-related experiments. Alice Chang helped in the forced-swim test. Prutha Patel and Alice Chang helped in analzying Fos immunostaining data. I have analyzed all the data from behavioral experiments for statistical significance, and presented them as a poster in two separate Society for Neuroscience meetings. All the electrophysiology recordings were done by Dr. John Larson in the Department of Psychiatry at the University of Illinois at Chicago.

TABLE OF CONTENTS

CHAPTER		PAGE
1	INTRODUCTION	1
1.1	Synaptic transmission	1
1.2	Ionotropic Glutamatergic receptors	3
1.3	NMDA receptors	5
1.3.1	Structure of NMDARs	5
1.3.2	Properties of NMDARs	6
1.3.3	Regional expression of NMDARs	7
1.3.4	Molecular diversity of NMDARs	9
1.3.5	NMDAR-dependent synaptic plasticity	10
1.3.6	Regulation of NMDARs via CTD interactions	12
1.3.6.1	PDZ-domain interactions	12
1.3.6.2	Interaction with kinases	13
1.3.7	Dissertation rationale	18
2	GENERATION OF Δ*PKC* MICE	21
2.1	Introduction	21
2.2	Methods	25
2.2.1	Targeting vector construction	25
2.2.2	Homologous recombination	26
2.2.3	Removal of the *Neo*^{r} Cassette by Cre Recombination	27
2.2.4	Genotyping	27
2.2.5	mRNA expression levels	28
2.2.6	Western Blotting	30
2.2.7	Histology	31
2.2.8	Visual placement test	31
2.3	Results	32
2.3.1	Genotyping assay and *Neo*^{r} cassette excision	32
2.3.2	*Grin2a* mRNA and GluN2A protein expression levels	34
2.3.3	General animal morphology and gross brain anatomy	35
2.4	Discussion	36
3	BEHAVIORAL CHARACTERIZATION OF Δ*PKC* MICE	45
3.1	Introduction	45
3.2	Methods	47
3.2.1	Experimental animals	47
3.2.2	Spatial working memory	47
3.2.2.1	Spontaneous alternation behavior	47

TABLE OF CONTENTS (Continued)

CHAPTER **PAGE**

3.2.2.2 Non-reinforced delayed alternation . . . 50
3.2.3 Recognition memory - Novel object recognition . . . 51
3.2.4 Repetitive behaviors - Marble burying . . . 51
3.2.5 Anxiety and depression-related behaviors . . . 52
3.2.5.1 Open-field exploration . . . 52
3.2.5.2 Light-dark box emergence . . . 52
3.2.5.3 Elevated plus maze exploration . . . 53
3.2.5.4 Forced swim test . . . 53
3.2.6 Impulsive behaviors - nose-poke training . . . 54
3.2.7 Behavioral induction of Fos expression . . . 55
3.3 Results . . . 57
3.3.1 General activity levels of Δ*PKC* mice. . . . 57
3.3.2 Spatial working memory of Δ*PKC* mice . . . 57
3.3.2.1 Spontaneous alternation in a four-arm and Y maze . . . 57
3.3.2.2 Delayed alternation in non reinforced T maze task . . . 61
3.3.3 Recognition memory . . . 63
3.3.3.1 Novel object recognition . . . 63
3.3.4 Perseverative behavior . . . 65
3.3.4.1 Marble burying . . . 65
3.3.5 Anxiety and depression-related behaviors . . . 65
3.3.6 Impulsivity test . . . 67
3.3.7 Fos expression in hippocampus after novelty exposure . . . 73
3.4 Discussion . . . 80

4 HIPPOCAMPAL SYNAPTIC PLASTICITY IN Δ*PKC* MICE . . . 86
4.1 Introduction . . . 86
4.1.1 GluN2A subunit, CTD and synaptic plasticity . . . 87
4.2 Methods . . . 89
4.2.1 Electrophysiology . . . 89
4.3 Results . . . 90
4.3.1 Input-output curves and paired-pulse facilitation . . . 90
4.3.2 LTP induced by TBS . . . 90
4.4 Discussion . . . 91

5 CONCLUDING REMARKS . . . 98
5.1 Kinase modulation of NMDARs . . . 98
5.2 Relevance to human pathology . . . 102

APPENDICES . . . 104
Appendix A . . . 105
Appendix B . . . 108
Appendix C . . . 109

TABLE OF CONTENTS (Continued)

CHAPTER **PAGE**

Appendix D 112

CITED LITERATURE 115

VITA 133

LIST OF TABLES

TABLE		PAGE
I	Primers and product sizes (in bp) for *Neo*^{r} excision PCR and Genotyping PCR	28
II	Primer sequences	29
III	Behavioral Phenotyping Assays	49
IV	Behavioral parameters measured during novelty-induced Fos induction experiments	74
V	Digestion Buffer	107
VI	PCR Master Mix	107
VII	RE digest master mix	107
VIII	Apparatuses used for behavioral phenotyping	109
IX	ACC protocol letters	112

LIST OF FIGURES

FIGURE		PAGE
1	A schematic representation of a NMDA Receptor	8
2	Activation of kinases by Calcium	17
3	Genotyping assay	33
4	Homologous recombination	34
5	*Neo*^{r} primers binding sites	38
6	PCR based assay for verifying *Neo*^{r} cassette excision	39
7	Representative images of Northern and Western blot gels for assaying levels of *Grin2a* and GluN2A respectively	40
8	Quantification of *Grin2a* mRNA and GluN2A protein expression levels in WT and Δ*PKC* mice	41
9	Growth and development of Δ*PKC* mice	42
10	Visual placement scores of WT and Δ*PKC* mice	43
11	Anomalous CA1 field in mutant hippocampal slice	44
12	Battery of behavioral tests done on WT and Δ*PKC* mice	48
13	Timeline for behavioral induction of Fos in the mouse hippocampus	55
14	Similar activity levels of Δ*PKC* and WT mice during a spontaneous alternation task in four-arm maze and Y Maze, and open field exploration	58
15	Decreased spontaneous alternation of Δ*PKC* in Y maze but not in four-arm maze	59

LIST OF FIGURES (Continued)

FIGURE **PAGE**

16 Reduced crossovers exhibited by Δ*PKC* mice in a four-arm maze during the 10 minutes alternation task 60

17 Decreased alternation of Δ*PKC* mice in a non-reinforced T Maze alternation task consisting of one forced choice trial followed by 14 free choice trials 62

18 Performance of Δ*PKC* and WT mice in every trial of the T Maze alternation task based on the percentage of mice that alternated correctly in each trial 63

19 Normal recognition memory in Δ*PKC* mice in a novel object recognition test 64

20 Δ*PKC* do not exhibit any repetitive/ perseverative behaviors in the marble burying test 66

21 Reduced anxiety-like behaviors exhibited by Δ*PKC* mice in an Open field, Light-dark box, and Elevated plus maze 68

22 Reduced anxiety-like behaviors exhibited by Δ*PKC* mice in an elevated plus maze 69

23 Risk assessment behaviors exhibited by Δ*PKC* mice in an elevated plus maze 70

24 Δ*PKC* mice did not show any any changes in behavioral despair response in the forced swimming test 71

25 Δ*PKC* do not exhibit any impulsivity to nose-poke for water reward. 72

26 Fos expression in the hippocampus of WT and Δ*PKC* mouse brains after novel environment exposure 75

27 Differential Fos expression in hippocampal region of Δ*PKC* mouse brains after novel environment exposure 76

28 Fos expression in the CA1 region of Δ*PKC* mouse brains after novel environment exposure 77

LIST OF FIGURES (Continued)

FIGURE **PAGE**

29 Fos expression in the CA3 region of Δ*PKC* mouse brains after novel environment exposure 78

30 Fos expression in the DG region of Δ*PKC* mouse brains after novel environment exposure 79

31 Basal synaptic transmission in hippocampal field CA1 of WT and Δ*PKC* mice 93

32 Paired-pulse plasticity in adult Δ*PKC* and WT mice 94

33 LTP in the SC-CA1 synapses of slices from adult WT and Δ*PKC* mice 95

34 LTP induced by TBS is not different in hippocampal field CA1 of WT and Δ*PKC* mice 96

35 Burst responses in SC-CA1 synapses of hippocampal slices from WT and mutant mice. 97

36 Body and brain weight of Δ*PKC* mice 108

37 Apparatuses used for SAB and recognition memory experiments . . . 110

38 Apparatuses used for anxiety and depression-related behavioral experiments 111

LIST OF ABBREVIATIONS

AMPA	α-amino-3-hydroxy-5-methyl-4-isoxazolepropionic acid
CA1 or 3	*cornu ammonis* 1 or 3
CaMKII	Calcium/calmodulin-dependent protein kinase II
CNS	central nervous system
CTD	C-terminal domain
dNTP	deoxynucleotide triphosphate
fEPSP	field excitatory post synaptic potential
GABA	γ-aminobutyric acid
GluR	glutamate receptor AMPA type
GluN2A	glutamate receptor NMDA type subunit 2A
GluN2B	glutamate receptor NMDA type subunit 2B
GluN2C	glutamate receptor NMDA type subunit 2C
GluN2D	glutamate receptor NMDA type subunit 2D
Grin2a	glutamate receptor ionotropic NMDA type 2A
*Grin2a*Δ*PKC*	mutant mice with phosphorylation site mutations (S1291A, Y1292, S1312, Y1387) in the C-terminal domain of GluN2A subunit of NMDA receptor

LIST OF ABBREVIATIONS (Continued)

LTD	long-term depression
LTP	long-term potentiation
mGluR	metabotropic glutamate receptor
µg	microgram
µl	microliter
mV	millivolt
M	Molar
Neo^r	neomycin resistance
NMDA	N-methyl-D-aspartate
NMDAR	N-methyl-D-aspartate receptor
PSD	post synaptic density
PKA	protein kinase A
PKC	protein kinase C
PKMζ	protein kinase M zeta
SH2 or 3	Src homology domain 2 or 3
Src	Src tyrosine kinase
WT	wild-type

SUMMARY

Synaptic transmission in adult brain is mainly mediated by glutamate released at the excitatory synapses, and γ-aminobutyric acid (GABA) released at inhibitory synapses (Curtis et al., 1961). Glutamate gates ionotropic glutamate receptors (iGluRs) that form ion channels at synapses. The N-methyl-D-aspartate receptors (NMDARs) are one of the four classes of receptors that belong to the iGluR family, and mediate a range of cellular functions in the central nervous system such as development of synapses (Yashiro and Philpot, 2008), learning (Morris et al., 1986; Tang et al., 1999; Brigman et al., 2011), and certain forms of synaptic plasticity (MacDonald et al., 2006; Paoletti et al., 2013). Repetitive high-frequency stimulation of presynaptic afferent fibers results in an increase in synaptic strength lasting for hours, and hence has been implicated in synaptic remodeling that occurs during learning and memory (Bliss and Lømo, 1973). Long-term potentiation (LTP) and long-term depression (LTD) of synapses are the most well-studied forms of long lasting synaptic plasticity in the mammalian central nervous system , which leads to strengthening and weakening of synaptic connections respectively, based on integration of synaptic inputs.

Activity-dependent plasticity in NMDAR containing synapses could be regulated by phosphorylation of specific amino acids in the C-terminal domain (CTD) of the receptor subunits. The CTD of the NMDAR has a number of protein binding motifs such as PDZ domains, clathrin adaptor protein (AP-2) binding domains (Prybylowski et al., 2005). The differential interaction of the NMDAR subunits with various postsynaptic proteins may result in regu-

lation of neuronal signal integration, and intracellular signaling pathways. The long CTD of GluN2A subunit, containing about 600 amino acids also has a number of serines and tyrosines which are targets for serine kinases (such as Protein kinase C (PKC), Calcium/calmodulin dependent kinase (CaMKII), Protein kinase A (PKA), cyclin-dependent kinase (Cdk-5)) and tyrosine kinases (such as Src). Phosphorylation of those residues alters the net charge of the protein, which may result in a change in protein conformation. Any change in the receptor protein structure may alter the interactions they may have with other cytosolic proteins (Kim et al., 2011). The fast kinetics and the reversibility of the phosphorylation reaction may also allow for rapid modulation of the receptor. A number of kinases are expressed in an adult brain which may have different substrates and activation profiles. Thus, these kinases may regulate activity-dependent synapse remodeling, learning, memory and cognition by (i) altering the properties of ion channel receptor (ii) affecting the number of those receptors on the synaptic membrane, or (iii) regulating synapse remodeling by affecting protein synthesis.

Previous work from our lab established that the phosphorylation of the Serines (S1291 and S1312) directly by PKC and tyrosines (Y1292 and Y1387) indirectly via PKC activation of Src Tyrosine Kinase positively modulate the receptor currents. Using the frog oocyte expression system, it was found that PKC-induced enhancement of currents through the GluN2A-containing NMDAR was diminished when those specific serine and tyrosine residues in the CTD were mutated to alanine and phenylalanine (that cannot be phosphorylated), respectively. To understand the behavioral and physiological significance of those sites *in vivo*,

the *Grin2a*Δ*PKC* mouse expressing GluN2A with those four mutated amino acids (S1291A, S1312A, Y1292F and Y1387F) was generated using homologous recombination.

The mutant mice were like their WT-littermate controls in their body weight, appearance, and general activity. Mutant and wild-type (WT) mice also have similar expression levels of *Grin2a* mRNA, and GluN2A protein. Although the *Grin2a*Δ*PKC* mice alternated above chance levels in a four-arm and Y maze spontaneous alternation tasks, they alternated at levels lower than WT mice only in the Y maze. Interestingly, the mutants also have decreased alternation in a non-reinforced T maze alternation task. This suggests that the mutant mice may have a mild spatial memory deficit. When these mutant mice were subjected to anxiety-associated tasks, they exhibited reduced anxiety-related behaviors such as increased time spent in the center of an open field, increased time in lit side of light/dark box, and increased entries and dwell times in the open arms of an elevated plus maze.

c-Fos (Fos) expression is a widely used indicator of neuronal activation. Immunostaining for Fos in the hippocampus after exposure of the animals to novel environments shows region specific differences between the mutants and WT mice. There was no increase in Fos levels in mutants after exposure to novel environments in CA1 and CA3 compared to home-cage (basal) Fos levels, in contrast, Fos levels increased in the WT mice in CA1, CA3 and dentate gyrus (DG). However, both groups had similar basal Fos levels in the CA1, CA3, and DG. To determine if the mutants had impaired synaptic plasticity in the hippocampus, the Schaffer collateral-CA1 synapses were stimulated using a theta-burst protocol. In hippocampal slices obtained from mutant mice, there was no impairment in LTP. Also, the mutant mice showed

no significant differences in input-output curves and paired-pulse facilitation. Taken together, these results suggest that PKC-mediated phosphorylation of at least one of those four sites regulates NMDAR-mediated signaling that modulates anxiety, and spatial working memory.

CHAPTER 1

INTRODUCTION

1.1 Synaptic transmission

An adult human brain is estimated to contain about 100 billion neurons (Azevedo et al., 2009). Vast networks of neurons communicate with each other through specialized anatomic structures called synapses. The term **synapses** coined by Sir Charles Sherrington in 1987, denotes the sites at which interneuronal communication required for normal brain function occurs (Sherrington, 1906). It is currently recognized that two main forms of synaptic transmission exists : electrical and chemical. At electrical synapses, information is transferred through channels in the cell membranes called gap junctions which connect the adjacent neurons (Furshpan and Potter, 1959). At chemical synapses, there is no cytoplasmic continuity and hence information is transferred via neurotransmitter released into the synaptic cleft (Loewi, 1935). The arrival of an action potential at the presynaptic terminal activates voltage gated calcium channels resulting in an increase in intracellular Ca^{2+} concentration. This causes synaptic vesicles containing neurotransmitter molecules to fuse with the cell membrane of one neuron (called the presynaptic neuron) releasing the neurotransmitter in the synaptic cleft. The neurotransmitter binds to receptor(s) on the membrane of a second neuron (called the postsynaptic neuron). These postsynaptic receptors are classified as either ionotropic or metabotropic based on their mechanism of eliciting postsynaptic changes. Upon neurotransmitter binding,

ionotropic receptors undergo a conformational change resulting in opening of an ion channel pore that allows passage of ions, while neurotransmitter binding to the metabotropic receptors (usually G-protein coupled receptors) results in activation of second messenger signaling molecules. All these receptors are mainly expressed throughout the central nervous system (CNS), but there is some expression in peripheral neuronal and non-neuronal tissues. For example, a number of studies have demonstrated the presence of AMPA receptor subunit 2/3 (GluA2 and GluA3), NMDAR subunit 1 (GluN1), and metabotropic glutamate receptor subunit 2/3 (mGluR 2/3) in the glomeruli, lungs, mast cells and in pancreatic islets (Gill et al., 1998; Gill et al., 2000). Glutamate receptors in these sites have been studied for their potential role as alternative targets for excitatory compounds in food, and for their role in cell injury (Gill and Pulido, 2001). In the adult brain, synaptic transmission is mainly mediated by glutamate released at the excitatory synapses, and γ-aminobutyric acid (GABA) released at inhibitory synapses (Curtis et al., 1961). Glutamate was not readily accepted as an excitatory neurotransmitter since, (i) it was ubiquitously present in high concentrations in the brain (not localized to synapses), and (ii) glutamate, like all other amino acids is a component of cellular metabolism (Lau and Tymianski, 2010). This led to a debate about establishing its role as a neurotransmitter involved in signaling. Apart from that, under certain conditions glutamate also had toxic effects on the nervous system known as excitotoxity which complicated its acceptance as a molecule essential for synaptic transmission (Gillessen et al., 2002). However, the discovery of various post synaptic receptors that can bind to glutamate led to acceptance of glutamate as a primary excitatory neurotransmitter in the mammalian CNS (Curtis and

Watkins, 1960; Krnjević and Phillis, 1963). Thus, glutamate, since its discovery in 1961 as an excitatory neurotransmitter in the brain now has been definitely shown to activate two main classes of postsynaptic receptors: (i) ionotropic glutamate receptors that are mostly permeable to cations and (ii) metabotropic glutamate receptors (mGluRs) that belong to a family of G-protein coupled receptors (Traynelis et al., 2010).

1.2 Ionotropic Glutamatergic receptors

Glutamate gates postsynaptic ionotropic Glutamate receptors (iGluRs) that form ion channels. The iGluR family consists of four classes of receptors: α-amino-3-hydroxy-5-methyl-4 isoxazolepropionic acid (AMPA), N-methyl-D-aspartate (NMDA), Kainate and orphan receptors (Sprengel, 2013; Mandolesi et al., 2009). All of the receptors, except for the orphan receptors, usually exist as a homomeric or heteromeric integral membrane protein complexes consisting of various protein subunits, and were initially identified and hence named based on their preferential pharmacological agonist. *In vivo*, these receptors mostly form a complex containing four subunits that belong to the same receptor class that form a central pore in the post synaptic membrane. At most mature synapses, the AMPA receptors are heterotetramers containing two of the GluA2 subunits along with two GluA1, GluA3, or GluA4 (Wenthold et al., 1992), although they are capable of forming homomeric complex containing GluA(1-4). The Kainate receptor subunits (Glu1-3) also form both homo- and heteromers, but to form functional channels, receptor complexes with GluK4 or GluK5 has to contain GluK1-3. Most of the NMDA receptors (NMDARs) at the synapses are mostly heterotetramers containing two subunits of GluN1 and two of the same subunits of from GluN2(A-D). However a few studies

have indicated the presence of triheteromeric complexes composed of GluN1 and GluN2A/B, GluN2A/C, GluN2B/D, GluN2A/D in specific brain regions (Luo et al., 1997; Dunah et al., 1998; Brickley et al., 2003).

These receptor subunits have about 20–40% amino-acid sequence homology between the classes, and a higher amino-acid sequence homology (50–80%) within the classes (Cull-Candy et al., 2001). Sequence analysis and detailed crystallographic analysis of the glutamate receptor subunit structures have revealed that they contain four domains: the amino-terminal domain (ATD), the ligand binding domain (LBD), the transmembrane domain (TMD) and the carboxy-terminal domain (CTD) (Sobolevsky et al., 2009; Wo and Oswald, 1995). The carboxy-terminal being the intracellular domain, has a number of protein binding motifs. The CTD of AMPA, NMDA and Kainate receptors are also closely associated with auxiliary proteins that modify the kinetics and efficiency of synaptic transmission (Sumioka, 2013; Wyeth et al., 2014). Thus, the auxiliary proteins could also contribute to modulating the spatial and temporal aspects for neurotransmission. Presynaptic iGluRs (AMPA, NMDA and Kainate receptors) mostly facilitate synaptic transmission, but may also have inhibitory actions (Pinheiro and Mulle, 2008).

Among these iGluRs, the most well studied are the AMPA and the NMDA receptors. In most of the excitatory synapses, the initial, fast and transient component of the excitatory post-synaptic current (EPSC) is mediated by the AMPARs while the slower modulatory component is contributed by the NMDARs (Forsythe and Westbrook, 1988). For instance, the rapid activation kinetics of AMPA receptors in the cerebral cortex has been shown to contribute to working

memory (Sanderson et al., 2010). As the predominant synaptic current, they are regulated to induce long-term potentiation (LTP) and long-term depression (LTD) of the synapses during learning and memory formation. On the other hand, postsynaptic NMDA receptors that mediate slow currents often are regulators of synaptic plasticity due to their coincidence detecting property and high Ca^{2+} permeability (i.e. the NMDAR is activated not only by the presence of glutamate but also by depolarized membrane potential) (Dingledine et al., 1999). This unique combination of AMPA and NMDA receptors at the postsynaptic membrane plays an essential role in higher order neurophysiological processes such as learning and memory (Bliss and Collingridge, 1993).

1.3 NMDA receptors

1.3.1 Structure of NMDARs

NMDAR subunits like all the other glutamate receptor subunits are integral membrane proteins that have two extracellular domains: an amino-terminal domain (ATD) and a ligand-binding domain (LBD), a transmembrane domain, and an intracellular carboxy-terminal domain (CTD). The LBD in the NMDARs have a 19% sequence identity and 68% homology between the various subunits (Traynelis et al., 2010). While it has been shown the the LBD of GluA2 receptor undergoes a conformational change in its structure after it binds to an agonist, LBD sequence homology between all the subunit of the glutamate receptors predict that this may be true in NMDARs too (Dong and Zhou, 2011). The ATD contains a short signal peptide that is required for membrane targeting, and is removed after the receptor is inserted into the membrane (Dingledine et al., 1999). The remaining sequences forming the ATD of

the functional NMDAR receptor has binding sites for divalent cations such as Zn^{2+}, subunit-selective modulators (such as ifenprofil to GluN2B) and extracellular proteins such as ephrin receptor (Choi and Lipton, 1999; Dalva et al., 2000; Perin-Dureau et al., 2002). The CTD of the NMDARs has about 600 amino acids and makes up about one-third of the GluN2 subunits. These CTDs are also the least conserved regions among NMDAR subunits, and bind to a number of intracellular proteins (Ryan et al., 2008).

1.3.2 Properties of NMDARs

The neuronal NMDAR subtypes containing GluN1 and GluN2 subunits have unique properties compared to other receptors in the family of iGluRs [Figure 1]. First, the NMDARs requires the binding of two distinct agonists (glutamate and L-glycine) for its activation (Johnson and Ascher, 1987). When the glycine concentration was less than 1 μM, its binding increases currents through the NMDAR channel (Johnson and Ascher, 1992). However, at concentrations higher than 10 μM the currents through the receptor decrease to about 20% of the NMDAR peak current, and at concentrations between 0.1 to 1 μM, negative cooperativity between the glutamate and the glycine binding site results in faster desensitization of the NMDAR (Benveniste et al., 1990). Although it has been generally accepted that the binding sites for glutamate and glycine interact with each other to regulate desensitization of the NMDAR, conflicting results have been reported in various studies using various preparations such whole-cell recordings, recordings from outside-out patches, suggesting that the NMDAR responses may vary across preparations (Sather et al., 1990; Lester et al., 1993). Second, it has a unique gating mechanism that requires a depolarized membrane potential apart from ligand

binding. Mg^{2+} ion that blocks the NMDAR channel pore is released due to the depolarized membrane potential contributing to voltage-dependent channel function (Johnson and Ascher, 1990). The NMDARs possess slow activation and deactivation kinetics. This allows the receptors to filter out low-frequency inputs and results in integration of synaptic activity (Seeburg et al., 1995; Larkum et al., 2009). Finally, NMDARs show a high Ca^{2+} permeability compared to other iGluRs (MacDermott et al., 1986; Mayer and Westbrook, 1987). Since Ca^{2+} is an important intracellular second messenger molecule that activates a number of calcium dependent enzymes, this unique property of the NMDAR is crucial in regulating certain types of synaptic plasticity (Berridge, 1998). This also allows for coupling of synaptic transmission to intracellular signaling cascades involving kinases to regulate other cellular properties.

1.3.3 Regional expression of NMDARs

The heteromeric NMDARs (GluN1/N2) have a unique regional and developmental expression pattern in a mouse and rat brain (Kirson and Yaari, 1996; Wenzel et al., 1997). The different kinetic properties of those subunits offer unique properties to both the neonatal and the adult brain when expressed in specific regions and at specific times. For example, during early stages of development in rats and mice, GluN2B subunit containing NMDARs are mostly expressed in the cortex, hippocampus and cerebellum (Wenzel et al., 1997). The slower deactivation kinetics of the Glu2B subunits helps in the circuit formation and development in a neonatal and early postnatal brain. Thus the GluN2B subunits may be critical in formation of neural circuits and it is not surprising that the complete knockout of GluN2B subunit in mice results in lethal mutation (Kutsuwada et al., 1996). The highest levels of GluN2D were

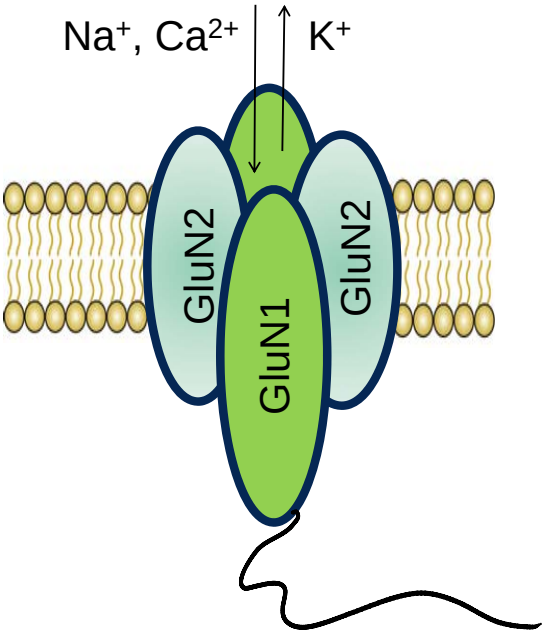

Figure 1: A schematic representation of a NMDAR. The NMDARs as shown in the image occur *in vivo* as heterotetramers containing two GluN1 subunits that bind to NMDAR co-agonist glycine and two GluN2 subunits that bind to glutamate.

detected in the thalamus, spinal cord, and midbrain and moderate levels were detected in the cortex and hippocampus by postnatal week 1 (Dunah et al., 1996). During the third week of postnatal development, the subunit composition of NMDAR switches from GluN2B/GluN2D to GluN2A containing receptors in the cerebral cortex, hippocampus, basal ganglia and olfactory bulb. There is also a switch in the cerebellum from GluN2B to GluN2C subunits during the first postnatal week. By postnatal week 3, the GluN2A levels peak in all the brain regions including cortex, thalamus, basal ganglia, olfactory bulb and cerebellum, while the levels of GluN2B and GluN2D decline by about twofold of neonatal subunit levels. In adult brain,

GluN2C-containing receptors were found to be predominantly expressed in the cerebellum, thalamus and olfactory bulb. This switch in NMDAR subunits during this **critical period** of development determines a point of transition between a developing neonatal brain and a fully mature adult brain. Overall, the GluN2B, GluN2D, and GluN3A are the dominant subunit types expressed in a neonatal brain which switches to a preponderance of GluN2A and GluN2C subunit types in an adult brain (Wenzel et al., 1997).

1.3.4 Molecular diversity of NMDARs

In vivo, like most of the other iGluRs, the NMDARs exist as heterotetramers (dimer of dimers) (Dingledine et al., 1999). Also, the subunit composition of each of the NMDAR subtypes confer distinctive biophysical properties which in turn determine the amplitude and kinetics of excitatory postsynaptic currents (EPSCs). Multiple isoforms of the receptors are expressed in various regions of the brain due to the the eight splice variants of the obligatory GluN1 subunits and the three types of GluN2 subunits (Zukin and Bennett, 1995; Klein et al., 1998; VanDongen and VanDongen, 2004). While the GluN1 subunit has three splice sites (one at the N-terminal, and two at the C-terminal), there have been no reports of splice sites in GluN2A. Splice variants of GluN2C usually have a truncated TMD, and GluN2C, GluN2B, and GluN2D also have splice sites in their 5'-untranslated region. While the oocyte and HEK cell expression system provided an approach to study the regulation of NMDAR channel properties using recombinant receptors, genomic or proteomic analysis of the receptors revealed the subunit composition of native NMDARs (Monyer et al., 1994; Vicini et al., 1998). Progress in molecular biology and gene targeting allowed researchers to generate mice with specific

subunit genes deleted to study various aspects of the NMDAR subunits such as their spatial and temporal expression in the brain. Specifically conditional knockout animals were used to determine the role of NMDAR subtypes on synaptic physiology (Akashi et al., 2009; Brigman et al., 2010). For example, it has been shown that the NMDARs containing GluN2A subunits display a rapid and sharp increase in channel opening terminating relatively quickly while the NR2B NMDARs result in a higher activation probability over an extended period of time (Cull-Candy et al., 2001). Thus, it could be inferred that the GluN2A-containing receptors with low glutamate affinity and fast kinetic properties might be more suited to respond to any synaptic activity while the GluN2B-containing receptors might be preferentially activated during sustained synaptic activity. A different class of NMDAR containing the GluN3A subunit is subsequently down-regulated within days after birth. The formation of NR3A containing heteromers (GluN1/GluN2/GluN3A) results in two important changes to the NMDAR when compared to the heterotetrameric GluN1/GluN2A or GluN2B; 1) the channels have reduced Ca^{2+} permeability and 2) lower sensitivity to Mg^{2+} blockade. It has been suggested that the down-regulation of GluN3A containing receptors is required during postnatal neurodevelopment to prevent premature stabilization of synapses (Roberts et al., 2009).

1.3.5 NMDAR-dependent synaptic plasticity

The most studied forms of long lasting synaptic plasticity in the mammalian central nervous system are the LTP and LTD, which leads to strengthening and weakening of synaptic connections respectively, based on integration of synaptic inputs. Ever since the discovery of LTP in the dentate gyrus due to stimulation of the perforant pathway in a rabbit hippocampus,

it has been shown to be occurring in the other hippocampal subregions and other brain regions such as amygdala, visual and somatosensory cortex (Bliss and Lømo, 1973; Bear and Rittenhouse, 1999; Feldman et al., 1999; Blair et al., 2001). NMDAR were implicated in LTP of SC-CA1 synaptic pathway, when the magnitude of LTP was observed to be decreased upon infusion of AP-5 (a competetive NMDAR antagonist) into that brain region (Collingridge et al., 1983). However, not all forms of LTP are NMDAR-dependent, since voltage-gated Calcium channels also can potentiate certain synapses (Frank, 2014). There are a number of ways by which the NMDAR channel subtypes can modulate certain forms of synaptic plasticity. First, the difference in kinetic properties such as charge transfer ratio, conductance, and decay time between the GluN2A and GluN2B subunits could regulate synaptic plasticity. It has been shown in HEK cells that the recombinant GluN1/GluN2B receptor channels have a lower probability of opening compared to GluN1/GluN2A. The NMDARs containing GluN1/GluN2A also show faster activation and deactivation kinetics compared to GluN1/GluN2B (Vicini et al., 1998; Cull-Candy et al., 2001). Using caged-glutamate to elicit excitatory postsynaptic currents (EPSCs) in dendritic spines of CA1 pyramidal neurons, it was shown that the GluN2B-containing receptor channel may have a greater calcium flux through them than the GluN2A-containing receptors (Sobczyk et al., 2005). Second, the CTD of these receptor subunits has a number of protein binding domains that facilitate interactions with a number proteins present in the post synaptic density (O'Brien et al., 1998; Prybylowski et al., 2005; Cousins et al., 2008). Finally, the temporal and spatial expression of these receptor subunits could also play an important role in modulating the synaptic plasticity at certain brain regions.

1.3.6 Regulation of NMDARs via CTD interactions

1.3.6.1 PDZ-domain interactions

The long CTD of the GluN2A and GluN2B subunits contain about 600 amino acids have a 30% sequence identity with most of the similar residues clustered as small regions. Thus, the two subunits may interact with the same proteins or with unique proteins resulting in either signal integration, or distinct signaling pathways, respectively. The CTD of the NMDAR has a number of protein binding motifs such as PDZ domains, clathrin adaptor protein (AP-2) binding domains (Prybylowski et al., 2005). Proteins that include PSD-93, PSD-95, SAP-97 and SAP102 that belong to family of proteins called membrane-associated guanylate kinases (MAGUKs) associate with the CTD of GluN2 subunit via PDZ domains or SH3/GK domains. It has been suggested that the preferential binding of MAGUKs to specific GluN2 subunits could result in differential effects on physiological processes such as trafficking of receptors, modulation of receptor current, and synaptic plasticity. For instance, interaction of PSD-95 and PSD-93 with the GluN2A and GluN2B subunits via the PDZ binding domains (PDZ1 and/or PDZ2) results in an increased surface expression of the NMDARs containing GluN2A/B subunits at the postsynaptic sites, while the PSD protein interaction does not affect the cell surface expression of GluN2C/N2B containing NMDARs (Prybylowski et al., 2005; Cousins et al., 2008). Further biochemical characterization revealed that the GluN2B preferentially binds to PDZ2 domain whereas GluN2A binds to both PDZ1 and PDZ2 domain of PSD-95 (Neithammer et al., 1996). Apart from stabilizing the receptors at the synapses, PSD-95 also facilitates the interaction of other proteins such as SynGAP, and various kinases with the NMDA re-

ceptors (Kim et al., 1998; Li et al., 2003). For example, selective association of GluN2B with SynGAP, a Ras GTPase activating protein, inhibits NMDAR-dependent ERK signaling (Kim et al., 1998; Kim et al., 2005). Thus, many proteins that interact with the CTD could regulate physiological events such as trafficking, and intracellular signaling.

1.3.6.2 Interaction with kinases

Certain forms of synaptic plasticity may require activation of protein kinases that transfer phosphate moieties to the side chains of the amino acids serine, threonine, and tyrosine in the intracellular CTD of the iGluR subunits [Figure 2]. Phosphorylation of those residues alters the net charge of the protein, which may result in a change in protein conformation. Any change in the receptor protein structure may alter the interactions they may have with other cytosolic proteins (Kim et al., 2011). The fast kinetics and the reversibility of the phosphorylation reaction may also allow for rapid modulation of the receptor. A number of kinases are expressed in an adult brain which may have different substrates and activation profiles. Interestingly it has been shown that mGluRs activated by glutamate can enhance NMDAR currents through the Pyk2/Src family of kinases in cortical neurons (Heidinger et al., 2002). Furthermore, activation of mGluR5 in the neurons of the subthalamic nucleus has been shown to potentiate NMDAR currents (Awad et al., 2000). These kinases may regulate activity-dependent synapse remodeling, learning, memory and cognition by a) altering the properties of ion channel receptor b) affecting the number of those receptors on the synaptic membrane, or c) regulating synapse remodeling by affecting protein synthesis. A few key studies that revealed the contribution of kinases modulation of NMDARs specifically in the context of synaptic plasticity, learning and

memory have been discussed below. Due the availability of vast literature on the contribution of these kinases to learning and memory, and since most of this dissertation research has been focussed on behavioral significance of PKC-modulation of GluN2A subunit, more emphasis has been placed on PKC regulation of NMDARs.

- **CaMKII.** The two major subunits of CaMKII in an adult brain are the αCaMKII and βCaMKII, although it has been shown that CaMKII exists as a homomeric or heteromeric holoenzyme consisting of twelve subunits (Hanson and Schulman, 1992). Those two major subunits play different roles in regulation of synaptic plasticity. For example, while the dissociation of βCaMKII from F-actin have been implicated in reorganization of cytoskeleton of dendritic spines during formation of long-term memories, the auto-phosphorylation of αCaMKII at T286 sustains the kinase activity due to its association with NMDARs. For a long time CaMKII has been touted as an ideal candidate for memory trace, since mice with mutated αCaMKII (T286A) show deficits in NMDAR-dependent spatial memory, and contextual fear memory learning (Irvine et al., 2011). However, the latter deficit can be reversed in T286 by using massed training paradigms. Thus, auto-phosphorylation of T286 may enable the mice to perform well in one-trial memory tasks by sustaining the synaptic activity levels above baseline (Radwanska et al., 2011). CaMKII can bind to the GluN2B subunit of the NMDAR which sustains the kinase activity of the enzyme contributing to LTP (Barria and Malinow, 2005). CaMKII also can phosphorylate S1303 in the GluN2B subunit, and may result in a slower dissociation of CaMKII from the receptor-kinase complexes (Omkumar et al., 1996). Since the GluN2A

and GluN2B subunits have different binding affinities to CaMKII, the NMDAR subunit composition also controls synaptic plasticity by regulating binding to CaMKII (Strack and Colbran, 1998; Barria and Malinow, 2005).

- **PKC.** Though all the isoforms of PKC are expressed in various brain regions, PKC isoforms that are dependent on calcium such as PKCγ and PKCβ have may have distinct functional roles in regulating short term synaptic plasticity (Chu et al., 2014). PKC enhances the currents through the recombinant NMDARs expressed in frog oocytes (Kelso et al., 1992; Logan et al., 1999). GluN1 has three serine sites that are phosphorylated by PKC. Phosphorylation of S896 and S897 by PKC increase the number of NMDARs trafficked onto the the plasma membrane of isolated hippocampal neurons (Scott et al., 2001). Phosphorylation of the Serines in the NMDAR C-terminus directly by PKC and indirectly via PKC activation of Src tyrosine kinase at two Serine and two Tyrosine (S1291, Y1292, S1312, and Y1387) positively modulates the receptor currents (Hsu, 1998). Thus, PKC enhances the currents through the receptor either as a result of increase in surface expression of the receptor or an increase in probability of opening. In contrast, PKC activity suppresses NMDA receptor-mediated currents due to a decrease in the number of synaptic NMDARs in isolated rat hippocampal neurons (Fong et al., 2002). The two serine sites in GluN2B CTD were identified to be substrates for PKC phosphorylation based on sequence identity between the CTDs of GluN2A and GluN2B. These sites are homologous to the S1291, and S1312 on GluN2A (Liao et al., 2001). In rat hippocampal slices LTP may be induced at least partially by PKC-dependent phosphorylation of

NMDARs (Lopez-Molina et al., 1993). Apart from modulating the receptor function directly, PKC also regulates binding of CaMKII by phosphorylating S1416 located within the CaMKII binding region on GluN2A subunit (Gardoni et al., 2001).

- **Tyrosine kinases.** Protein tyrosine kinases such as Src and Fyn phosphorylate tyrosines in the NMDAR subunits, and mostly result in enhancement of NMDAR-associated currents. It has been shown that PKC can activate Src signaling cascade, and thus G-protein coupled receptors that activate PKC can also indirectly modulate NMDAR function via Src (Lu et al., 1999). Though GluN2A, GluN2B and GluN2D have tyrosines that are targets for such kinases, it has been shown that GluN2B subunit has a greater number of phosphorylated tyrosines. While the major tyrosine phosphorylation sites in GluN2B (Y1252, Y1336 and Y1472) have been identified as substrates for Fyn kinase; the major tyrosine phosphorylation sites in GluN2A (Y1292, Y1325 and Y1387) have been identified as targets for phosphorylation by Src (Nakazawa et al., 2001; Yang and Leonard, 2001). The surface expression of NMDAR has also shown to be regulated by STEP (a phosphatase that targets Y1472), and casein kinase II (CKII) that phosphorylates S1480. Similar to the S1416 phosphorylation site on GluN2A that reveals crosstalk between two different kinases, Y1472 in GluN2B subunit also has been shown to be a substrate for both the STEP and CKII eventually regulating the surface expression of the NMDARs (Braithwaite et al., 2006; Sanz-Clemente et al., 2010).

- **Other kinases.** Protein kinase B, cyclin-dependent kinase-5 (Cdk5), and DRYK1-A have been shown to phosphorylate a number of serines in the NMDAR subunits, and could

regulate the surface expression and channel activity (Scott et al., 2001; Sutton and Chandler, 2002; Grau et al., 2014). PKA has been shown to increase NMDAR currents by increasing the channel opening probability and also influence its calcium permeability (Crump et al., 2001; Skeberdis et al., 2006). Activated PKA also regulates the targeting of the NMDARs to the surface of the membrane (Scott et al., 2003).

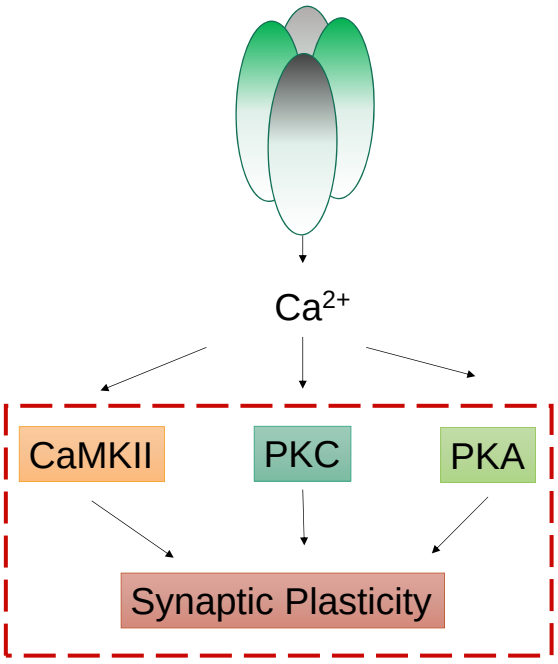

Figure 2: Activation of kinases by Calcium. Calcium flux through voltage-gated Ca^{2+} channels, Calcium-permeable AMPA receptors, or indirectly via activation of G-protein coupled receptors such as mGluR1/5 activate CaMKII and certain isoforms of PKC. The Ca^{2+} influx also recruits adenyl cyclase, which activates the PKA. Furthermore, several kinase knockout mice show alterations in certain forms of synaptic plasticity.

In summary, phosphorylation of specific amino acids in the NMDAR C-terminus could be one of the key mechanisms that could regulate NMDAR activity, and localization. Apart from the subunit-specific regional expression, temporal expression, and gating properties, the CTD of all the iGluRs contain various structural motifs that interact with scaffolding proteins (such as AKAPs), and are involved in numerous signal transduction processes (Westphal et al., 1999). A number of kinases and phosphatases also interact with Ser/Thr and Tyr residues in the CTD of the NMDAR subunits. This interaction regulates a number of ion channel properties like synaptic trafficking and membrane insertion. Though, all the phosphorylation site studies have identified many substrates for second messenger activated Ser/Thr kinases and tyrosine kinases, very few studies have focused on examining the behavioral and physiological significance of kinase-dependent NMDAR modulation in a living animal. Such animal models could reveal the existence of coordinated network of kinases and how each kinase in that network could differentially regulate specific NMDAR subunits which could in turn modulate the functional properties of the receptor channel.

1.3.7 Dissertation rationale

Synaptic transmission can be regulated by activity of kinases and phosphatases on certain residues in ionotropic receptors (Chen and Roche, 2007). In the adult brain, GluN2A-containing receptors remain the predominantly expressed NMDAR subtype in most areas of the brain. Regional and temporal expression of NMDAR subtypes could regulate activity-dependent changes in certain synapses. Also, the NMDARs themselves could be regulated by various kinases and phosphatases in the brain. Though a number of phosphorylation sites

have been identified on GluN2 subunits using the oocyte expression system, HEK cells and isolated mouse hippocampal neurons, the physiological relevance of all the data still remains unanswered. It is still not clear which phosphorylation sites may be more critical in regulating the NMDAR complex composed of the receptor with its scaffolding proteins and signaling proteins.

To address at least a part of that question, the *Grin2a*Δ*PKC* mouse was generated. Gene-targeted replacement in mice allowed selective inhibition of kinase activity on specific serines and tyrosines in the GluN2A subunit. In the oocyte expression system, phosphorylation of serines (S1291 and S1312) directly by PKC and phosphorylation of tyrosines (Y1312 and Y1387) indirectly by PKC via activation of Src tyrosine kinase positively modulates the receptor currents (Hsu, 1998; Liao et al., 2001). *Grin2a*Δ*PKC* mice with site directed mutations in two serine and two tyrosine residues (S1291A, Y1292F, S1312A, and Y1387F) in the GluN2A subunit without altering PKC action on any other proteins was used a mouse model to examine the behavioral and physiological significance of those sites. The S→A and Y→F substitution renders the amino acids non-phosphorylatable by a kinase, thereby allowing researchers to study the physiological significance of those phosphorylation sites in the GluN2A subunit. Each of the following chapters in this dissertation describe the general characterization of the mice, mRNA and protein expression levels of the mutated gene, behavioral phenotypes observed in different behavioral experiments, general activation of hippocampal neurons based on Fos expression and electrophysiological characterization of the *Grin2a*Δ*PKC* mouse hippocampal

SC-CA1 synapses using paired pulse facilitation, and theta-burst induced LTP of the synapses in hippocampal slices.

CHAPTER 2

GENERATION OF Δ*PKC* MICE

2.1 Introduction

Apart from interacting with a number of cytosolic proteins (such as PSD-95,PSD-93, SAP-102, Tubulin, Spectrin and Neto) the CTD of the GluN2A subunit also has a number of serines and tyrosines which are targets for various kinases (Husi et al., 2000). Such interactions could also modulate the currents through the receptor by changing the surface expression of the receptors in the post-synaptic density, and open probability of the channel. An increase in any of the above factors result in an increase in total amount of current flowing through the receptor resulting in an enhancement of synaptic transmission through those receptors. PKC phosphorylates serine residues and also activates another kinase called Src which in turn phosphorylates tyrosine residues in the sites in the GluN2A CTD. Chimeric NR2A constructs that contained varying lengths of truncated amino acids in CTD were made and expressed along with the NR1 subunit in HEK-293 cells. This was used to identify a region in GluN2A CTD specifically between amino acids 1267 and 1406 as a key structural determinant for PKC-mediated current potentiation in NMDA receptors (Grant et al., 1998). Using site-directed mutagenesis, specific amino acids on the CTD within that region were determined to be critical for the current enhancement in NMDA receptor by PKC (Hsu, 1998). S1291 and S1312 have been identified as PKC phosphorylation sites from oocyte expression studies based on PKC phos-

phorylation of its homologous sites on GluN2B (Liao et al., 2001), while Y1291 and Y1387 have been identified as Src phosphorylation sites from HEK cell studies (Yang and Leonard, 2001). The behavioral and physiological significance of those phosphorylation sites were determined *in-vivo* by using gene-targeted replacement strategy in mice.

Gene-targeted replacement using homologous recombination is a valuable technology that allows researchers to generate directed mutations at any specific locus. Germline transfer of the mutant alleles allows generation of offspring that could be used to study the effect of those mutations. This strategy also could be used to study the functional contribution of a specific amino-acid residue to a gene product. This procedure works because, even in the mouse with a relatively large genome size of 2.5 Gb, the in-built cellular DNA repair mechanisms work efficiently to align homologous regions resulting in chromosomal integration. While a large number of researchers use gene-targeting to generate knockout mice by disrupting the open reading frame of the gene, homologous recombination that swaps the normal copy with the mutant copy of the allele can be used to introduce subtle mutations. Those subtle mutations could be a single amino-acid insertion, substitution or deletion targeted to a gene of interest to study behavioral and physiological effects of those mutations in a mouse model of a human disease. However, altering an endogenous protein essential during critical periods of brain development could also result in embryonic lethality. For example, complete knockout of GluN2B results in pups that survive only for days after being born. They have severe locomotor deficits eventually resulting in death due to lack of suckling response (Kutsuwada et al., 1996). Hence, such severe phenotypes could be circumvented by using Cre/lox-P system.

The loxP site is a short 34 bp sequence that is usually placed flanking the exon of interest in a gene. An enzyme called Cre recombinase is used to excise the region of DNA between the two loxP sites. Thus, the mouse generated with the floxed (flanked by loxP) sequence contains the genetically altered allele in all tissues with a wild-type phenotype. Site-specific deletion or alteration of the gene could be obtained by breeding this floxed mouse to a Cre-expressing transgenic mouse.

Although, a number of researchers have used selection markers such as Neomycin resistance (*Neo^r*) and have studied the resulting phenotype and physiology of the mutant mouse without excising the *Neo^r*, there have been concerns that *PGK-Neo* cassette could influence the expression of several genes within a multi-gene locus (Pham et al., 1996). The role of Hox genes (specifically Hox-b4) in vertebrate segmentation was studied using mutant mice generated using two different approaches (Ramfrez-Solis et al., 1993). One of the mutants that was generated using gene targeted replacement resulted in a disruption of the target gene apart from retention of the *Neo^r* cassette, while another one was generated using a "hit and run" strategy that results in just gene disruption. Both the mutants show a homeotic transformation of C2 vertebrae while the mutant with the *Neo^r* cassettte also had a split sternum. This showed that the presence of the cassette could result in a additional unexpected phenotypes in mutant mice. The orientation of *Neo^r* selection cassette and the specific locus of deletion in the coding region in *Myogenic regulatory factor-4 (MRF4)* resulted in variable phenotypes in the mutant mice (Olson et al., 1996). Another clear example of the cassette effects was revealed during targeted deletion of 5′HS2 region of the *β-globin* gene locus. The 5′HS2 was previously

shown to regulate the expression of *β-globin*. When the wildtype 5′HS2 was replaced with the mutant allele containing the *Neo*^{r} cassette, it resulted in at-least a two fold reduction in expression of all the genes in the locus. In contrast, mice containing the mutant allele without the cassette resulted in a almost normal expression of all beta-like globin genes (Fiering et al., 1995). To avoid such conflicting results such as occurrence of additional phenotypes, and variation in expression levels of other genes in mutant mice with the *Neo*^{r} selection marker, those mutants were bred with Cre-expressing transgenic mice to completely excise the *Neo*^{r} cassette as described previously (Lakso et al., 1996).

A point mutation in a genome is a mutation that changes a single nucleotide in the sequence. Sometimes these mutations result in a chemically different amino-acid substitution in the protein that could produce an alteration in the protein structure and function. In mutant mice that were generated to study the significance of PKC phosphorylations, the point mutations were targeted to the CTD of the *Grin2a* gene resulting in substitution of four amino acids that could be phosphorylated by PKC or Src to their chemical equivalents that cannot be phosphorylated by PKC or Src, respectively. A missense mutation such as the one described above could result in mRNA or protein instability due to a number of factors. For example, if the mutation occurs at a folding region, it could result in protein misfolding, aggregate formation, or an unstable protein; while a mutation that occurs in a binding domain (protein-protein or DNA-protein binding) or a signaling region of the gene, it could affect signaling through the protein, mislocalization of the protein to a different subcellular organelle, altered protein activity or altered protein expression levels. Overall, this means that the mutations

that were introduced to study significance of site-specific PKC-mediated phosphorylation in mice could produce phenotypes that may not be related to PKC-mediated phosphorylation. Also, altered mRNA production is usually associated with mutations in residues that are involved in splicing events (Hawley and Mori, 2010). To avoid attributing any phenotype in mutant mice to varying mRNA levels or protein levels of the NMDAR receptor subunit that was mutated, the mRNA expression of *Grin2a* and protein levels of GluN2A in *Grin2a*Δ*PKC* mice and their control wild-type littermates was compared using modified Northern blotting and Western blotting. In addition, because the loss of *Grin2a* expression in GluN2A knockout mouse did not alter the whole animal morphology or the brain anatomy (Sakimura et al., 1995), no change was expected in *Grin2a*Δ*PKC* mouse either. Still, the overall anatomy of the *Grin2a*Δ*PKC* mouse was also examined.

2.2 Methods

2.2.1 Targeting vector construction

Mutagenesis of the *Grin2a* phosphorylation sites was accomplished by using PCR to amplify a 1.8 kb fragment spanning exon 12 of the mouse *Grin2a* gene. This fragment was cloned into the pCR4Blunt-TOPO vector and used as a template for serial site-directed mutagenesis with the QuikChange Site-Directed Mutagenesis Kit (Stratagene, CA, USA). The resulting plasmid pCR4Grin2a12-5'-AFAF contained the four desired amino acid substitutions: S1291A, Y1292F, S1312A, and Y1387F. For construction of the *Grin2a* targeting vector, DNA from bacterial artificial chromosome clones spanning the *Grin2a* gene was digested with SmaI, SnaBI, and BstEII, and 8.1 kb and 1.8 kb fragments spanning the *Grin2a* locus were isolated and cloned

into pBKSII, generating plasmids pBSGrin2a12-5′ and pBSGrin2a12-3′. These fragments represent the 5′ and 3′ arms of the *Grin2a* targeting vector, respectively. To replace the exon 12 region of the 5′ targeting arm with the phosphorylation site mutant, plasmid pBSGrin2a12-5′ was digested with EcoRV, releasing a 1.6 kb segment of exon 12. The mutant exon 12 was similarly released from the plasmid pCR4Grin2a12-5′-AFAF, and cloned into pBSGrin2a12-5′, creating plasmid pBSGrin2a12-5′-AFAF. The 5′ arm was then released from pBSGrin2a12-5′-AFAF with EcoRI and BamHI, and blunt-ended into the XhoI site of the targeting vector ploxPNT. Similarly, the 3′ arm insert was released from pBSGrin2a12-3′ with EcoRI and BamHI and blunt-ended into the KpnI site of ploxPNT, creating the targeting vector Grin2aKINR. The targeting vector therefore carries the 8.1 kb 5′ arm containing exon 12 upstream of the *Neo* gene, and the 1.8 kb 3′ arm downstream of the *Neo* gene. Accuracy and orientation of the cloned fragments was verified by sequencing across all cloning junctions.

2.2.2 Homologous recombination

The targeting vector Grin2aKINR containing the substitutions (S1991A, Y1292F, S1312A and Y1472F) along with a *Neo*^{r} was designed to replace the exon 12 of *Grin2a* gene by homologous recombination [Figure 4]. The targeting vector Grin2aKINR also had a loxP sites flanking the *Neo*^{r} cassette. The Grin2aKINR vector was linearized with NotI, electroporated into J1 embryonic stem cells and 500 Neo-resistant ES cell colonies were selected and expanded. PCR genotyping employed a primer located within the targeting construct, and one in the Grin2a locus outside the targeted area. Twenty clones were found to have undergone homologous recombination, and the mutated region was verified by sequencing select clones. Three of

the targeted clones were micro-injected into blastocysts from C57BL/6 mice, in collaboration with the University of Illinois at Chicago Transgenic Production Service. These blastocysts were returned to outbred surrogate mothers, yielding 14 chimeras that were up to 90% ES cell-derived. The best chimeras were crossed to C57BL/6 mice to obtain germline transmission of the targeted allele. Heterozygous animals were crossed to generate homozygous mice for the mutant *Grin2a* allele. These mutants were called *Grin2a*Δ*PKC-Neo* mice (shortened as Δ*PKC-Neo*).

2.2.3 Removal of the *Neo*^{r} Cassette by Cre Recombination

Δ*PKC-Neo* males were crossed with *EIIaCre* female mice that target the expression of *Cre recombinase* to the early mouse embryo under an adenovirus *EIIa* promoter (Lakso et al., 1996). Male heterozygotes which have completely excised *Neo*^{r} cassette were identified by using specific set of primers which bind to a sequence within the cassette or to an outside locus. All the pups were screened and about 6 male heterozygous mice with complete *Neo*^{r} excision were selected. These heterozygous mosaics were backcrossed to C57Bl/6J female mice. Heterozygous mice from the backcross were again screened for excised *Neo*^{r} cassette excision (using primers listed in Table I), and those selected animals were used as breeders. The mutant homozygous mouse strain was denoted as *Grin2a*Δ*PKC* (shortened as Δ*PKC*).

2.2.4 Genotyping

All of the mice used for behavioral and electrophysiological experiments were generated from heterozygous crosses. This breeding scheme also provided wild-type littermates for use as controls. Tail snips obtained from 14 - 21 day old mice were used to isolate pure genomic

TABLE I: Primers and product sizes (in bp) for *Neo*^{r} excision PCR and Genotyping PCR

Primers	WT	Δ*PKC*	Excised heterozygotes	Non-excised heterozygotes
Internal				
Neo F2/ R2		239		239
NeoB/OL1482		729		729
Genotyping				
Grin2aF10/R11	1328	1590	1328/1590	1328/1590

DNA. This DNA is used as a template for a PCR set up to amplify a segment of the *Grin2a* gene using specific primers (Grin2aF10 and Grin2aR11) [Appendix A]. A 50 µl PCR was setup with 1.5 µl of genomic DNA from tail snips as template DNA. The PCR cycle parameters were initial denaturation at 95 °C - 5 minutes, 35 cycles of (94 °C - 2 min; 58 °C - 2 min; 72 °C - 2 min), 72 °C - 5 minutes, 4 °C - 2 hours. About 10 µl of the PCR product was digested using RseI restriction enzyme, using standard digestion protocols [Appendix A]. The primers used for genotyping recognize a sequence in the *Grin2a* gene flanking a restriction enzyme site. This site was present in a WT allele but was absent in a mutant allele (due to a substitution mutation). The restriction digested PCR product was then run on a 2% agarose gel to determine the genotype of every animal.

2.2.5 mRNA expression levels

All animals were anesthetized using a a mixture of 100 mg/kg of Ketamine and 16 mg/kg of Xylazine, and their brains were dissected. mRNA levels of *Grin2a* were determined from

TABLE II: Primer sequences

Primer	Sequence (5′-3′)
Grin2aF10	AACTGCACTCCAGTGTCTGCTG
Grin2aR11	AACTAAGCGTTGGTCATCCCCG
NeoB	CCTTCTTGACGAGTTCTTCTGAGG
NeoF2	GATCTCCTGTCATCTCACCT
NeoR2	ATGATCTCGTCGTGACCCAT
OL1482	ACACCATCGTGGCTGTCTGG

RNA isolated from the whole brains of WT and Δ*PKC* mice. About 20 µg of pure RNA was isolated using the TRIZOL method (Rio et al., 2010). The purity of the RNA samples was determined from the absorbance values measured at 260 nm and 280 nm using a spectrophotometer. The RNA was loaded in a single well of a six-lane 1% MOPS/formaldehyde gel, which was transferred onto a Nylon membrane using a neutral buffer containing 0.5 M Tris-HCl at pH of 7 and 1.5 M NaCl. The membrane with the RNA samples was hybridized to biotinylated probes overnight at 55 °C. The probes were PCR products obtained using primers specific for *NR2A* and *GAPDH* (Kinney et al., 2006; Liu et al., 2003), and were biotinylated using North2South Biotin Random Prime Labeling Kit (Thermo-Scientific,MA,USA). The membrane was washed thoroughly at-least three times using a stringency wash buffer provided in the kit and a blocking buffer was added to cover the membrane. The probes were detected using

a Streptavidin-HRP solution and the membrane was subsequently developed using a Luminol enhancer solution. The developed images were obtained and processed using the Bio-rad Chemi-DocMP imaging system and Image-Lab (an built-in software in the Chemi-Doc).

2.2.6 Western Blotting

Whole brains were dissected from anesthetized mice, snap-frozen in liquid nitrogen and stored at -80 °C until further analysis. Brain tissue lysate was prepared by homogenizing the whole brain in modified RIPA buffer containing 150 mM NaCl, 1% IGEPAL CA630, 0.5% Sodium deoxycholate, 0.1% SDS, 50 mM Tris - pH 8.0 and 10X protease/phosphatase inhibitor cocktail (Sigma, MO, USA). Protein concentration in the lysate was determined using Bradford assay (Bio-Rad,CA,USA), and lysates were denatured by incubating them at 95 °C in 2X Laemelli sample buffer. Samples containing 50 µ g of protein were loaded per well in Any kD Mini Protean TGX gel (Bio-Rad) and transferred onto PVDF membranes. After the transfer, the membranes were incubated in blocking buffer containing 5% BSA in TBS-T for 1 hour at room temperature, followed by overnight incubation at 4 °C in TBS-T containing primary antibodies against GluN2A protein and GAPDH (EMD-Millipore, MA,USA). The membranes were then washed in TBS-T and incubated for 2 hours in diluted secondary antibody (HRP conjugate Goat Anti rabbit obtained from Millipore). After a quick wash in TBS-T, the blots were developed using a chemiluminescent detection system (Clarity WB ECL, Bio-Rad) on a Bio-rad ChemiDocMP system. These blots were quantified using Image Lab software for ChemiDoc (Bio-Rad). Each animals' GluN2A protein intensity levels were normalized to its respective

GAPDH intensity and these values were averaged among three animals in each group (WT and ΔPKC).

2.2.7 Histology

For cresyl-violet staining, mice were anesthetized using a a mixture of 100 mg/kg of Ketamine and 16 mg/kg of Xylazine. After the animals attained a deep level of anesthesia, they were transcardially perfused at room temperature with phosphate buffered saline (PBS), followed by a fixative containing 4% formaldehyde. Brains were postfixed for one hour at 4 °C in the high pH fixative solution (4% formaldehyde solution containing 0.05 M Sodium Borate , pH 9.5) and then transferred to 20% sucrose in PBS until slicing. Serial 35 µm slices were prepared from frozen slices and were stored in a cryopreservative solution until they were processed for cresyl violet staining as described elsewhere (Paul et al., 2008).

2.2.8 Visual placement test

To determine if the mice used for various behavioral and electrophysiological experiments were impaired in vision, they were tested using the visual placement test paradigm. In this test, the mouse was held using its tail, and was gradually lowered on to the wired-cage top from a height of 15 cm. The mouse was observed and scored on a 0–3 point scale based on its forelimb extension (0 - no forelimb extension; 1 - forelimb extension upon nose contact; 2 - forelimb extension upon vibrissae contact; 3 - vigorous forelimb extension).

2.3 Results

2.3.1 Genotyping assay and *Neo*^{r} cassette excision

The genotype of every animal in the colony was determined using a PCR/ Restriction digest protocol established in the lab using the genotyping primers listed in Table I. A 2% agarose gel was loaded with the samples obtained from the restriction digestion of PCR products and post-stained using 10000X solution of Gel-Red. As shown in Figure 3, the WT allele containing the mutation was cut by the RseI enzyme resulting in a smaller product about 1350 bp while the mutant allele without the restriction site was not affected by the enzyme. The sizes of various products are listed in Table I. The mice were then group-housed (maximum 4 per cage) based on their genotype with an ear-punch used to distinguish WT and mutant animals in the colony. Within a cage, individuals were identified based on unique tails colored using Sharpie markers. Thus, the genotyping assay provided a monitoring system to distinguish WT, heterozygous, and homozygous mice.

As shown in Table I, and Figure 5 two sets of primers and PCR conditions were used to assay for *Neo*^{r} excision. The internal primers NeoB, NeoF2 and NeoR2 bind within the *Neo*^{r} cassette, while the flanking primer OL1482 binds outside the *Neo*^{r} cassette.Table I also lists the PCR product sizes for the genomic DNA templates isolated from Δ*PKC*, heterozygotes and control littermates. The PCR products were run on 2% agarose gels to confirm excision over three generations after complete excision of the *Neo*^{r} cassette.

As shown in Figure 6, a complete excision of *Neo*^{r} cassette, resulted in an absence of a PCR product when the internal primers were used. The PCR that was run using the flank-

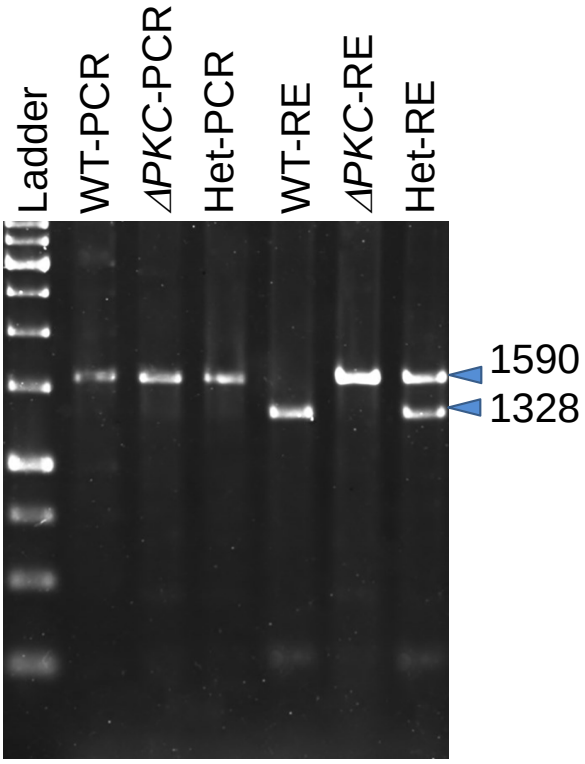

Figure 3: Representative gel from genotyping assay. The agarose gel lanes were loaded with 10 µl of either PCR products (PCR) or Restriction digested PCR product (RE) obtained from tail snips of WT, Δ*PKC*, and heterozygote mice. The PCR products are about 1590 bp in size, and the digestion of the PCR product containing the WT allele with a restriction enzyme results in a shorter product of about 1328 bp. The small blue triangles indicate the product size in bp.

ing primers OL1481 and OL1482 did not give the predicted product sizes even after multiple PCR optimization runs. Hence, to confirm complete excision of the *Neo*^{r} cassette, every PCR reaction was run thrice as three independent runs in different times with control reactions. The positive control template for the *Neo*^{r} was the genomic DNA extracted from PCR was the Δ*PKC-Neo*, while the genomic DNA from WT animals was used as the negative control. This

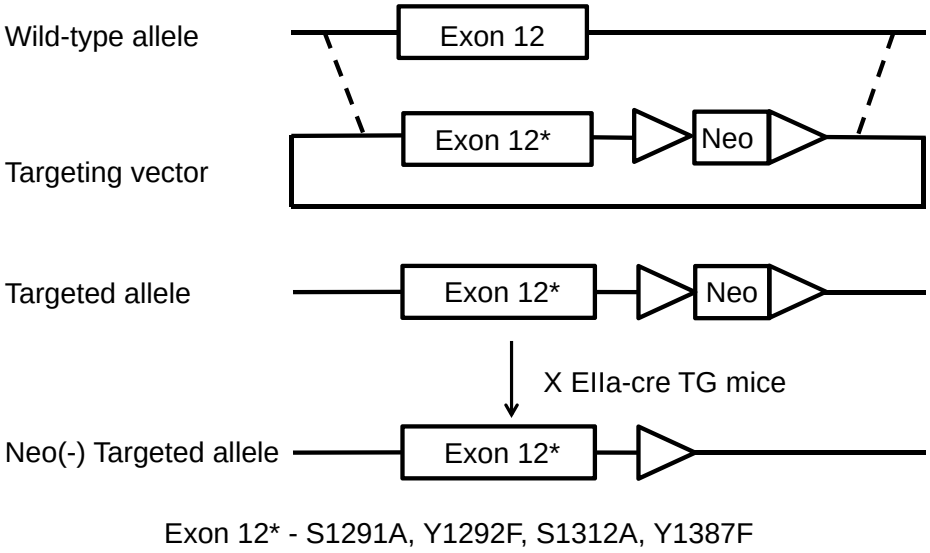

Figure 4: A schematic representation of homologous recombination process. A targeting vector containing the PKC-mediated phosphorylation site mutations (S1291A, Y1292F, S1312A, and Y1387F) with a *Neo*^{r} replaced the exon 12 of WT *Grin2a* gene by homologous recombination. Δ*PKC-Neo* mice with were crossed with *EIIa-Cre* mice to generate Δ*PKC* mice.

is due to the fact that the *Neo*^{r}-excision PCR relied on absence of a product to confirm excision which means there is a risk of a false negative due to some problems in the PCR components or cycle parameters.

2.3.2 *Grin2a* mRNA and GluN2A protein expression levels

Northern blot analysis confirmed the presence of a high molecular weight band that represents the signal obtained when the RNAs obtained from WT and mutant brain lysates are hybridized onto biotinylated probes specific to *Grin2a* and *GAPDH*. In Figure 7, the GluN2A subunit is detected as a 170 kDa band while the GAPDH protein appears as a 36 kDa band

in the western blots. The mRNA and protein levels of the GluN2A subunit in the WT and mutant mice brain were determined using a modified Northern blotting and western blotting technique respectively. Both the RNA and protein subunit levels were normalized to its GAPDH levels in the brain lysates. The intensity of signals obtained from the blots was quantified using the Image lab software by using standard settings for background subtraction. The expression levels of *Grin2a* mRNA and GluN2A subunit were similar in WT and Δ*PKC* mice [Figure 8].

2.3.3 General animal morphology and gross brain anatomy

Young and adult mice from both the groups (WT and Δ*PKC*) were randomly chosen and weighed periodically at at 1, 3 and 6 months. At postnatal day 30, both the WT and Δ*PKC* mice weighed about 15 g, and their weights increased to about 27 g by 3 months and to about 40 g by 6 months [Appendix B, Figure 9a and Figure 9b]. Hence, there was no change in body weight between the two groups of mice. For determining the RNA/protein levels, and c-fos immunostaining studies described in Chapter 3, whole brains were dissected, observed and weighed. There were no detectable changes in the shape and size of brains extracted from both the groups of mice [Appendix B]. Both the groups of mice were not impaired in vision since they had similar scores in the visual placement test [Figure 10]. As shown in Figure 9c, cresyl-violet staining of 35 µm coronal sections obtained from brains of the two groups of mice did not show any morphological changes in the hippocampus, and cortex. However, one of the mutants out of 14 showed an abnormal CA1 hippocampal field [Figure 11].

2.4 Discussion

A gene-targeted replacement strategy using homologous recombination was used to insert a mutated *Grin2a* allele in the mouse genome, to study the effect of specific PKC-mediated phosphorylation sites *in vivo*. For generating Δ*PKC* mice, a Neomycin resistance cassette (*Neo*^{r}) was used as a marker to determine which embryonic stem cells have incorporated the vector containing the mutations. This *Neo*^{r} cassette was flanked by two loxP sites. Though it is highly unlikely that the *Neo*^{r} cassette within the *Grin2a* locus, might affect the behavior and physiology of the mutant mice, the *Neo*^{r} cassette was removed by breeding male Δ*PKC-Neo* mice with *EIIa-Cre* female mice. The *Neo*^{r} cassette excision was successfully confirmed over three generations of offsprings using two sets of primer pairs (each containing at least one internal primer that binds to the *Neo*^{r} cassette). Using two flanking primers (OL1481 and OL1482), the DNA extracted from mutant animals containing the *Neo*^{r} cassette and with the excised *Neo*^{r} cassette were run thrice as in independent PCR runs with proper controls. Thus, *Neo*^{r} was completely excised in the genome of mutant animals from the mouse colony.

To maintain the mouse breeding colony, a trio mating scheme using heterozygous mice ensured the availability of animals for research. However, the large number of offspring animals, also resulted in a continuous need for genotyping individual mice. All the mice were used for all the experiments were individually identified using a combination of genotyping assay and ear-punches. Only males were used in the study to avoid confounding behavioral and physiological results due to the influence of hormonal cycle in female mice.

The expression levels of both the *Grin2a* mRNA and the GluN2A protein in the mutant Δ*PKC* mice were found to be similar to those found in WT mice. Though the mRNA expression level is a good read-out of protein levels, there are instances where the mRNA expression does not correlate with protein expression levels (Chen et al., 2002; Gygi et al., 1999). Of all of the factors that determine steady state protein levels, comparable mRNA levels could be a result of similar transcription process in the two groups of mice. Hence, the levels of GluN2A subunit in the mice could still be regulated by various factors such as mRNA degradation, translation, and protein degradation. Most importantly, to ensure that any phenotypic changes we observed in the mutants are attributed only to the mutations and not due to aberrant transcription and translation of the *Grin2a* gene the mRNA and the GluN2A protein were compared between the wild-type and mutant mice. There were also no abnormalities found in the brain sections obtained from the Δ*PKC* mice, and the gross brain morphology was indistinguishable from their age-matched control WT littermates. There was also no observable change between the two groups of mice in body weight during development of the animal to adulthood.

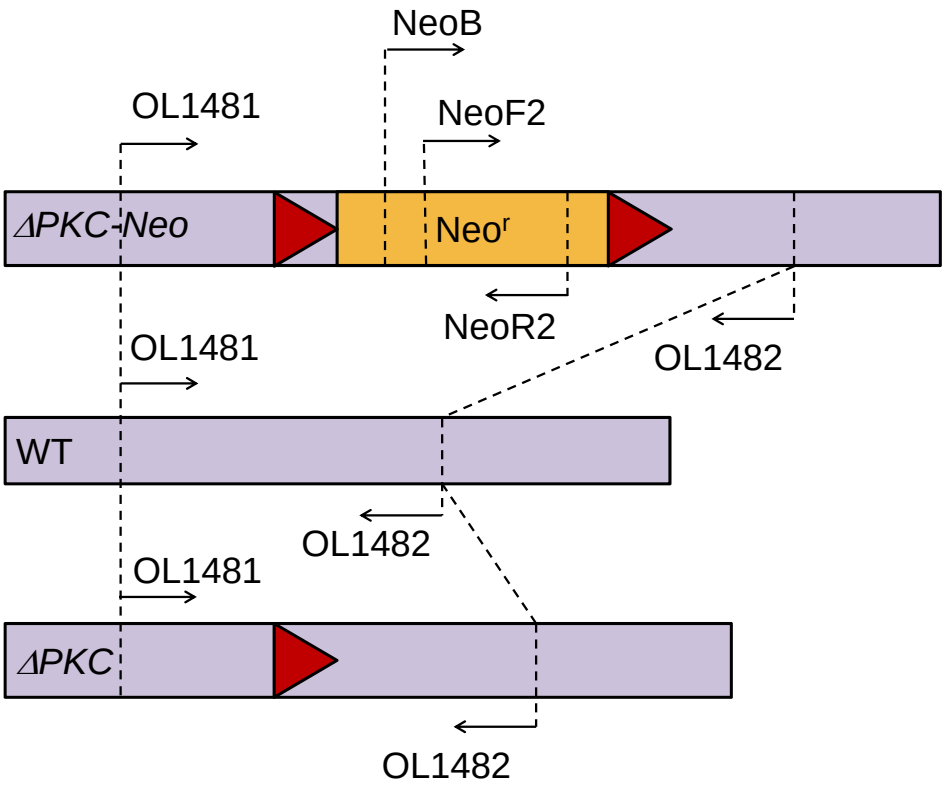

Figure 5: A schematic representation of WT, heterozygous and homozygous mutant *Grin2a* alleles showing the position of flox sites and primer binding sites. The targeting vector has the flox sites represented in the figure as red triangles, which are targets for the cre recombinase. The excision process leaves behind one flox site within the *Grin2a* locus. The primer binding sites in Δ*PKC-Neo* mice and WT mice are also indicated. OL1482 and OL1482 are flanking primers which bind outside the *Neo*^{r} cassette but within the *Grin2a* locus. NeoF2 or NeoB and Neo R2 are internal primers which bind within the *Neo*^{r} cassette locus. Another set of primers NeoB and OL1482 were used to confirm the results from the two PCRs.

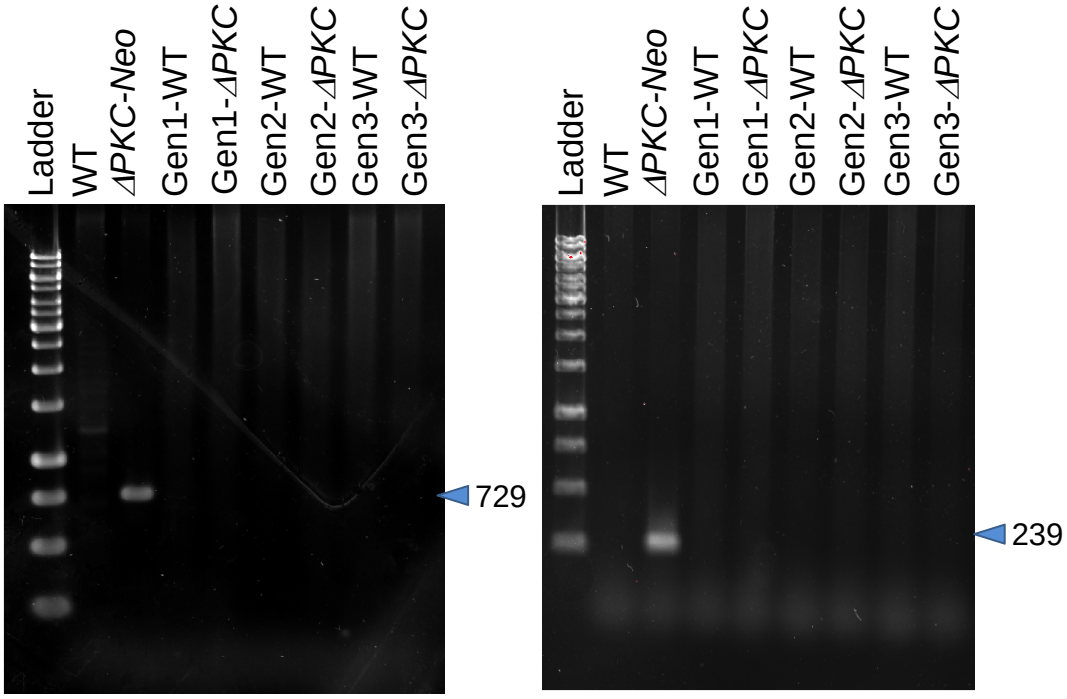

(a) **(b)**

Figure 6: Gel images from PCR assay used for verifying *Neo*^{r} cassette excision. (a) Representative gel image from PCR using Internal/Flanking primers - NeoB and OL1482. (b) Representative gel image from PCR using internal primers - NeoF2 and NeoR2. Genomic DNA from each mouse was used as a template for three independently set up PCR reactions using proper controls. the excision was also confirmed over three generations of mice from the colony.

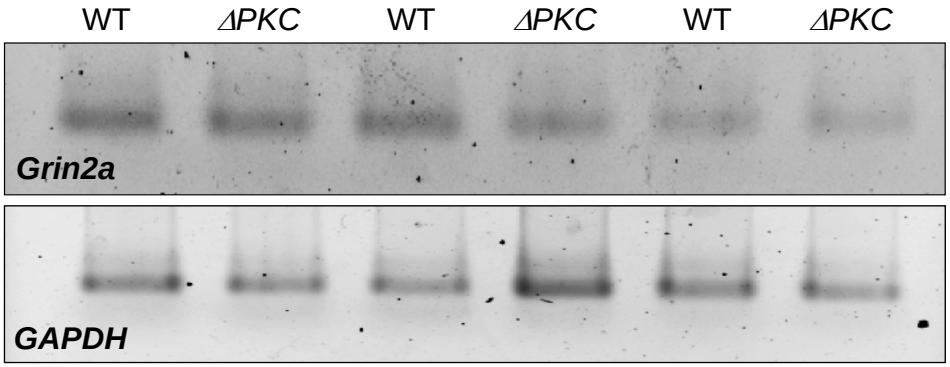

(a)

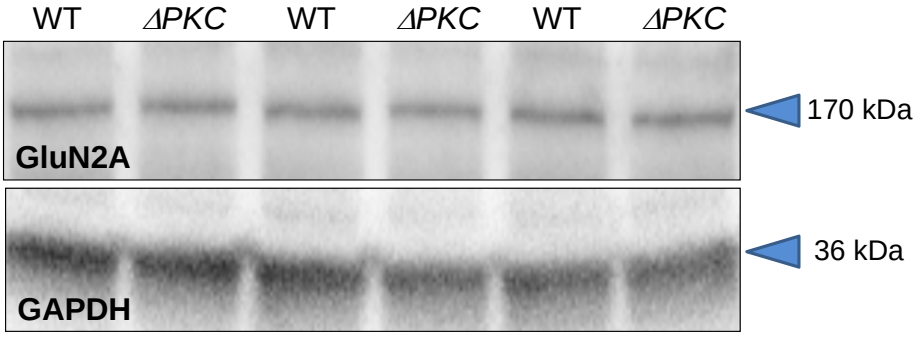

(b)

Figure 7: Representative images of Northern and Western blots. (a) Each lane contains equal amounts of about 1 µg RNA isolated from either WT or mutant mouse brain in 7 µl RNA solution and 7 µl of loading dye. The RNA isolated from brain lysates of both WT and mutant mice were hybridized to either biotinylated *Grin2a* or *GAPDH* probes, and detected using chemiluminescent nucleic acid detection kit purchased from Thermo-Scientific. (b) Each lane was loaded with equal amounts of protein (50 µg) isolated and purified from either WT or mutant mouse brain. The gel was run with 1X Tris-Glycine buffer at 75V, transferred onto PVDF membranes, blocked and incubated in primary antibodies targeted to mouse GluN2A subunit and GAPDH. The blots were then developed using Clarity WB ECL Chemiluminescent detection kit, and images using Biorad-ChemiDoc imaging system.

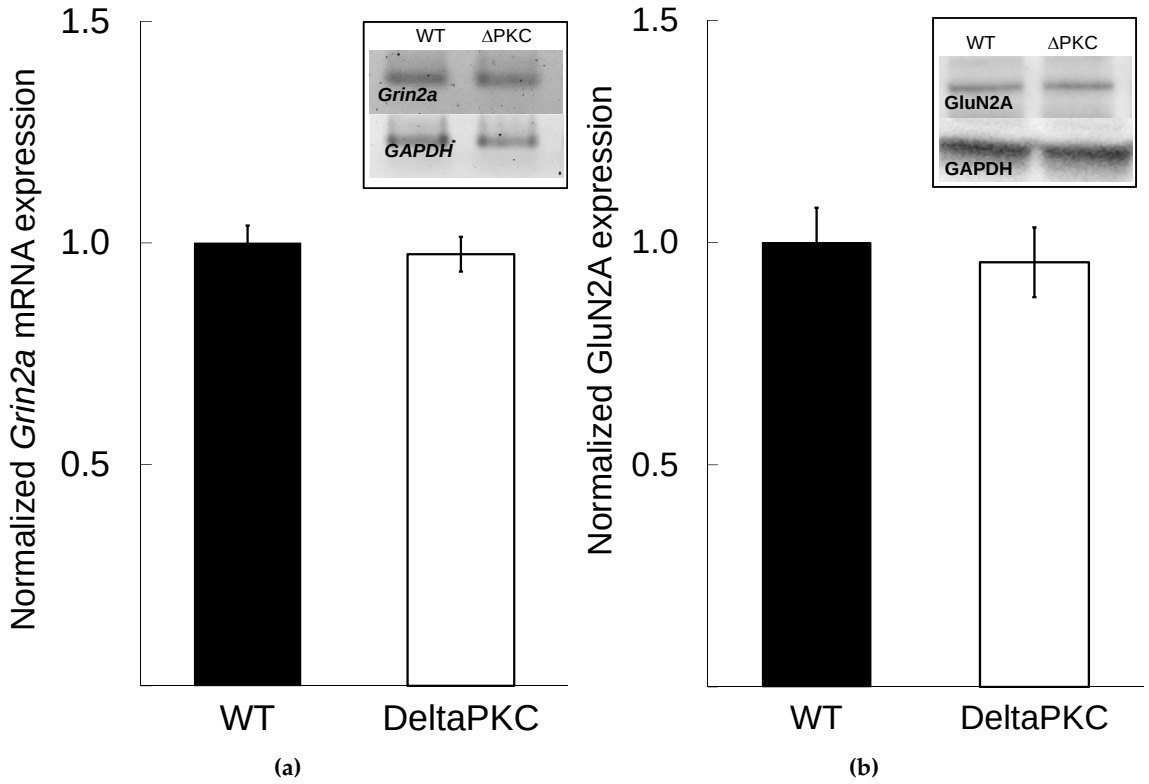

Figure 8: mRNA and protein expression levels of GluN2A subunit. Quantification of (a) RNA and (b) protein levels in lysates obtained from whole brain homogenates of WT and Δ*PKC* brain. Histogram represents mean ± S.E.M, obtained by normalizing the signal intensities of the *Grin2a* mRNA or GluN2A protein levels to *GAPDH* or GAPDH expression levels in the WT and mutant mouse brain. The inset in the right corner of each quantification is a representative image of western blot of one animal. There was no significant difference in the quantities of normalized mRNA ($F_{1,4}$=O.18,p=.69) and protein ($F_{1,4}$=0.66,p=.22) expression levels of GluN2A subunit between the WT and mutant mice. n=3 for both the groups, and each of the blots probed with GluN2A antibody was stripped and reprobed using GAPDH antibody.

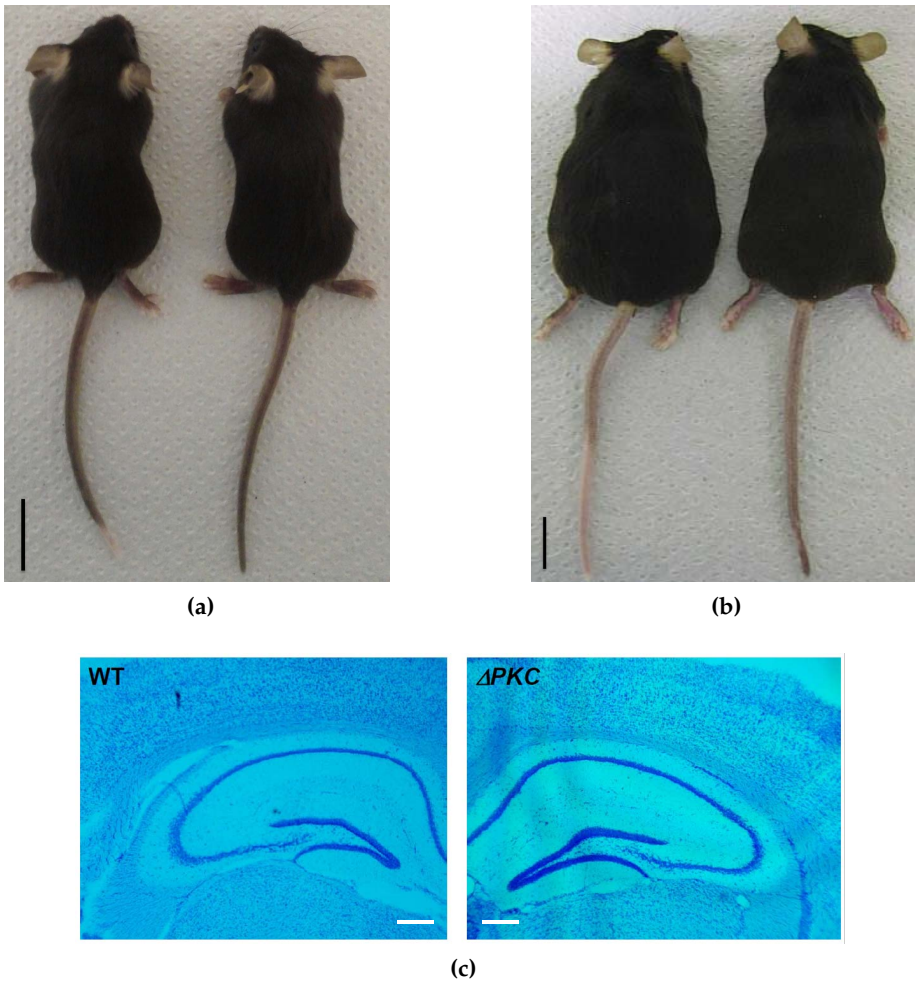

Figure 9: Growth and development of Δ*PKC* mice. (a) One-month old and (b) adult (six-month old) WT and Δ*PKC* mice were not different in size and growth rate through adulthood. Black scale bars: 1 in. (b) There was no difference observed when the hippocampal regions of the WT and Δ*PKC* mice were compared. White scale bars: 125 µm.

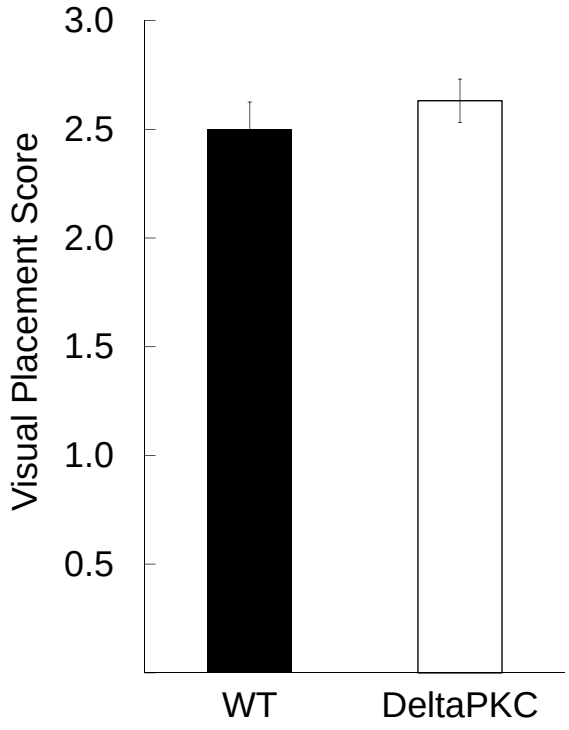

Figure 10: Visual placement scores of WT and ΔPKC mice. Every mouse was lowered on to the wire-cage of a mouse cage, and scored on a scale of 0–3 based on forelimb extension. The higher the score the more rapid was the forelimb extension, and implied no visual impairment. Both the groups of mice had similar scores in the visual placement test ($F_{1,37}$=0.65,p=.42, WT:n=20; ΔPKC:n=19).

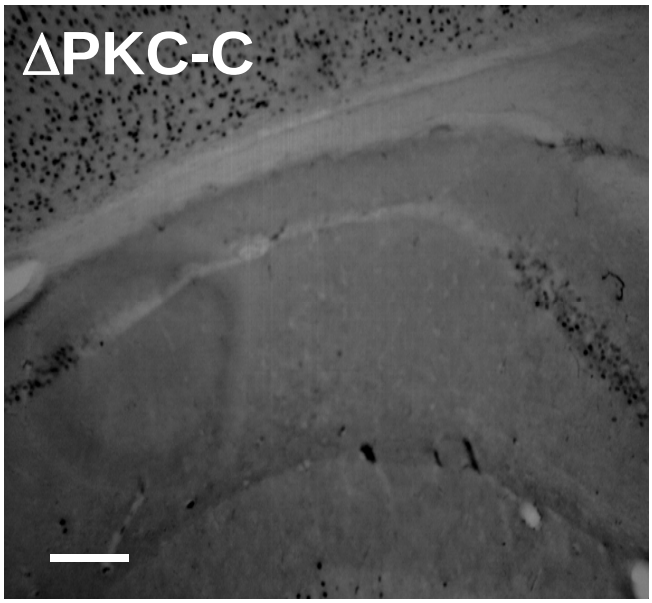

Figure 11: Anomalous CA1 field in mutant hippocampal slice. Apart from Fos immunostaining, 2-4 slices from each mouse was also stained using Cresyl-violet to determine if there were any abnormalities in hippocampal fields, cell numbers or morphology. In one of 14 mutants obtained for Fos immunostaining, CA1 cells in the hippocampus were found to be missing, while the DG and CA3 looked normal. The mutant was not included in the data analysis for counting the Fos(+) cells since it might skew basal Fos levels. White scale bars: 125 μm.

CHAPTER 3

BEHAVIORAL CHARACTERIZATION OF ΔPKC MICE

3.1 Introduction

Among all the structural domains in the NMDAR subunits, the CTD of the subunits reveal the most diversity in terms of amino-acid residues and length (Traynelis et al., 2010). Also, the CTD has a number of binding motifs for intracellular proteins involved in synaptic plasticity and neuronal signaling. Hence, a number of studies have focussed on physiological contributions of specific GluN2 subunits using transgenic mice that have over-expressed or completely deleted subunit, or mutating certain residues in the CTD that alters the binding motif of the subunit. However, *in vivo* studies in such transgenic mice could reveal any causal links that may exist between the behaviors observed in mice and the physiological changes.

Various studies have established the behavioral significance of the GluN2 subunits, using knockout and over-expression of various subunits in the brain. When the GluN2A subunit was over-expressed in the mouse forebrain, the mice show deficits in long-term memory, and not short term memory in various behavioral tests such as spatial maze, novel object recognition, and cued/contextual fear conditioning (Cui et al., 2012). However, the GluN2A knockout mice exhibited reduced anxiety-like behaviors (in an elevated plus maze, light-dark box, and open field), and antidepressant-like behaviors (in a forced-swim test) (Boyce-Rustay and Holmes, 2006). Mice lacking the GluN2A subunit also have deficits in the formation of spatial memory,

and show impairments during acquisition of conditioned eye-blink response task (Bannerman et al., 2008; Kishimoto et al., 1997). Thus, the findings from GluN2A knockout mouse study implicated the GluN2A subunit in learning and, regulation of emotional and cognitive function. In contrast, another research group found that GluN2B over-expression in the forebrain resulted in enhancement of learning and memory, and inflammatory pain perception (Tang et al., 1999; Wei et al., 2001), and its conditional deletion results in both spatial and non-spatial memory impairment (Engelhardt et al., 2008). Such studies reveal the differential contribution of the GluN2 subunits to various behaviors in mice. Specifically, the importance of the GluN2 subunit CTDs was evident in when the CTDs were swapped in mice. Thus, the differential interaction of the two subunits (GluN2A/N2B) with cytosolic proteins could contribute to different vertebrate behaviors and also increased signaling complexity (Ryan et al., 2008; Ryan et al., 2013). Interestingly, the mice with CTD of GluN2B swapped with CTD of GluN2A showed reduced general activity, while the mice with CTD of GluN2A swapped with CTD of GluN2B showed reduced anxiety-like behavior, motor coordination and perceptual learning, establishing the subunit-specific CTD contribution to various behavioral phenotypes. Given that PKC modulates NMDARs by directly phosphorylating serine residues and indirectly phosphorylating tyrosine residues via Src kinase, the behavioral consequence of mutating specific PKC-mediated phosphorylation sites on the GluN2A subunit was examined in mice. Hence, Δ*PKC* mice with PKC-mediated phosphorylation site mutations (S1291A, Y1292F, S1312A, and Y1387F) were generated and characterized under various behavioral tests.

3.2 Methods

3.2.1 Experimental animals

All experiments using animals were carried out in accordance with the guidelines for animal use issued by the Office of Animal Care and Institutional Biosafety at University of Illinois-Chicago [Appendix D]. Heterozygous mice carrying alleles of *Grin2a* containing the phosphorylation mutations (S1291A, Y1292F, S1312A, Y1387F) - flanked by loxP sites were bred to yield littermate controls (WT, Δ*PKC* for all experiments). Most of the behavioral experiments were done with mutants before Cre-mediated excision of Neo^r. Student's *t*-test comparing the data obtained from behavioral experiments (such as for the four-arm maze alternation, and T maze alternation tests) using Δ*PKC-Neo* and Δ*PKC* mice show that they were not significantly different. Except for the forced-swim test (which was performed only using Δ*PKC* mice), the data from both the groups of mutants were used for all the experimental analysis. All the behavioral experiments were done between 9 AM and 12 PM, and were analyzed by researchers blind to the genotype of the animal. All the apparatuses used for behavioral experiments were cleaned using 70% ethanol between individual mouse trials. Table VIII lists various tests and the parameters measured during those tests for behavioral characterization [Appendix C].

3.2.2 Spatial working memory

3.2.2.1 Spontaneous alternation behavior

Spontaneous alternation behavior was observed in the mice using in a four-arm maze and Y maze (Hughes, 2004). The arms of the maze, made of black plexiglass were 30.5 cm in length. The walls of the arm were 7.5 cm. These arms were arranged to form either a plus or a Y

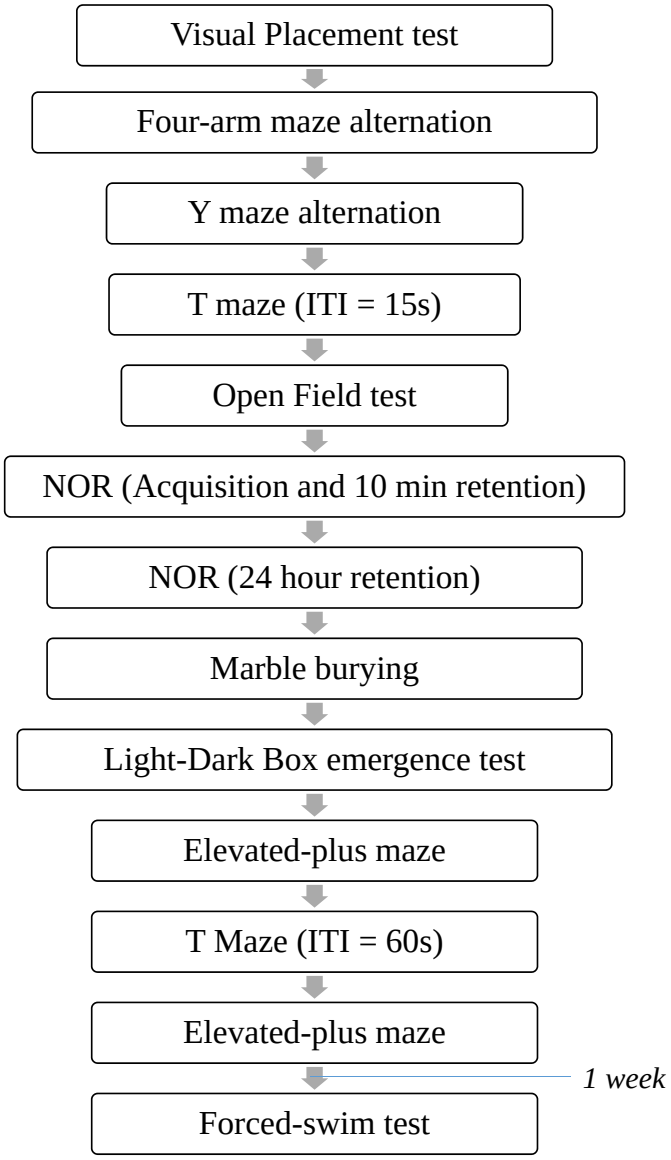

Figure 12: Battery of behavioral tests done on WT and Δ*PKC* mice. Every mouse was subjected to the battery of behavioral experiments that included tests for general activity, spatial memory, visual recognition memory, repetitive and perseverative behaviors, anxiety and depression-related behaviors. All the tests were performed sequentially everyday between 9 AM to 12 PM with one exception. After completion of the elevated plus maze test, the mouse was subjected to the forced swim test only after a week.

TABLE III: Behavioral Phenotyping Assays

Behavior	Ethological parameter(s)
General activity	Arm entries in four-arm and Y maze Line crossings in open field
Spatial working memory	Spontaneous alternation in four-arm and Y maze Non-reinforced Forced and free alternation in T maze
Recognition memory	Discrimination index in the novel object recognition test
Perseverative, repetitive behavior	Marbles buried and displaced in the Marble burying test
Anxiety	Time spent in the central area in an open field Time spent in lit compartment of LDB Time spent and entries in open arms in EPM
Depression	Immobility and latency to swim in FST

shape where each animal was allowed free access to explore the maze for 10 minutes and the arm entries were recorded by the experimenter. An arm entry was considered to be valid only when all four limbs are inside an arm. A set of unique entries into each of the four arms during a four-choice sequence in a four-arm maze or unique set of entries in a three-choice sequence in a Y maze was termed as an alternation. The spontaneous alternation rate was calculated as the ratio of actual alternations to maximum possible alternations. The probability that the mouse performed the alternation task by chance is 9.4% (for a four-arm maze), and is 22.2% (for a Y maze) (Lennartz, 2008). The number of arm entries made by WT and Δ*PKC* mice while exploring the maze in 10 minutes was used to assay their activity levels. In a four-arm

maze, apart from determining the percentage of spontaneous alternation and total exploration time, total number of crossovers and crossovers during a spontaneous alternation were also counted. A crossover in a four-arm maze was defined as a set of entries made by the mouse when it entered an arm across from the arm it previously visited. For total crossovers, arm entries such as AC,CA,BD or DB over the entire 10 minutes were counted. A sequence of arm entries such ACBD, BDAC, CADB or DBAC was counted as a crossover during alternation.

3.2.2.2 Non-reinforced delayed alternation

In a non-reinforced T maze delayed alternation task, the mouse was placed at the stem of the T-shaped maze which acts as the start arm. The stem of the T maze was 69 cm, and the walls were 7.5 cm. The left and the right arms were 30.5 cm long. The entire test consisted of one free choice trial and 14 free choice trials with a inter trial interval (ITI) of either 10 seconds or 60 seconds per animal. During the forced-choice trial, the mouse was forced to turn left or right by blocking off the other arm, while during the free-trial the mouse was allowed to make its choice. However, after the mouse has entered an arm during a free-choice trial the other arm was blocked off using sliding doors. The choice made by the mouse (left/ right) and the time taken to explore the arm were recorded in a data-sheet during the experiment. After exploration of one arm, the mouse was returned to the start arm and was confined for about 10 seconds in the holding area before it was allowed another free choice. Performance was measured as the percentage of alternations between the two arms (Deacon and Rawlins, 2006). Another set of experiments were performed using an ITI of 60 seconds, and the alternation rates were measured.

3.2.3 Recognition memory - Novel object recognition

Individual mice were habituated to the testing box (made of clear plexiglass material) for two consecutive days prior to testing by placing them in the box for 10 minutes. On the testing day, each mouse was placed in the cage containing two identical objects and allowed to explore for 10 minutes (training phase). One of the objects was replaced with a novel (new) object and the animal was allowed to explore for 5 minutes (testing phase). The identical objects were two plastic beakers with a red tape stuck around the surface, and the novel object was a two nalgene bottle caps with serrated edges taped together. The two objects were similar size, but were different in texture, shape and color. The time between the object switch was 10 minutes for assessing short-term memory and 24 hours for long-term memory. The entire session was recorded with a Canon PowerShot ELPH 300 HS camera mounted onto a clamp, and the magnification was adjusted so that the entire testing area was visible. The time spent by the animal interacting with the object such as sniffing, touching with paws and any activity done facing the object within 2-3 cms was analyzed from the video file. The premise of the experiment was based on the fact that mice being exploratory animals tend spend increased time with a novel object than a familiar object (Broadbent et al., 2010). Thus, the novel object discrimination index was calculated as the ratio or percentage of time spent interacting with the novel object to total time spent interacting with both the familiar and novel object.

3.2.4 Repetitive behaviors - Marble burying

The experiment was performed in a rectangular rat cages measuring 48 cm X 26 cm X 20 cm with approximately 1.5 inches of bedding material. Twenty clear marbles (diameter of 19 mm)

were placed over the bedding in a 4 x 5 pattern, equidistant from each other. A mouse was placed in the cage and allowed to explore the area for 10 minutes. After 10 minutes, the number of marbles displaced and buried were counted. Using a camera, a picture was taken before the mouse was placed in the cage, and after it was allowed to explore. The images were used to determine the number of displaced marbles. The marbles were considered to buried if they were more than a centimeter below the bedding.

3.2.5 Anxiety and depression-related behaviors

3.2.5.1 Open-field exploration

The open-field (OF) test apparatus was constructed of a rectangular, clear plexiglass material (72.5 cm X 72.5 cm X 30.5 cm) comprising of four walls and an open roof for recording the overall activity. Individual mice were allowed to roam for 5 minutes in the chamber with lighting provided by overhead fluorescent fixtures (32 W per bulb, two bulbs right above the apparatus). This experiment was based on the fact that mice exhibit thigmotaxis (which is defined as the inclination of a mouse to explore the area closer to the walls of an open field). Increased dwell time in the center of the field along with an increased number of entries towards the center were behaviors that indicated reduced levels of anxiety and higher exploration (Prut and Belzung, 2003). The entire session was recorded with a Canon PowerShot ELPH 300 HS camera mounted onto a pole stand with a clamp, and analyzed at a later time.

3.2.5.2 Light-dark box emergence

The light dark box (LDB) tested the behavioral response of rodents to brightly lit areas and exploratory behavior in response to stressors such high intensity light and novel environ-

ment (Bourin and Hascoët, 2003). The experimental setup consisted of a large box (75 cm X 50 cm X 30 cm), which was separated into two compartments - a relatively darker area that makes up a third of the box area and the remaining was illuminated to produce a brighter lit area. A 60 W bulb was placed directly on the lit compartment from the top. The wall between the two compartments had a small opening (7 cm X 7 cm) that allowed mice to freely move between lit and dark areas. A session lasted for 10 minutes and it was recorded with a digital camera clamped on top of the lamp to detect the activity of mice going from one compartment to the other.

3.2.5.3 Elevated plus maze exploration

The elevated plus maze (EPM) is made of two open arms (arms without any walls) and two closed arms (which have 15 cm walls on both sides). The arms measured 30 cm X 5 cm, and the entire maze was elevated from the ground by 40 centimeters. Each mouse was placed in the center of the maze and both the arm entries and duration were recorded by an observer blind to the genotype of the animal. Anxiety levels were measured based the number or entries, and dwell times in the open arms during 5 minutes (Walf and Frye, 2007).

3.2.5.4 Forced swim test

The forced swim test was used to assess depression-like behavior in mice. A clear plexiglass cylinder (15 cm diameter, 24 cm height) was filled with distilled water at 30 °C to a depth of 10 cm. The mouse was gently placed in cylinder and the behavior of the mouse was recorded for 6 minutes. After 2 minutes, during the swim test various behaviors such as swimming, climbing, and immobility were scored. Reduction in immobility without increase in general

locomotor activity was interpreted as anti-depression like behavior. Apart from immobility during the last 4 minutes of swim test, the latency to immobility from the start of the test period was also determined.

3.2.6 Impulsive behaviors - nose-poke training

Both the WT and ΔPKC mice were weighed for three consecutive days to determine their average weight and weighed every day until they reached their target weight which was 80% of their individual weights. They were provided with food pellets *ad libitum* while they were deprived of water and provided with 1 ml distilled water until they reached the target weight. After all the animals reached their target weight, they were trained in an enclosed testing chamber made of black acrylic that consisted of an alley measuring 60 cm X 10 cm as described previously (Larson and Sieprawska, 2002; Larson et al., 2008). The vertical end walls at each of smaller side had two sniff-ports (inner diameter = 1.5 cm) for nose poke responses and one small cup in the floor for water delivery. The water delivery was controlled by electrically-driven solenoid valves (General Valve Co., Fairfield, NJ), based on nose-pokes that were detected using infrared photo-beam breaks. Prior to training them to distinguish between four random pairs of odors, a shaping procedure was used at the end of which the mice were familiarized to the apparatus and also to reinforce nose-poke responses in either sniff-port. The nose-poke training consisted of two 20-trial sessions per day, in which the mice were reinforced with a drop of water (12.5 µl) for a nose poke in either sniff port at one end of the alley. A single trial lasted 120 s with an ITI of 10 s for correct response (nose-poke) or an ITI of 30 s for an incorrect response (no nose-poke). The lamps at both the ends of the alley were lit dur-

ing the ITI and was extinguished over the end at which the mice were reinforced with water. Each mouse was trained until it has made 90% reinforced response consecutively over three days. On the third day when they all reached the criteria, the latency to nose-poke for water was determined. Shorter latency to nose-poke may indicate impulsivity.

3.2.7 Behavioral induction of Fos expression

Fos levels in the hippocampus were measured after the mouse was exposed to three different novel environments: a new cage in a different room, open field made of plexiglass floor and walls measuring 72.5 X 72.5 X 30.5 cm, and an elevated plus maze [Figure 13]. The mouse

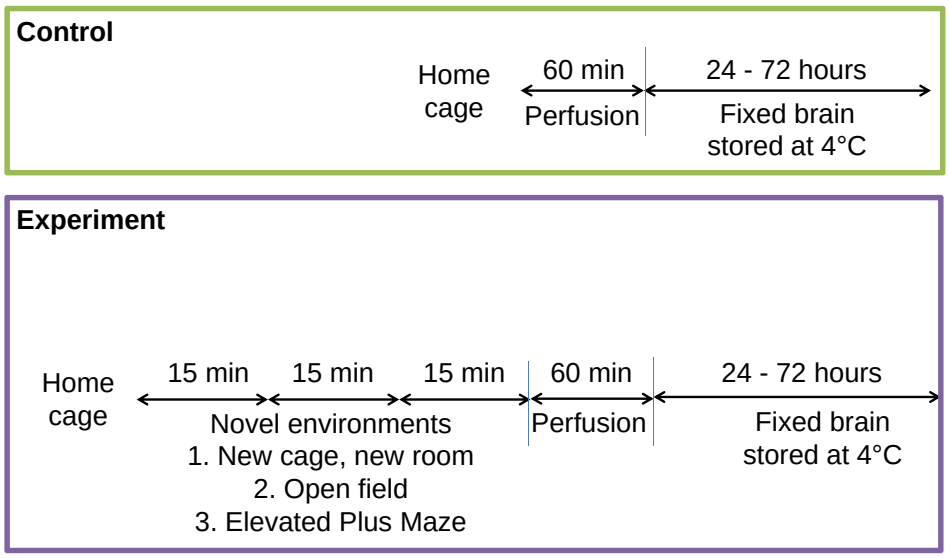

Figure 13: Timeline for behavioral induction of Fos in the mouse hippocampus. A diagram showing the timeline for control and experimental animals perfusion. Mice from their home-cage were the controls, and mice exposed to novel environments were experimental animals.

was placed in each environment and allowed to explore it for 15 minutes and subsequently moved to another (Wirtshafter, 2005). After approximately 60 minutes, the mouse was anesthetized using a a mixture of 100 mg/kg of Ketamine and 16 mg/kg of Xylazine. To obtain basal Fos levels, control animals were perfused immediately after anesthesia. After the animals attained a deep level of anesthesia, they were transcardially perfused rapidly with phosphate buffered saline (PBS), followed by a fixative containing 4% formaldehyde. Brains were postfixed for one hour at 4 °C in the high pH fixative solution (pH 9.5) and then transferred to 20% sucrose in PBS until slicing. Serial 35 µm slices were prepared from frozen slices and were stored in a cryopreservative until they were processed for Fos immunoreactivity (Wirtshafter and Sheppard, 2003). The slices were washed thrice in PBS, and incubated in Anti c-Fos (Ab-5) (4-17) Rabbit primary antibody (Millipore) in PBS with 2% normal goat serum. After 48 hours incubation, the slices were rinsed again in PBS, and incubated in biotinylated anti-rabbit IgG for 2 hours and then rinsed in PBS. c-Fos immunoreactivity was obtained after the tissue was processed using Vectastain Elite ABC Kit (Vector Labs). The tissues were then rinsed and stained using diaminobenzidine with nickel to obtain a contrasting image. After a final rinse, the slices were mounted in subbed slides and cover-slips were placed on them. Small round objects 5-10 35 µm that were darkly stained compared to the background were counted as Fos immunogenic sites. Fos immunoreactivity was counted as Fos(+) cells per 100 35 µm of the hippocampal regions since the dentate gyrus, CA3, and CA1 are all relatively linear structures.

3.3 Results

3.3.1 General activity levels of Δ*PKC* mice.

Parameters from four different behavioral experiments (four-arm maze, Y maze, and open field) were used to determine the general activity levels of the mutant mice, to ensure that motor deficits do not influence the various parameters measured during all the behavioral tests. First, in a four-arm maze and Y maze the total arm entries made by the mouse were measured for 10 minutes. In both the mazes, the total number of arm entries made by WT and mutant mice was not significantly different [Figure 14a, and Figure 14b]. Next, the number of line crosses made by the mouse during the entire test duration of 5 minutes in an open field was measured as an indicator of general locomotor activity, and the total line crosses made by both the groups of mice were similar [Figure 14c]. Thus, all the three general activity parameters (arm entries in four-arm maze, arm entries in Y maze, line crosses in an open field, and transitions in a light dark box) measured during various tests indicated that there was no change in the activity levels of the mutants when compared with their WT controls.

3.3.2 Spatial working memory of Δ*PKC* mice

3.3.2.1 Spontaneous alternation in a four-arm and Y maze

Spontaneous alternation in radial mazes have been used to test spatial working memory in mice as it is a less stressful than the Morris water-maze (Sarnyai et al., 2000; Hughes, 2004; Dudchenko, 2004). Alternation in a maze is defined as the tendency to choose and explore an arm that was not recently explored, and the alternation is considered to be spontaneous if it occurs without any reinforcement (such as food reward or training). The alternation rate was

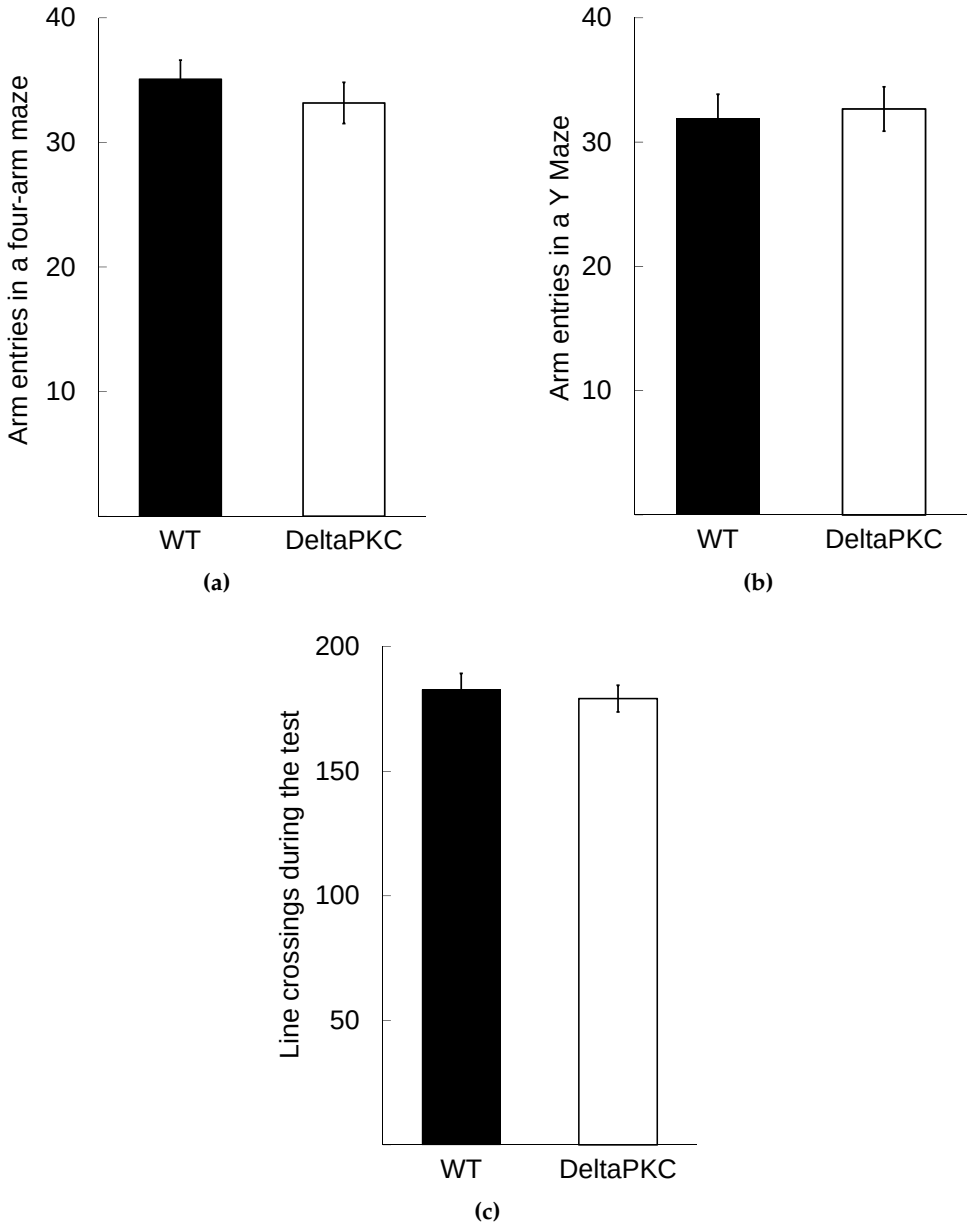

Figure 14: Similar activity levels of Δ*PKC* and WT mice in four-arm maze, Y maze, Open field and Light-dark box. General activity levels of the WT and Δ*PKC* mice in (a) four-arm maze (n = 30 in each group) and (b) Y maze (n = 12 in each group), measured as total number of arm entries made by the mice were similar (Four-arm maze: ($F_{1,58}$=0.71,p=.40), Y maze: ($F_{1,22}$=0.09,p=.76)). (c) Line crossings during the test duration in an open field was not different ($F_{1,44}$=0.17,p=.68). All data are mean ± S.E.M.

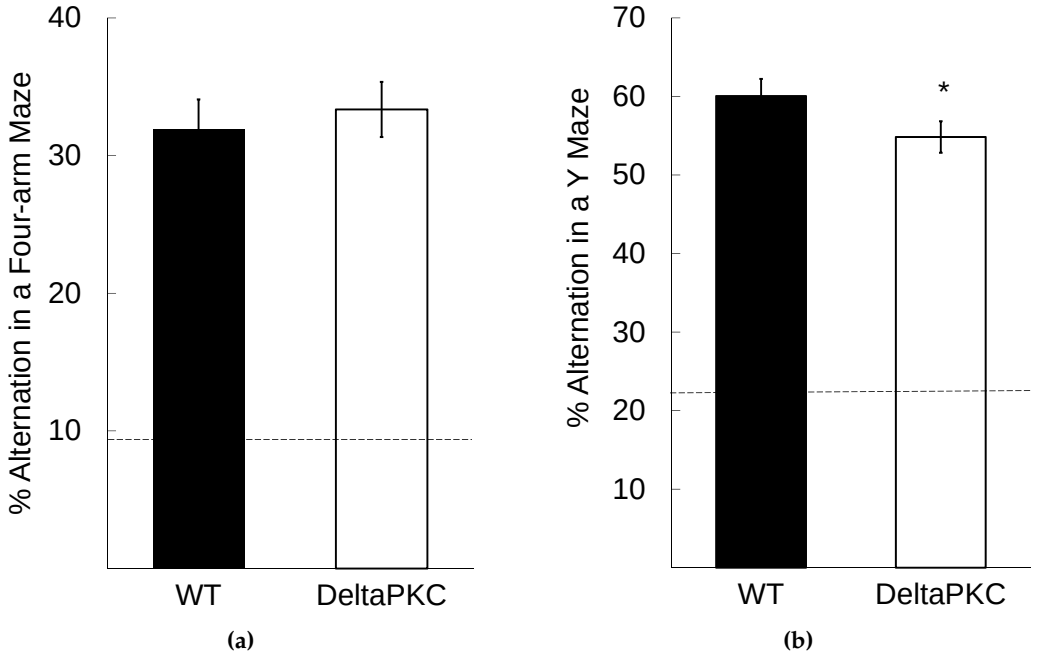

Figure 15: Decreased spontaneous alternation of Δ*PKC* mice in Y maze but not in four-arm maze. Spontaneous alternation rate of both the WT and Δ*PKC* mice in the (a) four-arm maze (n = 30 per group) and (b) Y maze (n = 12 in each group). There was no difference in the spontaneous alternation levels of the two groups of mice in four-arm maze during the test duration of 10 minutes ($F_{1,58}$=0.26,p=0.66). However, Δ*PKC* mice alternated at lower levels than the WT mice in a Y maze ($F_{1,22}$=4.94,p=0.04). All data are mean ± S.E.M. *$p < .05$

the total alternations made by the mouse during the test expressed as percentage of maximum possible alternations. In a four-arm and Y maze, the mice were allowed to explore for 10 minutes and their arm entries were recorded during the test. While the mutant mice alternated at levels similar to WT mice in a four-arm maze, they showed significantly lower alternation levels than WT mice in a Y maze as shown in Figure 15.

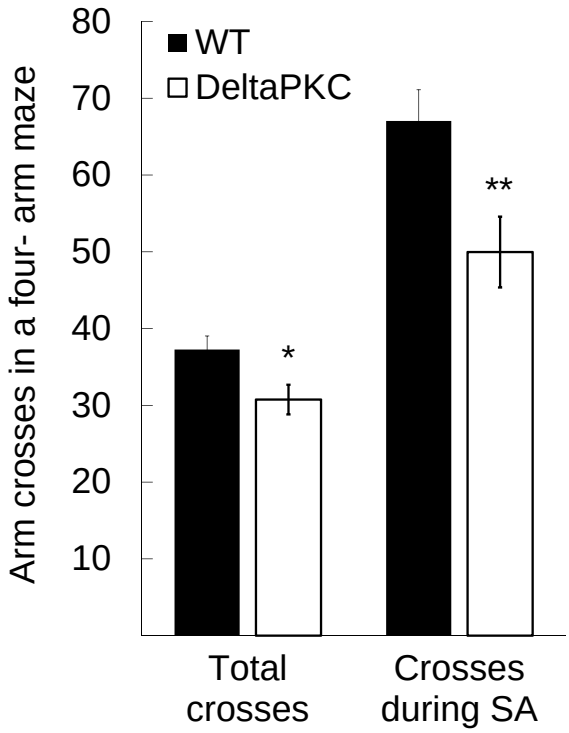

Figure 16: Reduced crossovers exhibited by ΔPKC mice in a four-arm maze during the 10 minutes alternation task. ΔPKC mice (n = 30) had a significantly lesser number of crossovers during a spontaneous alternation ($F_{1,58}$=7.65,p <.01) compared to the WT controls (n = 30), and also during the entire test duration ($F_{1,58}$=6.33,p <.05) in the four-arm maze. A crossover was defined as any arm entry made into an arm that was located right across it such as A to C or B to D and vice versa. A sequence of entries such as ACBD, DBCA was defined as a crossovers during an alternation. All data are mean ± S.E.M. **p <.01, *p <.05.

3.3.2.2 Delayed alternation in non reinforced T maze task

Although spontaneous alternation in a four-arm and Y maze was considered to be a task dependent on spatial working memory of the animal, a number of studies have questioned the use of such radial mazes (Dudchenko, 2004). However, both the versions of these mazes when used for continuous spontaneous alternation tasks, are useful to measure locomotor activity. A modified T maze consisting of one forced trial followed by 14 free-choice trials was used to determine spatial working memory in mutant mice. In this modified T maze task, ΔPKC had lower number of alternations than WT mice with similar levels of exploratory activity [Figure 17a anf Figure 17b]. This indicated that the mutant mice could have a mild spatial memory deficit. An inter-trial interval (ITI) of 15 seconds was used for the first set of experiments. It was observed that by increasing the ITI to 60 seconds, the performance of the both the groups of mice increased. This could be interpreted as a reduction in impulsive behaviors.

To determine if there was any difference in performance levels of the two groups of mice over successive trials, the number of animals that alternated correctly based on the the previous arm entry was plotted as a function of the trial number. It showed that the number of mutant mice that alternated correctly was always lower than the number of WT mice until 11th trial for 15 s ITI, and until the 10th trial for 60 s ITI [Figure 18]. The performance of the mutants were similar to the WT mice after the 11th and 10th trial for the T maze alternation task with ITI of 15 s and 60 s, respectively.

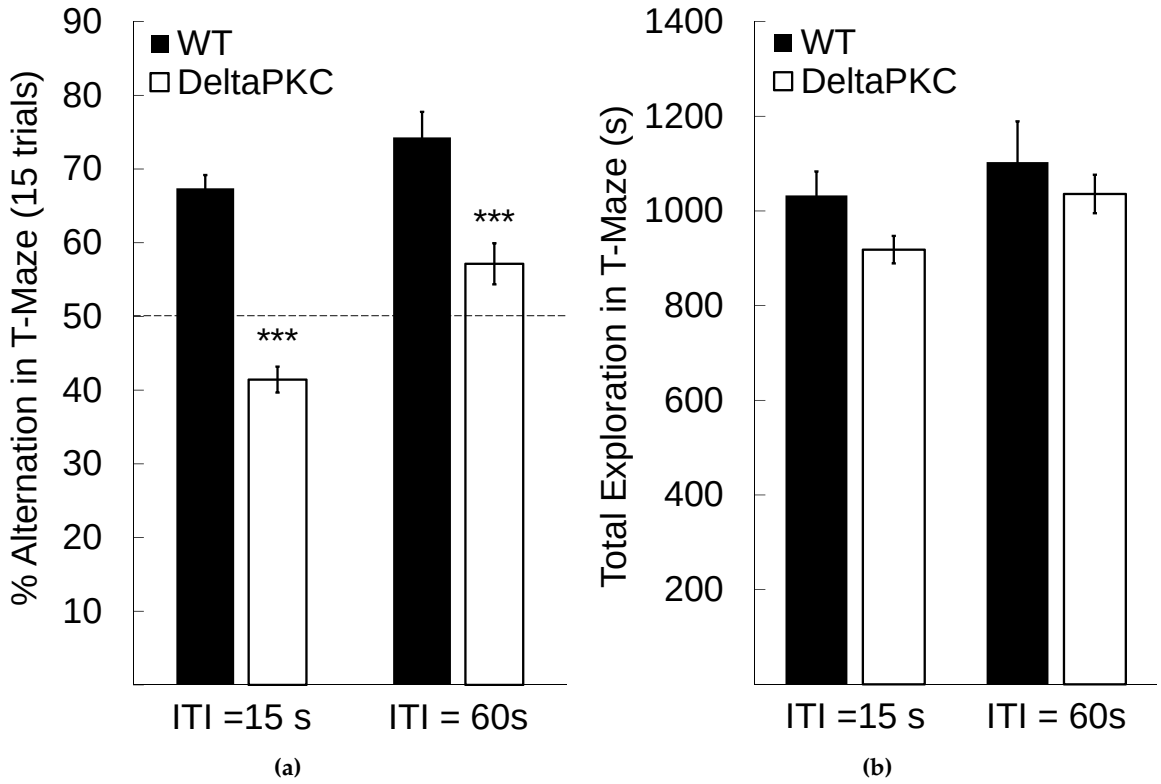

Figure 17: Decreased alternation of Δ*PKC* mice in a non-reinforced T Maze alternation task consisting of one forced choice trial followed by 14 free choice trials. (a) Mean alternation rate of Δ*PKC* mice was significantly lower than WT mice in the T maze alternation task. The alternation task involved one forced choice trial followed by 14 free choice trials with an ITI of either 15s (n = 30 in each group) or 60s (n = 15 per group). Irrespective of the inter-trial interval during the task, Δ*PKC* mice alternated at significantly lower levels than the WT mice (ITI=15s: $F_{1,58}$=104,p <.001, ITI=60s:$F_{1,28}$=14.98, p <.001). (b) The total time spent by both the groups of mice in exploring the arms was similar during both the alternation tasks with varying ITIs (ITI=15s:$F_{1,58}$=3.84,p=.52, ITI=60s:$F_{1,28}$=0.5,p=.49). All data are mean ± S.E.M. ***p <0.001.

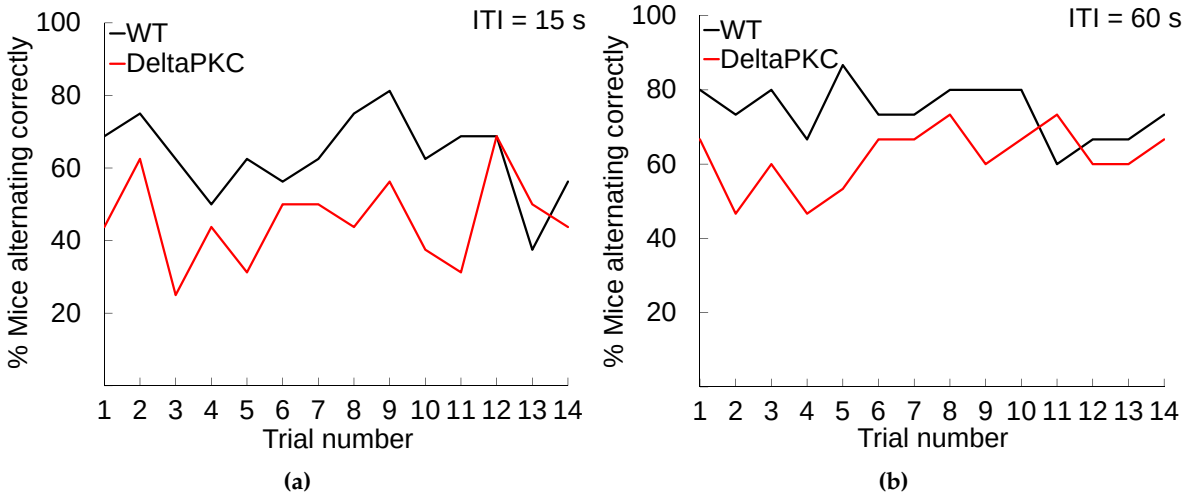

Figure 18: Performance of Δ*PKC* and WT mice in every trial of the T Maze alternation task based on the percentage of mice that alternated correctly in each trial. Percentage of WT and Δ*PKC* mice that alternated correctly in every trial was plotted for every trial in the delayed T maze alternation task with an ITI of (a) 15 s and (b) 60 s. Each data point represents the percentage of either WT or Δ*PKC* that made the correct choice in each trial.

3.3.3 Recognition memory

3.3.3.1 Novel object recognition

The novel object recognition test was used to assess the short-term recognition memory of mice by exposing the WT and Δ*PKC* to set of familiar object and a novel object (Broadbent et al., 2010; Oliveira et al., 2010). Similar recognition indices between the WT and mutant mice on exposure to the novel object in 10 minutes, and 24 hours later indicated that the Δ*PKC* mice had an intact short-term and long-term recognition memory [Figure 19].

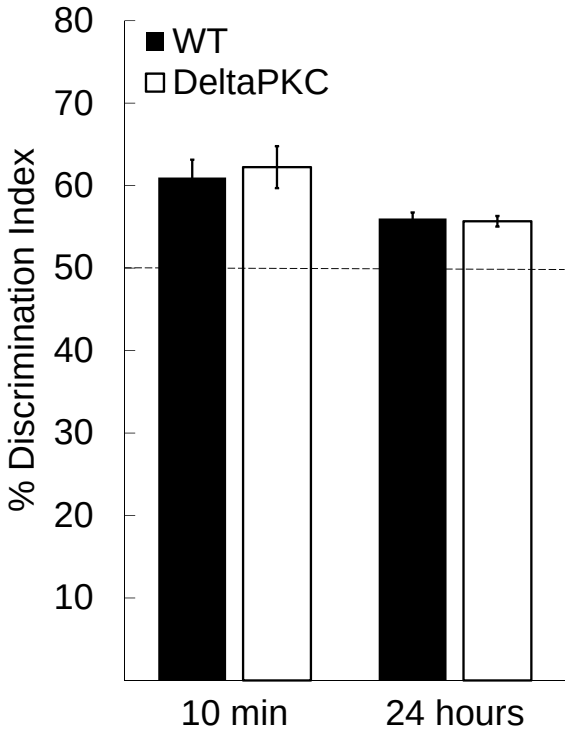

Figure 19: Normal recognition memory in Δ*PKC* mice in a novel object recognition test. Δ*PKC* mice had similar recognition index compared to the WT controls when exposed to the novel object 10 minutes and 24 hours after they were familiarized with an identical set of objects. (NOR-10min:($F_{1,26}$=0.129,p=.72);NOR-24h:($F_{1,26}$=0.095,p=.76)). n = 14 in each group. All data are mean ± S.E.M.

3.3.4 Perseverative behavior

3.3.4.1 Marble burying

Mouse marble burying was considered to be a repetitive behavior that persists even after multiple exposures to the environment containing the marbles (Thomas et al., 2009). Alternation below chance levels in a non-reinforced T Maze (ITI of 30s), and reduced crossovers in a four-arm maze by the Δ*PKC* mouse indicated that they may have alternated at WT levels in the four-arm maze by having a side preference (Deacon and Rawlins, 2006). To determine if they have any repetitive/perseverative behaviors, the marble burying test was performed, and it was found that both the number of marbles displaced and buried were similar between the WT and Δ*PKC* mice indicating that the Δ*PKC* may not have any repetitive behaviors [Figure 20].

3.3.5 Anxiety and depression-related behaviors

When the WT and mutant mice were subjected to various anxiety tasks, the mutants exhibited reduced anxiety-related behaviors including increased time spent in the center of an open field [Figure 21a] and increased time in light side of light/dark box [Figure 21b]. The number of transition the mouse made between the lit and dark compartment through a small door was correlated to exploratory activity (Bourin and Hascoët, 2003). Both the groups of mice had similar number of transitions between the two compartments indicating similar levels of exploratory activity due to habituation to the new environment over time [Figure 21c]. In an elevated plus maze, the mutants had increased dwell times in the open arms of an elevated plus maze [Figure 22a]. The mutant mice also had increased number of open arm

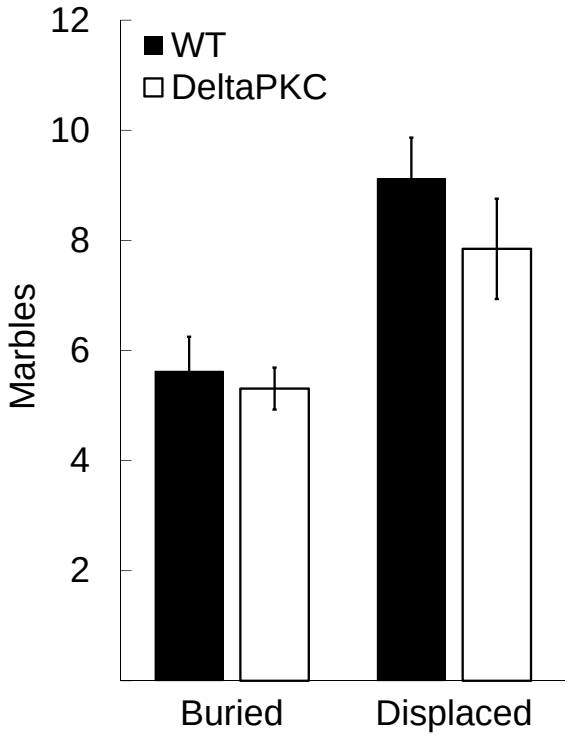

Figure 20: ΔPKC do not exhibit any repetitive/ perseverative behaviors in the marble burying test. After 10 minutes exploration of the area containing 20 marbles, the number of marbles displaced and buried were similar between the WT and Δ*PKC* mice. (Buried marbles:($F_{1,19}$=0.16,p=.67); Displaced marbles:($F_{1,19}$=1.23,p=.75)). All data are mean ± S.E.M.

entries with no change in total arm entries compared to WT mice during the test [Figure 22b and Figure 22c]. The mutant mice also display increased head dips from open arms but not from protected areas such as closed arms and center of the elevated plus maze [Figure 23a and Figure 23b]. Also, the WT and mutants have similar number of stretch attenuated postures while exploring the open arm [Figure 23c]. However, those mutant mice did not display any depression-like behavior in the forced swim test. The total time spent immobile in the last 4 minutes during the forced swim test was not significantly different between the two groups of mice, and they also had similar latency to immobility during the test [Figure 24a and Figure 24b]. Active behaviors such as swimming and climbing (measured as number of episodes) were also not significantly different between the WT and Δ*PKC* mice [Figure 24c].

3.3.6 Impulsivity test

Most of the mice strains show reduced anxiety also tend to be impulsive (Loos et al., 2009). The Δ*PKC* mice also have reduced performance when subjected to a T maze non-reinforced alternation paradigm irrespective of ITI, which may indicate impulsivity. Increased locomotor activity in an open field and elevated plus maze, and increased time spent interacting with a novel-object may be considered to be indicators of impulsive behaviors. However, there was no such behaviors observed when the mutants were tested using those behavioral paradigms. When both the groups of mice were trained to nose-poke for olfactory discrimination test, the latency to nose-poke for water-reward during the session when all the animals reached the criterion was determined. It was found that both the WT and Δ*PKC* mice had similar latency to nose-poke for water reward [Figure 25].

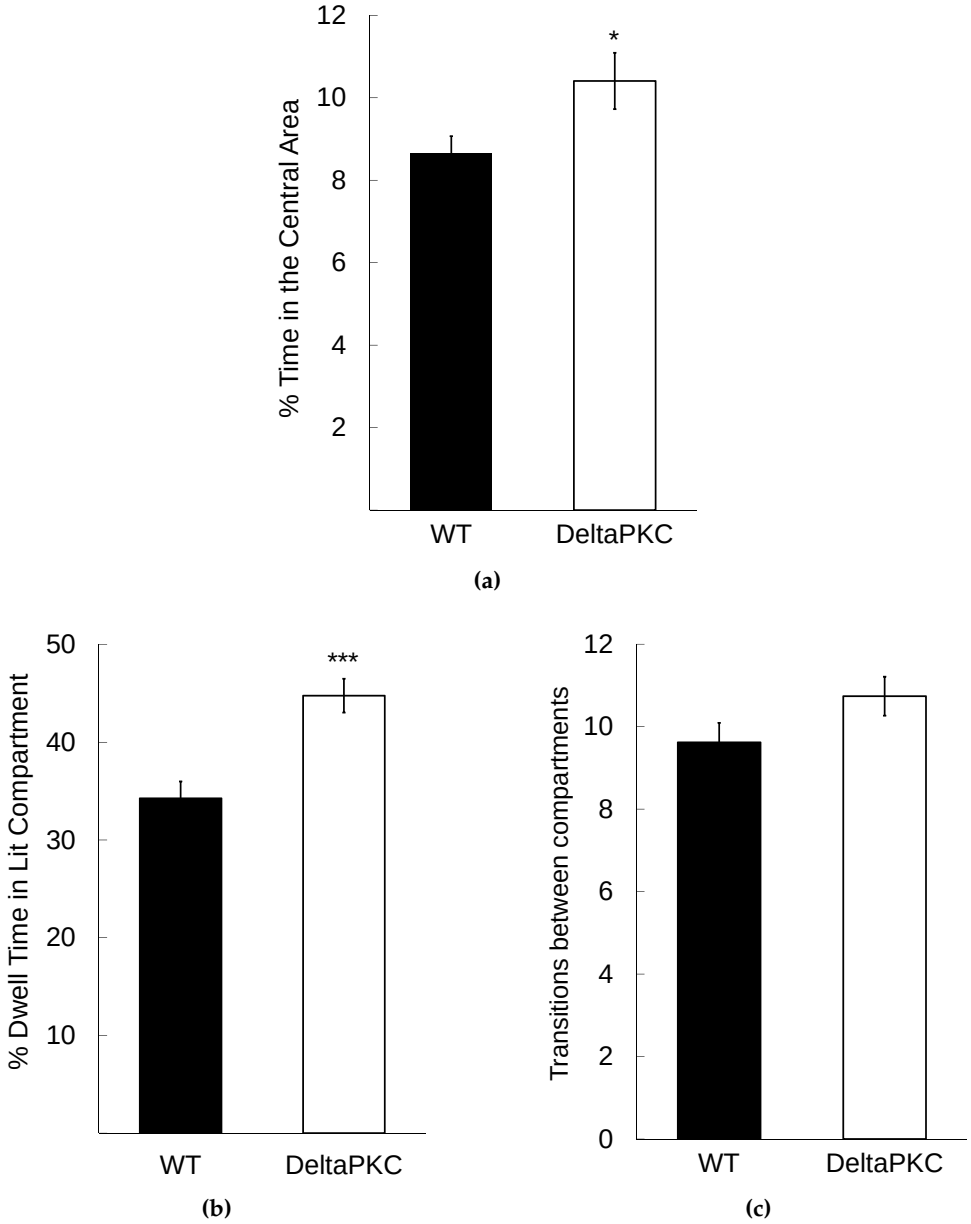

Figure 21: Reduced anxiety-like behaviors exhibited by ΔPKC mice in an Open field and Light-dark box (a) Time spent by ΔPKC mice in the center of an open field was increased ($F_{1,44}$=11.56,p=.03,n = 23 per group). (b) ΔPKC mice spent significantly more time in the lit compartment of the light-dark box than their WT controls ($F_{1,42}$=15.18,p <.001, n = 23 WT and 21 ΔPKC mice). (c) Both the groups of mice have similar levels of exploratory activity as indicated by their total transitions between the two compartments ($F_{1,42}$=2.22,p=.14) . ***p <.001,*p <.05.

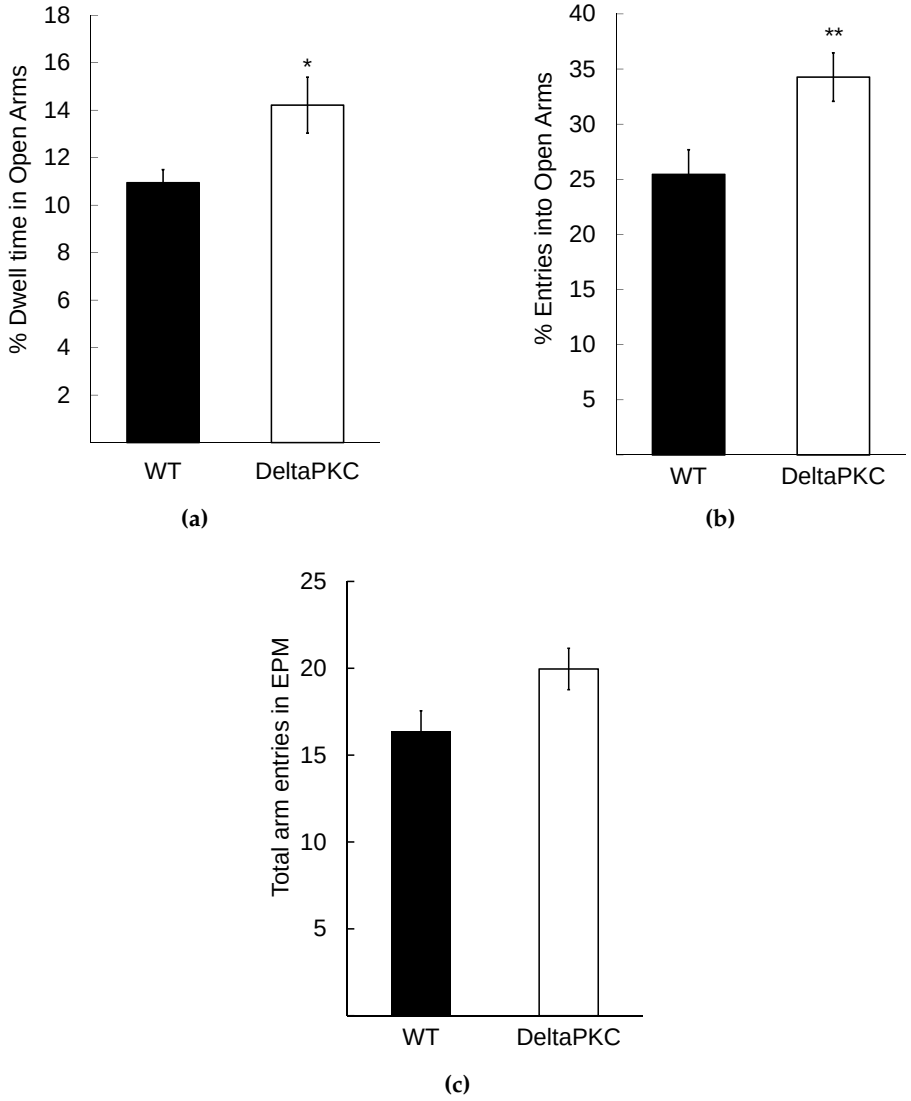

Figure 22: Reduced anxiety-like behaviors exhibited by Δ*PKC* mice in an elevated plus maze (a) Δ*PKC* mice show increased dwell times in the open arms of an elevated plus maze ($F_{1,48}$=10.96,p <.01). (b) Δ*PKC* mice show increased entries into open arms ($F_{1,48}$=6.32,p=.02). (c) The total arm entries made by the Δ*PKC* mice was not different from the WT mice ($F_{1,48}$=3.53,p=.07, n = 25 per group).**p <.01,*p <.05.

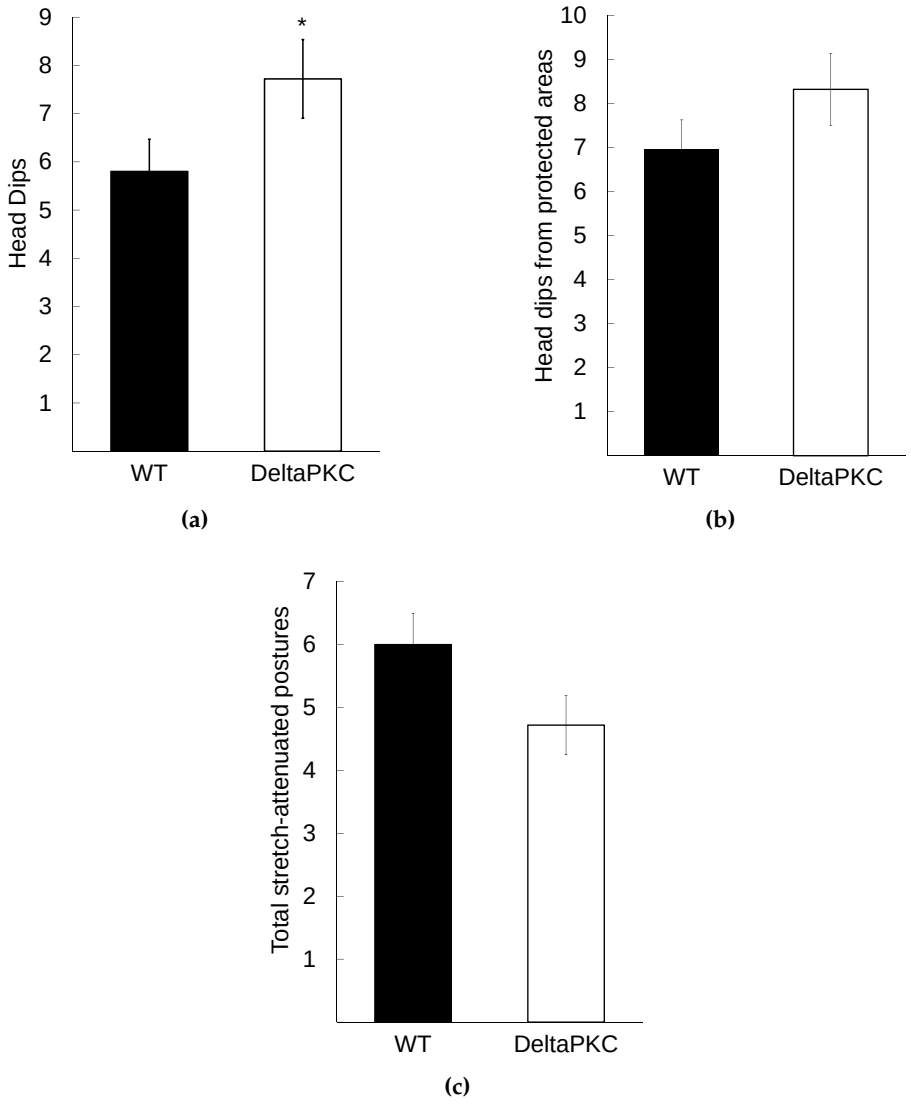

Figure 23: Risk assessment behaviors exhibited by ΔPKC mice in an elevated plus maze. (a) The ΔPKC mice have increased number of head dips after they entered the open arms ($F_{1,48}$=5.31,p <.05). (b) WT and ΔPKC mice show similar number of head dips from protected areas ($F_{1,48}$=2.08,p =0.07). (c) Both the groups of mice also exhibit similar number of stretch attenuated postures while exploring open arms ($F_{1,48}$=2.05,p =0.16). n=25 in each group, *p <.05.

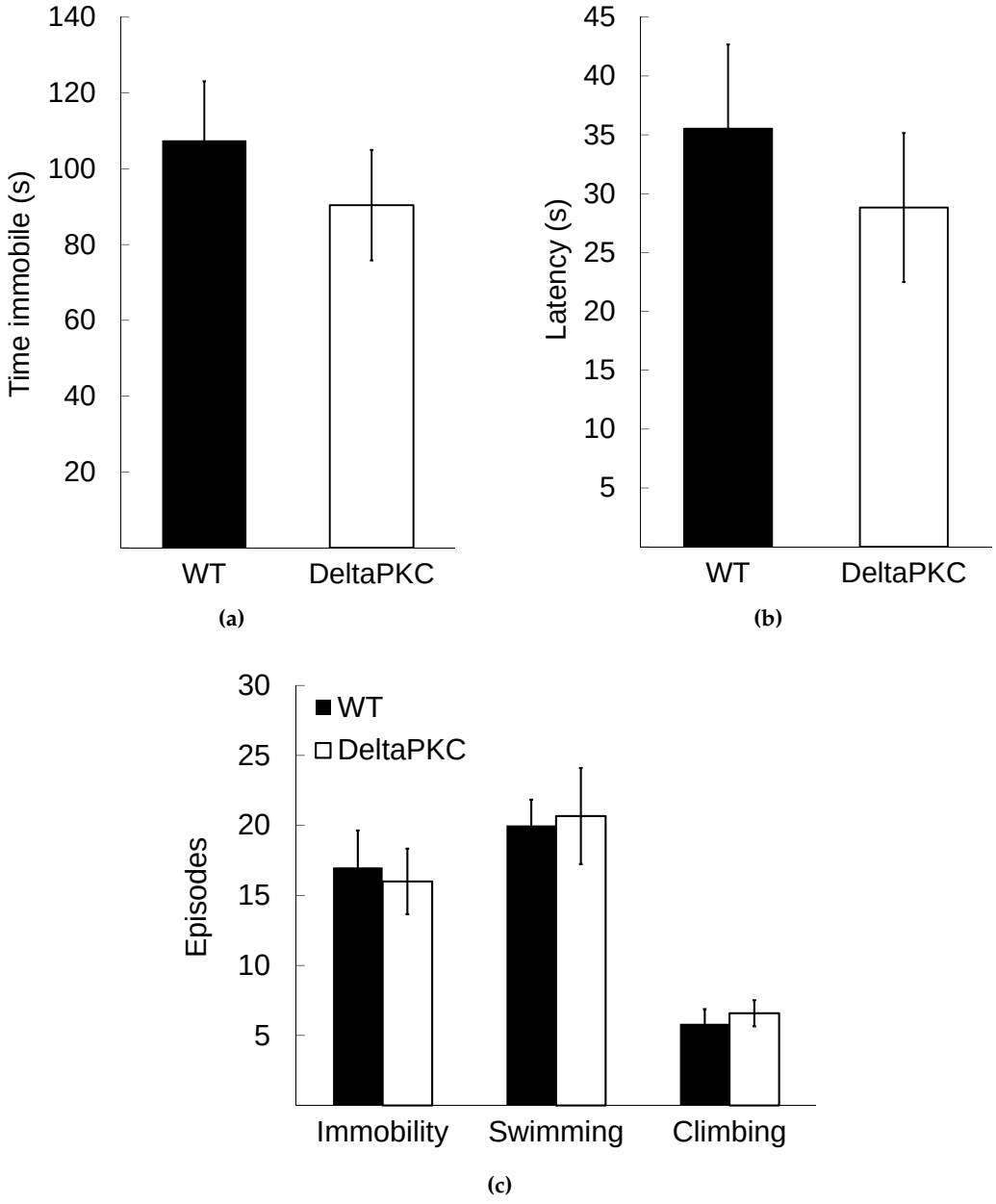

Figure 24: Δ*PKC* mice did not show any any changes in behavioral despair response in the forced swimming test. (a) Total immobility score in the last 4 minutes of forced swim test of Δ*PKC* and WT mice did not differ significantly ($F_{1,22}$=0.63,p=0.43). (b) Latency to the first episode of immobility did not vary between two groups of mice ($F_{1,22}$=0.49,p=0.69). (c) Total number of immobile, swim, and climb episodes in the last 4 min of the test did not differ between the two groups of mice (Immobility:$F_{1,22}$=0.08,p=0.78; Swimming:$F_{1,22}$=0.03,p=0.87; Climbing:$F_{1,22}$=0.33,p=0.6). All data are mean ± S.E.M. n = 12 per group.

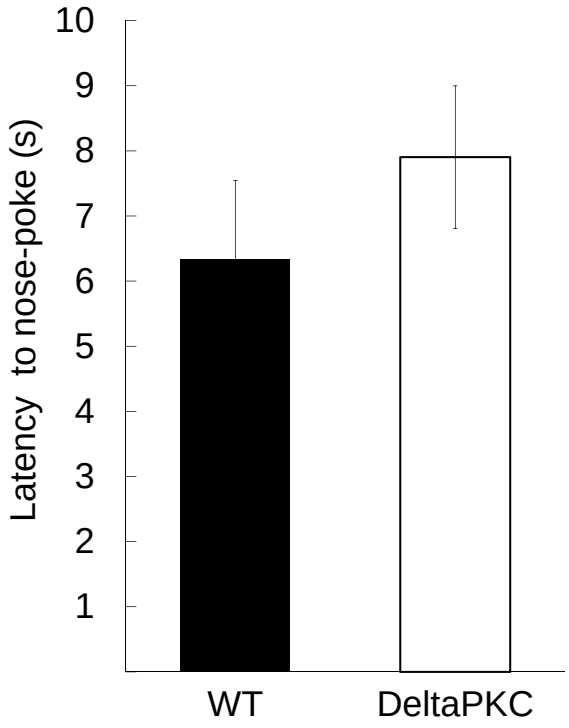

Figure 25: Δ*PKC* do not exhibit any impulsivity to nose-poke for water reward. During the initial training phase for olfactory discrimination tests both the groups of water-deprived mice were trained to poke their noses through a sniff-port for obtaining water reward. The latency to nose-poke in the last session when they all reached criteria were similar between the WT and Δ*PKC* mice ($F_{1,12}$=1.92,p=.19; WT:n=6, Δ*PKC*:n=8). All data are mean ± S.E.M.

3.3.7 Fos expression in hippocampus after novelty exposure

c-Fos (*Fos*) an immediate early gene, has been used in a number of studies as a neuronal activation marker. Placement of a rat in a novel environment has been shown to elicit robust *Fos* expression in hippocampus, and Fos protein levels in mice peak at about an hour after the placement (Wirtshafter, 2005; Montag-Salaz et al., 1998). Δ*PKC* mice display reduced anxiety levels and have decreased Y/T maze alternation rate compared to their littermate controls. To detect if this behavioral phenotype correlates with Fos levels in WT and Δ*PKC* mice hippocampus, the two groups of mice were exposed to three different novel environments for 15 minutes each. When the mouse was placed in each of the novel environments, various behavioral parameters such as total line crossings and time spent in center of the open field, number of closed, open arm entries and time spent in open arms in an EPM, and grooming bouts and time spent grooming in a new cage were measured. It was determined that the mutant mice exhibited significantly reduced anxiety-related behaviors in the EPM and open field compared to WT controls [Table IV]. All the behavioral experiments were analyzed as mentioned in methods section of this chapter. Exposure to the three novel environments for 15 minutes each also elicited a robust Fos expression in the Dentate Gyrus (DG), CA3 and CA1 regions of WT mouse hippocampus. However, in mutant mouse hippocampus only the DG showed an increase in Fos expression upon placement in the three novel environments, while no change was observed in CA1 or CA3 [Figure 26]. Interestingly, the magnitude of Fos increase in the DG of mutants was still significantly lower than the magnitude of Fos increase in DG of WT mice. Also a one-way ANOVA comparing the control Fos levels of WT and Δ*PKC*, indicate that

TABLE IV: Behavioral parameters measured during novelty-induced Fos induction experiments

Parameter	WT	Mutant	p value for F-statistic
OF - line crosses	166.8	173.6	0.70
OF - % center time	8.0	11.0	0.05
EPM - total arm entries	20.3	22.6	0.60
EPM - % open arm entries	26.0	40.1	0.04
EPM - % open arm time	11.9	14.9	0.03
EPM - Stretch attenuated postures	5.5	6.5	0.45
EPM - Head dips (open)	5.7	8.5	0.02
EPM - Head dips (protected)	7.8	7.9	0.97
New cage - grooming duration (s)	26.4	25.0	0.78
New cage - grooming bouts	8.0	7.6	0.87

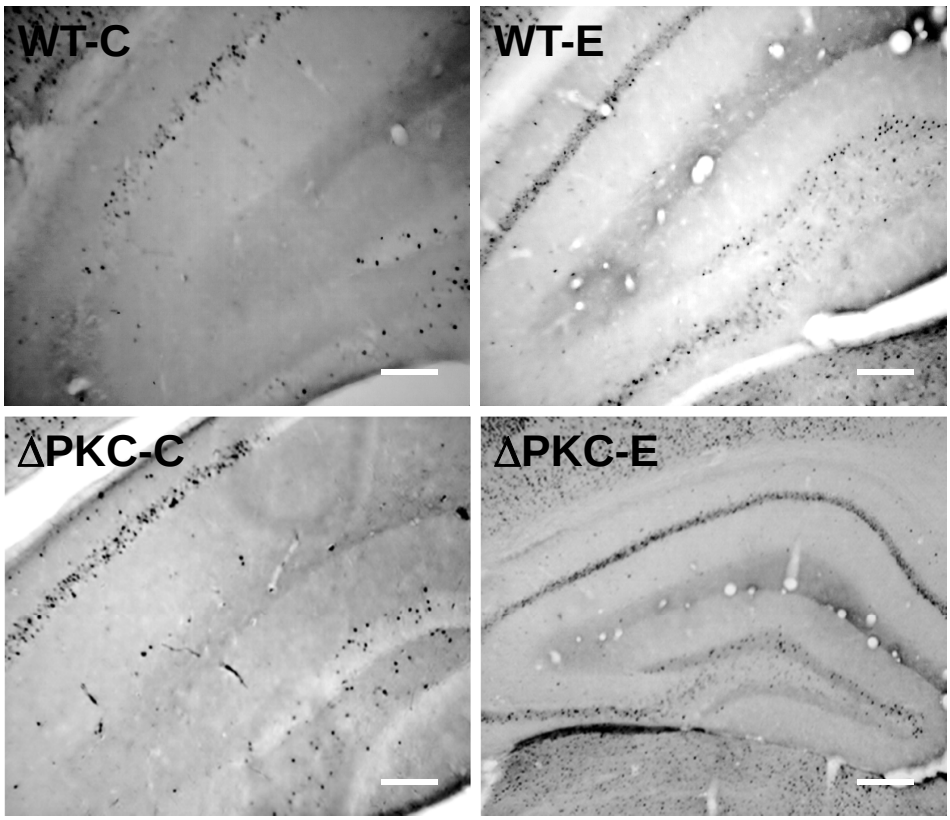

Figure 26: Fos expression in the hippocampus of WT and Δ*PKC* mouse brains after novel environment exposure. Representative images showing control Fos levels in hippocampus of WT and Δ*PKC* from home-cage animals (WT-C and Δ*PKC*-C) and exposure induced Fos expression in experimental animals (WT-E and Δ*PKC*-E). White scale bars represent 125 µm.

they were similar (Control-CA1: ($F_{1,10}$=4.52,p=.93), Control-CA3: ($F_{1,10}$=2.15,p=.17), Control-DG: ($F_{1,10}$=2.13,p=.18)). Thus, the lower Fos expression in the hippocampus of Δ*PKC* mice was found to be consistent with the anxiolytic-like behavioral phenotype of the Δ*PKC* mice. Representative images showing Fos expression in various hippocampal regions of WT and Δ*PKC* are shown in Figure 28, Figure 29 and Figure 30.

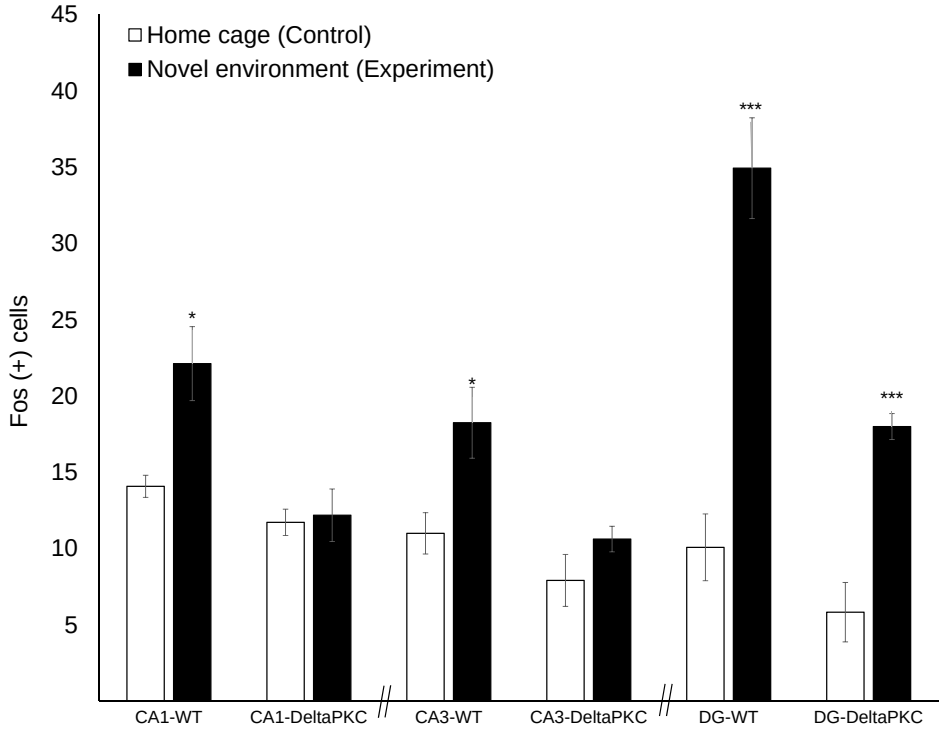

Figure 27: Differential Fos expression in hippocampal region of Δ*PKC* mouse brains after novel environment exposure. Control Fos level in brains of both the groups of mice in their home-cages was not significantly different in DG, CA1, and CA3. All the hippocampal regions of WT-E group had a significant increase in Fos levels compared to its home-cage levels (WT-CA1: ($F_{1,12}$=7.54,p=.02), WT-CA3: ($F_{1,12}$=6.10,p=.03), WT-DG: ($F_{1,12}$=31.55,p <.001)). However, the Δ*PKC*-E group had an increased Fos only in the DG, and not in CA1 or CA3, compared to its home-cage levels (Δ*PKC*-CA1: ($F_{1,12}$=0.05,p=.82), Δ*PKC*-CA3: ($F_{1,12}$=2.33,p=.15), Δ*PKC*-DG: ($F_{1,12}$=39.38,p <.001)). n = 6 per group (home-cage), and n = 8 per group (novel environment), ***p <.001,*p <.05.

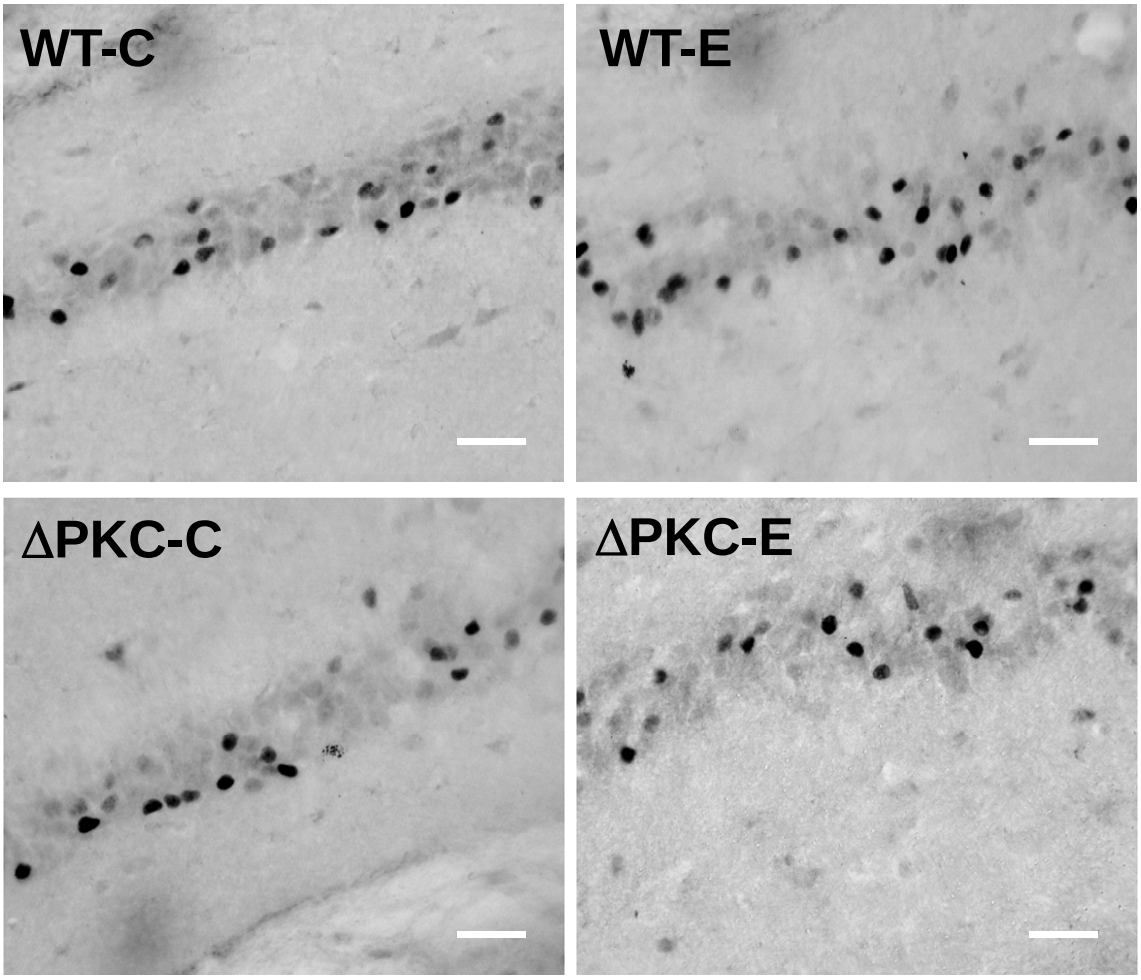

Figure 28: Differential Fos expression in the CA1 region of Δ*PKC* mouse brains after novel environment exposure. Representative images showing control Fos levels in CA1 region of WT and Δ*PKC* hippocampus from home-cage animals (WT-C and Δ*PKC*-C) and exposure induced Fos expression in experimental animals (WT-E and Δ*PKC*-E). White scale bars represent 50 µm.

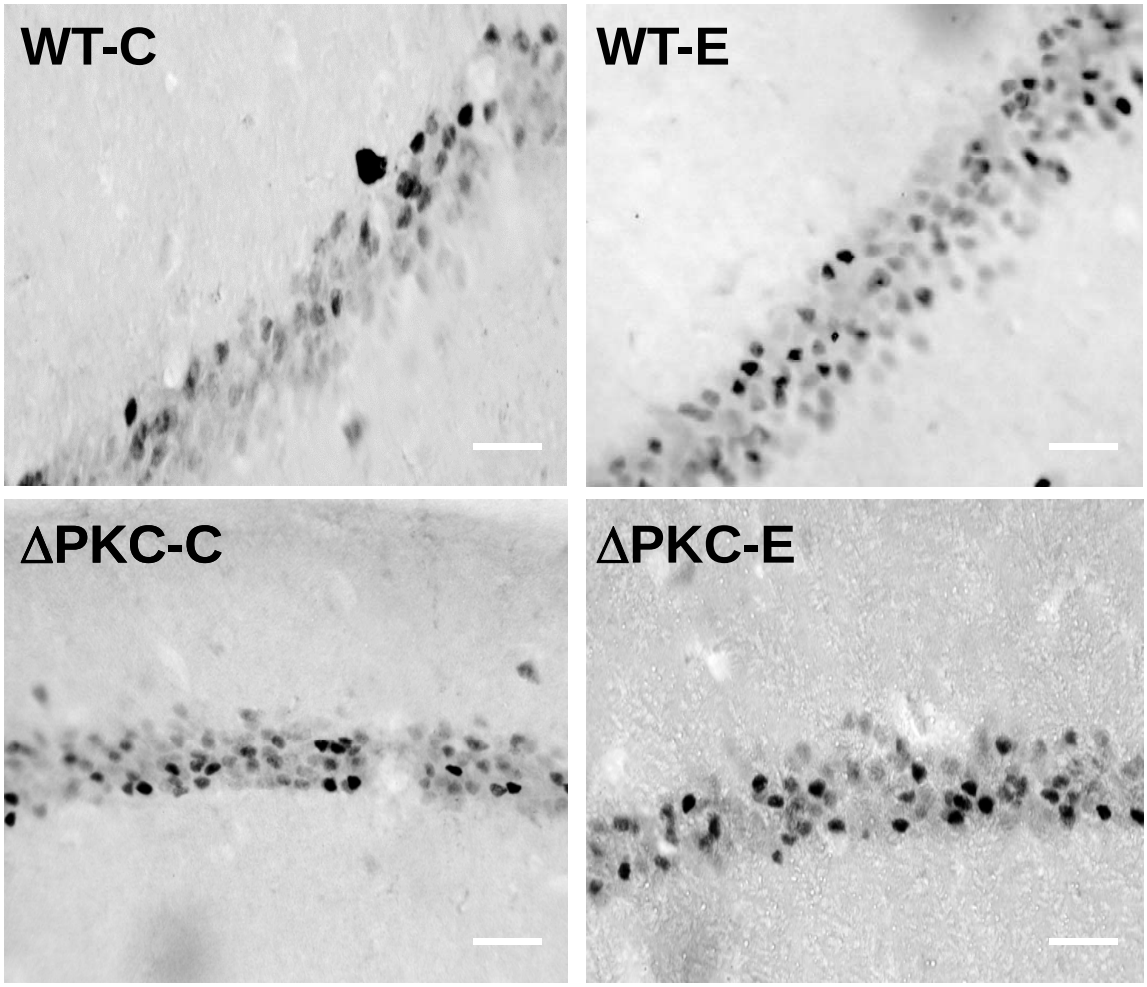

Figure 29: Differential Fos expression in the CA3 region of Δ*PKC* mouse brains after novel environment exposure. Representative images showing control Fos levels in CA3 region of WT and Δ*PKC* hippocampus from home-cage animals (WT-C and Δ*PKC*-C) and exposure induced Fos expression in experimental animals (WT-E and Δ*PKC*-E). White scale bars represent 50 µm.

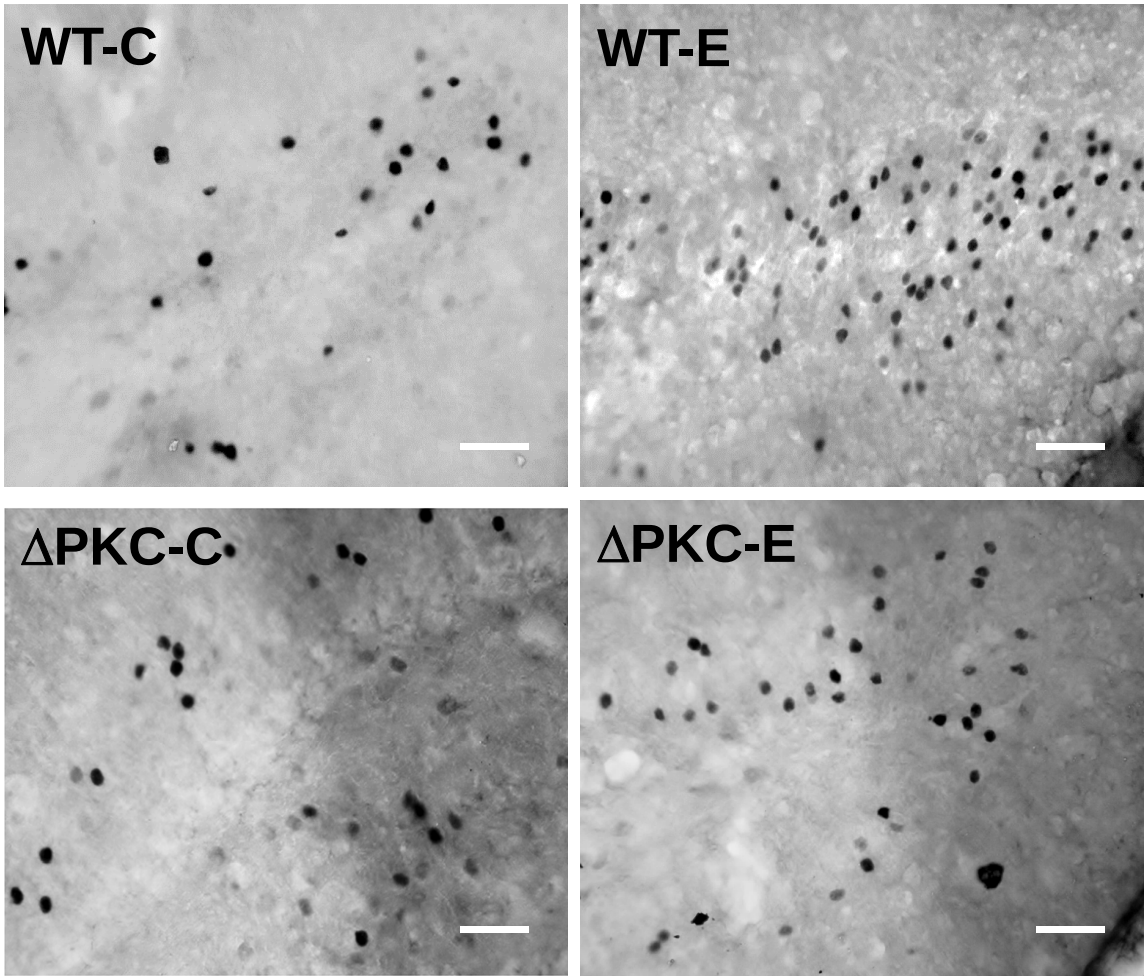

Figure 30: Differential Fos expression in the DG region of Δ*PKC* mouse brains after novel environment exposure. Representative images showing control Fos levels in DG region of WT and Δ*PKC* hippocampus from home-cage animals (WT-C and Δ*PKC*-C) and exposure induced Fos expression in experimental animals (WT-E and Δ*PKC*-E). White scale bars represent 50 µm.

3.4 Discussion

Spontaneous alternation was used as a measure of spatial working memory (Hughes, 2004). Alternation rate in mazes reflect the frequency with which least recently explored arms were chosen. Apart from laboratory-bred mice and rats, a number of other species such as cats, gerbils, rabbits, monkeys and humans has been shown to exhibit spontaneous alternation (Richman et al., 1986). Interestingly, this phenomenon was not specific to mammals since other species such as paramecia, cockroaches, and fruit-flies and chickens exhibit alternation under specific conditions such as forced trial alternations, and shorter inter-trial intervals (Richman et al., 1986). For maze exploration, the mice could use variety of navigational techniques such as use of extra-maze cues (such as auditory stimuli, visual stimuli), intra-maze cues (such as odor) and path integration (using vestibular information) (Eisenberger et al., 1970; Lennartz, 2008; Wallace et al., 2002). Continuous alternation tasks in four-arm maze and Y maze is more advantageous over the discrete T maze alternation that involve inter-trial handling of mice. This usually increases the stress levels in a mouse resulting in an unfavorable association with the arm from which the mouse was removed. However, a modified T maze alternation paradigm in which the mouse was allowed a maximum of 2 minutes to explore an arm, after the end of which it was gently nudged into the T maze stem area avoids the above mentioned negative association (Gerlai, 1998). One advantage of the delayed alternation task is that it allows testing the sensitivity of the genetic or physiological manipulation done in the animal by varying the ITI. Another advantage of the T maze alternation paradigm, is that it eliminates side preferences that may be adopted by an animal. An animal with a side preference may per-

form above chance levels obscuring any impairments in spontaneous alternation (Deacon and Rawlins, 2006). Most often the cognitive demand of the alternation task may be increased by increasing the ITI, thereby eliminating the effects of weaker treatments or subtle mutations in an animal. However, most of the rat and mice studies that involve food reward for reinforcing the correct choices in a T maze, showed that there was an inverse relation between the ITI and alternation rate during acquisition (Clayton, 1966; Jaffard et al., 1981). Since the alternation of the mutant in a T Maze with an ITI of 60 seconds was higher than its alternation with an ITI of 10 seconds, it is possible that the mutants were making more impulsive choices at lower ITIs. This was also consistent with the finding that the number of mutant mice that made correct choices during every trial for both the ITIs was lower than the number of WT mice that made correct choices during the T maze alternation trials [Figure 18]. Hence, increased impulsive choices made during the trials may be the reason for reduced performance of the mice in a T maze alternation task. In experiments performed on mutant mice with swapped CTD of the GluN2A and GluN2B, both the subunits were shown to contribute to impulsive behaviors in mice (Ryan et al., 2013).

Δ*PKC* mice, like the GluN2A knockout (GluN2A-KO) mice, and the GluN2A CTD deletion mice (GluN2A-ΔC also showed a reduced anxiety-like phenotype in an open field test, light-dark box emergence test, and elevated plus maze (Boyce-Rustay and Holmes, 2006; Ryan et al., 2013). Comparing the percentage time spent in open arms by all of these mutant mice to their WT controls in the elevated plus maze test reveals an interesting factor. The percentage change in open entries between the WT and mutant is positively correlated with the number of

residues mutated or deleted in the GluN2A subunit. For example, the difference between the percentage of open arm entries between the WT and GluN2A-KO mice was about 20% while the GluN2A-ΔC mice and their respective WT differed by about 10%. The percentage arm open entries between WT and Δ*PKC* mice differed by about 5%. All the mutant mice (GluN2A KO, GluN2A-ΔC, Δ*PKC*) had a pronounced anxiolytic phenotype, and so there could be a possibility other residues in GluN2A subunit involved in modulating emotional behavior. Also, since the GluN2A knockout mice may be more anxiolytic than the other two mutants (based on comparison of parameters such as open field entries and dwell times in open arms) other residues in either the LBD or the TMD may also be involved in modulating emotional behavior. Furthermore, the anxiolytic phenotype in the Δ*PKC* have been validated using other behavioral tests such as the light dark box and open field test. However, the parameters obtained for those two tests (such as time spent in the center of an open field, and time spent in lit compartment of the light-dark box) could not be compared since the test duration varied between the studies. Both the GluN2A KO and GluN2A-ΔC mice also had an increased locomotor activity in the open field test. However, the Δ*PKC* did not show any such increased activity in the open field test. The general activity levels of the Δ*PKC* were similar to their WT controls in a four-arm maze, Y maze and an open field. This shows that there may be other residues in the CTD of GluN2A subunit that regulate motor activity. It is also important to note that there might be strain specific differences, methodology differences, laboratory breeding conditions between all these mutant mice which may contribute to such differential behaviors. Increased levels of plasma corticosterone has been shown to be positively correlated with risk

assessment behaviors such as head dips and stretch-attenuated postures observed in an elevated plus maze (Walf and Frye, 2007). However, the Δ*PKC* mice may have higher number of head dips from open arms than the WT mice due to increased number of open arm entries in an elevated plus maze. Overall, the results from behavioral analysis of Δ*PKC*, and the other GluN2A mutant mice provides evidence that the GluN2A subunit of the NMDAR in modulation of anxiety. Interestingly, mice with a different tyrosine mutation on its GluN2A (Y1325F) show antidepressant-like behavior in forced swim test (Taniguchi et al., 2009). To avoid bias in forced swim test due to abnormal locomotor activity, episodes of swimming, and climbing behaviors during the test duration were also measured (Slattery and Cryan, 2012). This behavior was not seen when the Δ*PKC* mice were tested for depression-like behavior in the same test. In the forced swim test, the Δ*PKC* mice exhibited the similar episodes (or bouts) of swimming, climbing, and immobility as WT control mice.

Δ*PKC* mice exhibit reduced alternation in a T maze and reduced anxiety-related behaviors. Mice strains that exhibit reduced anxiety-related behaviors in various behavioral tests tend be impulsive (Sanchez-Roige et al., 2012; Greco and Carli, 2006). Increased locomotor activity in a novel environment, and increased exploration of a novel object have been shown to be predictors of impulsivity in mice (Bevilacqua et al., 2010). Anxiety-like behaviors in mice are generated due to the conflict between the natural tendency of mice to explore novel environment (that result in approach) and their innate tendency to avoid aversive stimuli (that result in avoidance). Hence, increased exploration in an aversive novel environment may also indicate impulsivity, rather than an anxiolytic phenotype. However, analysis of traditional

measures of anxiety and impulsivity in various mice strains showed that the parameters that predict anxiety-related behaviors had a low correlation with levels of impulsivity (Loos et al., 2009). Although the five-choice serial reaction time task has been established as a behavioral paradigm to investigate impulsivity in mice, other measures such as nose-pokes to food/water reward in an operant conditioning chamber, and aggression in home-cage can also be used to predict impulsivity (Simpson et al., 2010). Since the Δ*PKC* mice do not have increased locomotor activity in a novel environment, and do not show any overt signs of aggression in home-cage, they may not be impulsive. However, specific tests can be done to determine if the reduced anxiety and lower alternation of Δ*PKC* mice in a T maze could be a result of increased impulsivity.

To understand at least a part of the cellular mechanism underlying the modulation of anxiety-like behaviors, the Δ*PKC* mice were exposed to three novel environments (two of which are used in anxiety tests), and the levels of neuronal activation in hippocampus was studied. The critical role played by the hippocampus in both anxiety and spatial working memory, was one of the main reasons for determining the neuronal activation levels in specific hippocampal regions based on Fos immunostaining. Fos, an immediate early gene (IEG) has been shown to be expressed in many regions of a rodent brain after exposure to various physiological conditions including exposure to a novel environment, traumatic brain injury, after seizure-induction, noxious stimulation of the spinal cord, and inflammation (Herrera and Robertson, 2006; Kreiss et al., 2003; Wirtshafter, 2005). Fos expression in hippocampal subregions (DG, CA1, and CA3) has been studied to understand the hippocampal encoding

of information from a novel context. Furthermore, calcium influx through both NMDARs and voltage-dependent calcium channels could cause an increase in intracellular calcium that result in enhanced Fos expression (Morgan et al., 1987). Fos expression levels in the WT mice exposed to novel environments are in accordance with previously published studies that show a regional variation in Fos expression with the highest levels in DG followed by CA1 and CA3, although the paradigms used for Fos induction were different from the previously published studies (Barbosa et al., 2013; Satoko et al., 2013; Labrousse et al., 2012). The mutant mice exposed to novel environments showed Fos levels in DG, CA1, and CA3 that were significantly lower than the Fos levels measured in the same regions in WT mice exposed to the same novel environments. However, the mutant mice showed an increase in Fos levels in their DG compared to their home-cage levels which might indicate that the cells in the DG may be more sensitive to the environment. Despite the increased Fos levels in the DG of mutants after exposure to the novel environments, their increased Fos levels were still lower than the Fos levels in the DG of WT mice. Hence, the Δ*PKC* mice show a show a decreased activation in the hippocampal areas known to be involved in anxiety-related pathways (Engin and Treit, 2007; Kheirbek et al., 2013; Zhang et al., 2014).

Overall, Δ*PKC* mice exhibited reduced anxiety, and also may have a mild impairment of spatial working memory. Thus, the present study reveals that the phosphorylation of specific serines or tyrosines in GluN2A by various kinases could affect the behavior of mice. The mechanism underlying the modulation of emotional behavior by GluN2A subunit still remains unexplored.

CHAPTER 4

HIPPOCAMPAL SYNAPTIC PLASTICITY IN ΔPKC MICE

4.1 Introduction

The plasticity of synapses in the CNS contributes to different functions of the brain through all the stages of development. Glutamate receptors at excitatory synapses in the CNS play a critical role during formation of synapses during development, integration and processing of different forms of sensory information during learning and memory (Bliss and Collingridge, 1993). Such activity-dependent change in synaptic efficacy could be simulated using hippocampal slice preparations. For example, repetitive stimulation of the perforant pathway afferent fibers results in long-term potentiation of synaptic transmission by increasing the efficiency of the synaptic transmission and also by changing the excitation state of the neurons in the postsynaptic membrane (Bliss and Lømo, 1973). Since the discovery of such long-lasting synaptic activity at the perforant pathway, two major forms of synaptic plasticity has been widely studied namely LTP and LTD. As the name suggests, while LTP usually results in an enhanced synaptic activity, LTD reduces the synaptic transmission efficacy. Both LTP and LTD are region-specific, synapse-specific and also depend on the frequency of stimulation (Kumar, 2011). One of the most well-characterized forms of NMDAR-dependent LTP occurs in the CA3-CA1 Schaffer collateral synapses in the hippocampus. Although the current enhancement observed during LTP was mainly through AMPA receptors, activation of postsynap-

tic NMDARs was required to to induce LTP at the CA3-CA1 synapse (Grover and Teyler, 1994). Calcium flux through the activated NMDARs was shown to be the critical component of LTP. However, the calcium flux through the NMDARs can also result in LTD of synapses, though typically it can be simulated in hippocampal slices using a low-frequency stimulation to the presynaptic neuron. Thus, NMDAR-dependent LTP may be considered to be the form of synaptic plasticity that occurs when the calcium flux is maximal, while smaller calcium flux contributes to occurrence of LTD (Bloodgood et al., 2009). This influx of calcium results in activation of calcium-dependent kinases implicated as a necessary for LTP induction (Chen and Roche, 2007). Apart from the calcium flux, differential kinetic properties of the NMDAR subunits, their region-specificity and their expression at specific developmental stages also influence the induction of LTP or LTD at specific synapses (Yashiro and Philpot, 2008).

4.1.1 GluN2A subunit, CTD and synaptic plasticity

Subunit-specific differences in calcium permeability, spatial and temporal expression has prompted a number of researchers to attempt finding contrasting roles for the NMDAR subunits in governing the direction of synaptic plasticity. For example, since the developmental switch to predominantly GluN2A-containing NMDARs has been shown to be be important during the developmental critical period, GluN2A subunits were proposed to be critical for ensuring normal development of the brain (Quinlan et al., 1999; Philpot et al., 2003). Also, light-deprivation experiments done on mice showed that the ratio of GluN2A:GluN2B decrease when the mice were reared in dark, and also lowers the threshold for LTD induction (Philpot et al., 2007). Furthermore, GluN2A knockout mice have normal critical periods during de-

velopment, and have no deficits in development of somatosensory cortex indicating that the shift in subunits may be regulated by other regulators such as kinases and phosphatases. Despite the pharmacological evidence that exists for subunit-specific contributions to induction of LTP/LTD, and regulation of synaptic plasticity; problems with specificity of the GluN2A subunit-selective antagonist NVP-AAM007 used in those experiments, leaves the question of subunit contribution to LTP/LTD to be studied more precisely. Certain forms of synaptic plasticity may require activation of protein kinases that transfer phosphate moieties to the side chains of the amino acids serine, threonine, and tyrosine in the intracellular CTD of the iGluR subunits. Any change in the receptor protein structure may alter the interactions they may have with other cytosolic proteins (Kim et al., 2011). These kinases may regulate activity-dependent synapse remodeling, learning, memory and cognition by a) altering the properties of ion channel receptor b) affecting the number of those receptors on the synaptic membrane, or c) regulating synapse remodeling by affecting protein synthesis. Using HEK cells, a region in GluN2A CTD between amino acids 1267 and 1406 was shown to be a key structural determinant for PKC-mediated current potentiation in NMDARs (Grant et al., 1998). S1291 and S1312 have been identified as homologous sites for PKC phosphorylation on GluN2B, using oocytes (Liao et al., 2001), while Y1292 and Y1387 in GluN2A have been identified as Src phosphorylation sites using HEK cells (Yang and Leonard, 2001). Thus, the physiological significance of PKC-mediated phosphorylation of those specific sites was determined using electrophysiology. Specifically, the hippocampal synaptic plasticity was determined by theta-burst stimulation of Schaffer-collateral (SC)-CA1 synapses.

4.2 Methods

4.2.1 Electrophysiology

Six month old mice (WT and ΔPKC) were sacrificed, and transverse hippocampal slices were prepared as described (Larson et al., 1999). Slices were maintained at 36 $\pm$ 1 °C in an interface between an atmosphere of humidified 95% O_2/5% CO_2 and a perfusion medium (124 mM NaCl, 3 mM KCl, 1.2 mM KH_2PO_4, 26 mM $NaHCO_3$, 10 mM D-glucose, 2.5 mM $CaCl_2$, 2.5 mM $MgSO_4$, and 2 mM Na-ascorbate). Both the preparation of slices and electrophysiological experiments were performed blind with respect to genotype of the mice. Field excitatory postsynaptic potentials (fEPSPs) were recorded with a glass micropipette placed in stratum radiatum (SR) of CA1b. These dendritic fEPSPs were evoked by stimulation of Schaffer/commissural synapses with bipolar electrodes placed in stratum radiatum (SR) of field CA1a or CA1c. Basal synaptic transmission was assessed based on input-output curves generated using stimulation currents of 2.5-160 µA. Inter-pulse intervals (IPI) of 50, 100, 200, 400, and 800 ms were used to assess paired-pulse facilitation. The degree of facilitation was determined as the percent increase in initial slope of the second response relative to that of the first response in each pair where the paired pulses were separated by 20 ms. LTP was induced by theta-burst stimulation (TBS) and consisted of five bursts (4 pulses, 100 Hz) repeated at at 5 bursts per second. The magnitude of potentiation was determined as potentiation present 30 and 60 min after TBS, and was expressed as a percentage of the pre-TBS baseline value.

4.3 Results

4.3.1 Input-output curves and paired-pulse facilitation

In hippocampal slices obtained from WT and Δ*PKC* mice, the responses to increasing stimulus intensity were compared. For the entire range of the input-output curve, the responses were not significantly different between the WT and Δ*PKC* mice (t_{20}=0.93 ,p=.36). The magnitude of maximal evoked fEPSP was similar between the WT and Δ*PKC* mice [Figure 31]. Paired-pulse synaptic plasticity was also similar in slices from WT and Δ*PKC* mice [Figure 32].

4.3.2 LTP induced by TBS

LTP in the hippocampal slices were obtained by TBS stimulation protocol (Larson et al., 1999). Stimulation of the SC fibers using the TBS protocol induces an initial potentiation that stabilizes after 10–15 minutes of induction. Typical and average results for slices from adult mutant and WT mice are shown in [Figure 33]. Furthermore, two levels of TBS were used for LTP induction, one using 5 bursts and another one using 10 bursts, and there was no significant differences between the field potential responses to the two levels of TBS between the two groups of mice [Figure 34]. There were also no clear differences in these response patterns to 5 and 10 TBS in slices from WT and mutant mice and The total area of negativity underlying the first burst was not different between WT and mutant mice (WT: 131.4 + 8.7 mV-ms, n = 12; Mutant: 137.8 + 10.9 mV-msec, n = 11; (t_{21}=0.46,p=.6)) [Figure 35]. While the normal basal synaptic transmission in mutant mice suggested that there were impairments in AMPAR-mediated currents, the similar waveforms evoked during TBS in both the groups of mice suggested that there was no impairment in NMDAR-mediated postsynaptic currents.

4.4 Discussion

Previous work done in our lab showed that in oocytes injected with mutated *Grin2a* RNA (S1291A or S1312A), the current enhancement after PKC activation was reduced to about 60% compared to 120% in control WT *Grin2a* RNA. Hence, it was hypothesized that in hippocampus of the mice with those mutations, there might be altered synaptic transmission or synaptic plasticity due to the alanine which cannot be phosphorylated by PKC. However, since the mutated GluN2A subunits were present since E0 age of the mice, there might be some compensation due to other GluN2-containing or triheteromeric (GluN1/N2A/N2B) NMDARs trafficked onto the post-synaptic membrane of the hippocampus to maintain normal synaptic transmission, and current enhancement during the LTP-induction protocol (Tovar et al., 2013). It has been shown that GluN2B subunit-containing NMDARs are located predominantly on extrasynaptic membranes (Lozovaya et al., 2004). Furthermore, NMDARs with GluN2B subunits also have a higher glutamate sensitivity and deactivate slower than the GluN2A with NMDARs (Paoletti et al., 2013). Such extrasynaptic receptors can get activated via glutamate spillover from neighboring synapses (Rusakov and Kullmann, 1998). There is also the possibility that the mutated GluN2A-containing NMDARs are trafficked onto the extra-synaptic region rather than the synaptic regions and hence may influence the opening of L-type Ca^{2+} channels contributing to LTP (Zhao et al., 2005). Thus, LTP induction in mature hippocampal synapses could be dependent on both GluN2A and GluN2B, wherein the GluN2A forms an ion channel contributing to calcium influx, and the CTD of GluN2B subunit binds to various cytosolic proteins critical for LTP induction (such as PSD-95, β-catenin, and CRMP-2) (Al-

Hallaq et al., 2007; Barria and Malinow, 2005; Foster et al., 2010; Mayadevi et al., 2002). The experiments done so far indicated there were no alterations in LTP of hippocampal SC-CA1 synapses that were investigated using TBS protocol. Future whole-cell patch recordings and stimulations using a range of frequencies that could induce either potentiation or depression of hippocampal synapses may also reveal if there were any other impairments in SC-CA1 hippocampal synapses (or other synapses in the brain). Preliminary biotinylation experiments using oocytes show that the PKC-mediated phosphorylation sites that were mutated in this study were involved in modulation of number of NMDARs on the surface (Lin et al., 2006; Skeberdis et al., 2001). However, whether the mutations influence the probability of opening of individual NMDARs in the postsynaptic membrane in the mutant mice remains to be investigated. Hence, all the above mentioned possibilities might explain the normal hippocampal synaptic electrophysiology observed in the ΔPKC mice.

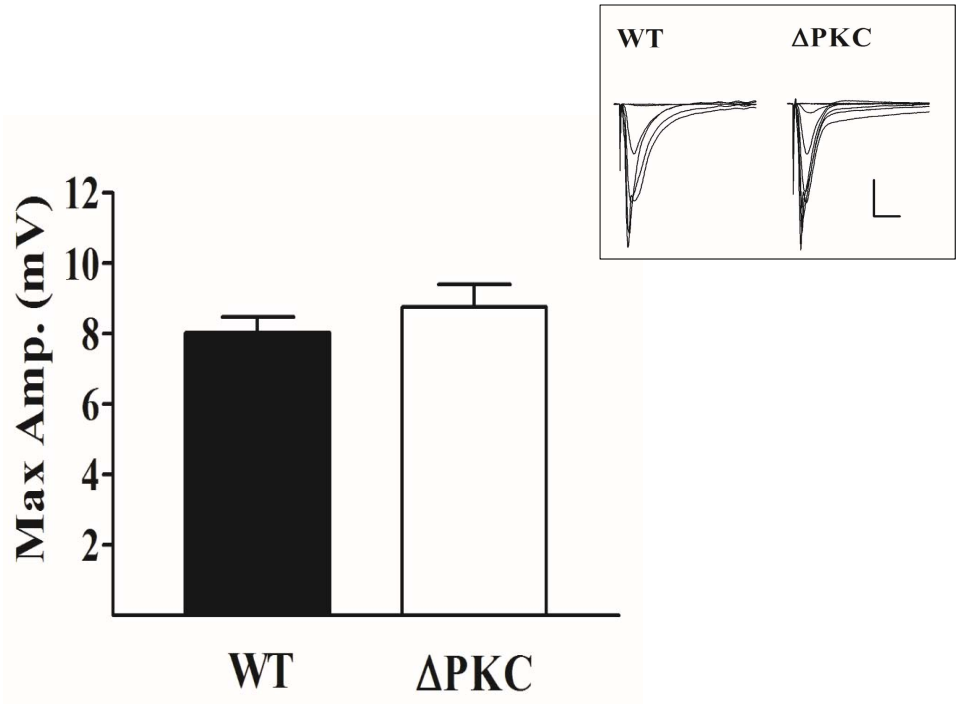

Figure 31: Basal synaptic transmission in hippocampal field CA1 of WT and Δ*PKC* mice. The maximal fEPSP amplitudes obtained by stimulation of WT and Δ*PKC* mouse slices were similar (t_{20}=0.93,p=0.35). The inset on the top-right shows the fEPSPs evoked by stimulus intensity ranging from 1.6-16 mA (WT) and 2.5-40 mA (Δ*PKC*) in typical slices. Each trace is an average of four responses. Calibration: 2 mV, 10 ms. Data are mean ± S.E.M. N = 11 WT and mutant slices.

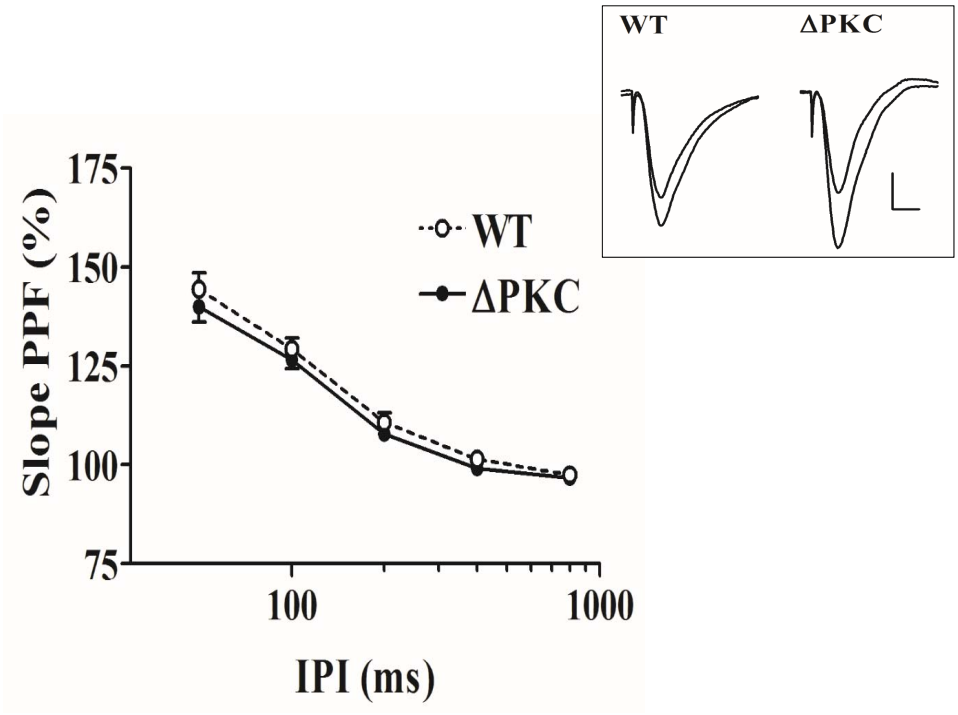

Figure 32: Paired-pulse plasticity in adult Δ*PKC* and WT mice. Paired-pulse curves showing the effect of IPI ranging between 50 to 800 ms on synaptic plasticity in the WT and KO slices. For the paired-pulse facilitation curves, five inter-pulse intervals were tested per slice. Two factor repeated measures ANOVA (Main effect of genotype:$F_{1,20}$=0.81,p=.38, Main effect of IPI: $F_{4,80}$=303.50,p <=0.0001, Interaction:$F_{4,80}$=0.38,p=.82.). The inset shows the recordings of first and second responses evoked in WT and Δ*PKC* mice at an inter-pulse interval (IPI) of 50 msec. Calibration: 1 mV, 10 ms. Data are mean ± S.E.M. N = 11 WT and mutant slices.

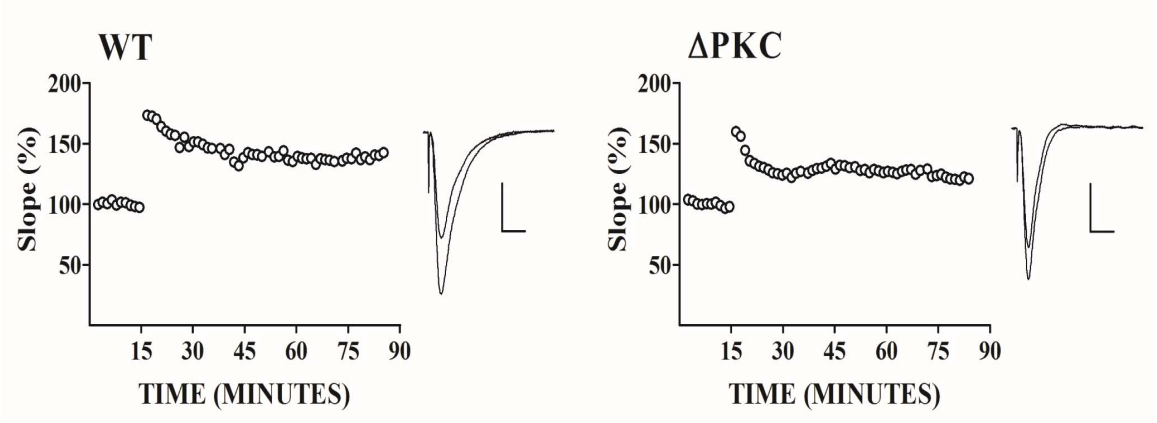

Figure 33: LTP in the SC-CA1 synapses of slices from adult WT and Δ*PKC* mice. fEPSP amplitude was plotted against time before and after 10 theta bursts (arrow) in slices from adult WT and mutant mice. Each circle represents the average of four consecutive responses and is normalized to the average of baseline period (100%). The traces to the left of LTP curve show superimposed recordings taken immediately before and 60 min after TBS. Calibration: 1 mV, 10 ms. *N* = 11 WT and mutant slices.

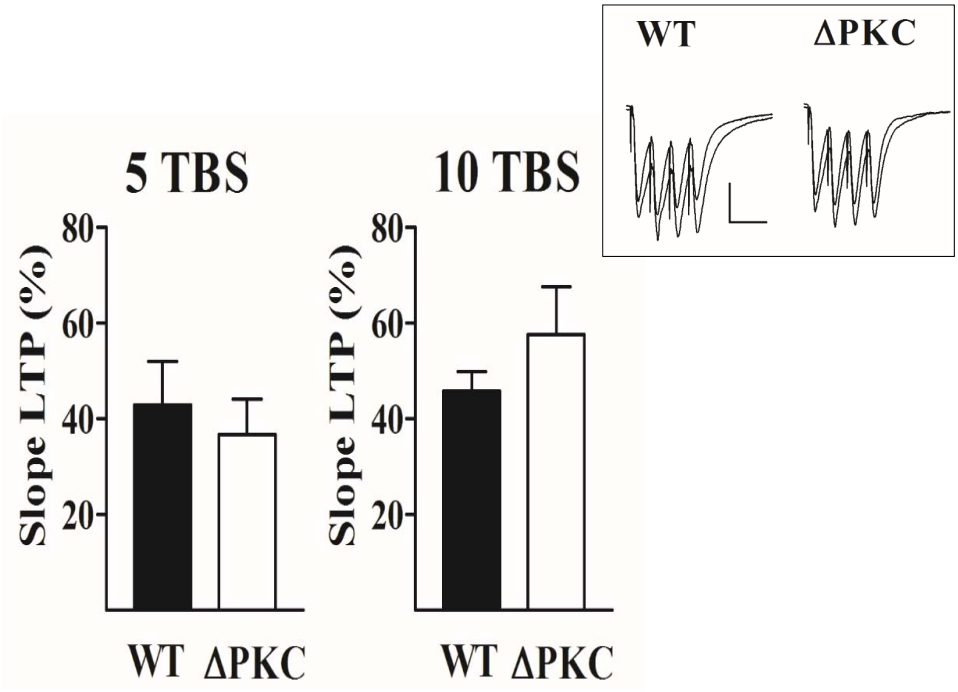

Figure 34: LTP induced by TBS is not different in hippocampal field CA1 of WT and Δ*PKC* mice. The average degree of fEPSP potentiation obtained from WT (open circles) and eight mutant (filled circles) mice after 5 or 10 theta bursts. Two-factor ANOVA on the slope LTP at 60 min post-TBS: (Main effect of genotype:$F_{1,25}$=0.11,p=.74, Main effect of burst number: $F_{1,25}$=2.48,p=.13, Interaction: $F_{1,25}$=1.26,p=.27).

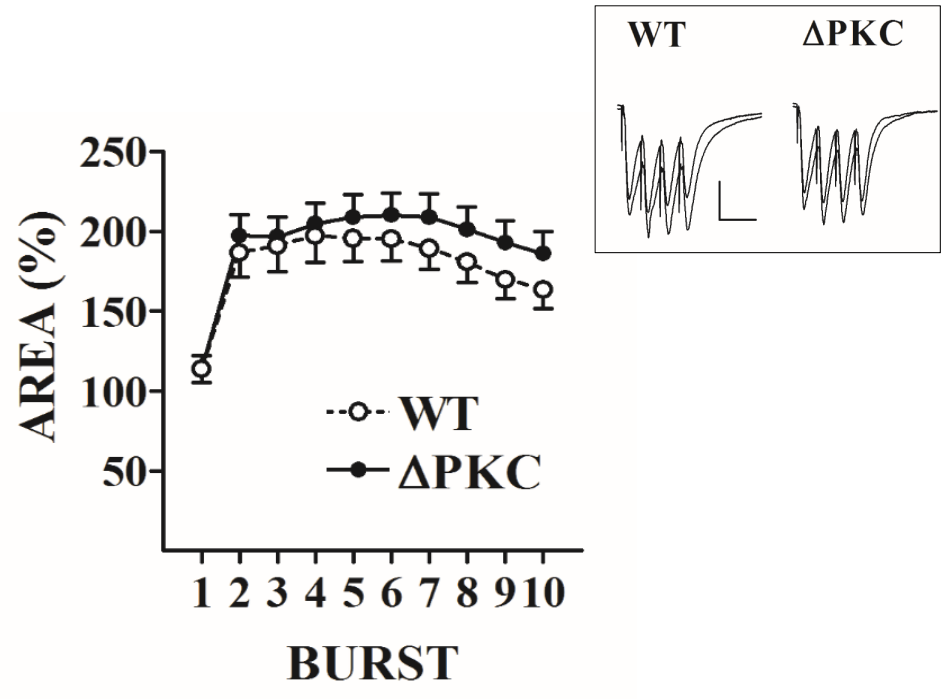

Figure 35: Burst responses in SC-CA1 synapses of hippocampal slices from WT and mutant mice. Burst response in representative WT and mutant mice showing superimposed recordings to first and a second burst. Graph shows the enhancement of burst 2-10 response area relative to the area evoked by the first burst. Analysis of variance yielded a significant effect of burst number ($F_{8,168}$=22.18,p <.0001) but no main effect of genotype ($F_{1,21}$=1.21,p=.25). The interaction was significant ($F_{8,168}$=2.07,p=.04) but none of the direct WT and mutant comparisons were significant. Calibration: 2 mV, 20 ms. 5 bursts:N = 6 WT and 8 mutant slices, 10 bursts:N = 7 WT and 8 mutant slices).

CHAPTER 5

CONCLUDING REMARKS

5.1 Kinase modulation of NMDARs

With critical roles in brain functions ranging from basic synaptic transmission to learning and formation of memory, the NMDARs are considered as one of the most important excitatory neurotransmitter receptors in the brain. NMDAR-dependent synaptic plasticity in different brain regions can be rapidly regulated by phosphorylation (Mammen et al., 1999). Phosphorylation of certain amino acids in the CTD of GluN2 subunits introduces a negative charge in the protein, which may change the conformation and stability of the receptor (Choi et al., 2011). Thus, it is one of the few key processes that can regulate various cellular processes such as synaptic remodeling during development, learning and excitotoxicity (Dingledine et al., 1999). Though a number of studies have characterized the NMDAR subunits using pharmacological, electrophysiological and genetic manipulations (using both conditional and knockout strategies), the modulation of NMDARs by kinases is yet to be understood. This is because:

- There are a number of kinases which can regulate a single NMDAR subunit. For example the CTD of GluN2A subunit contains serines that are substrates for kinases like PKA, PKC and CaMKII, and also tyrosines that are phosphorylated by Src (Chen and Roche, 2007).

- Some kinases also interact other kinases via directly phosphorylating them or by binding to residues close to the binding motif of other kinases. For instance, PKC has been shown to phosphorylate Src kinase (Lu et al., 1999), and also regulates binding of CaMKII by phosphorylating S1416 located within the CaMKII binding region on GluN2A subunit (Gardoni et al., 2001).
- Certain kinases may differentially interact with specific subunit, which may spatially regulate the functioning of NMDARs containing specific subunits (Yang et al., 2012).

. Though a number of phosphorylation sites have been identified on the GluN2 subunits using oocytes expression system, HEK cells and isolated mouse hippocampal neurons, the physiological relevance of all the data still remains unanswered. It is still not clear which phosphorylation sites may be more critical in regulating the NMDAR complex composed of the receptor with its scaffolding proteins and signaling proteins. To address at least a part of that question, the Δ*PKC* mouse with site directed mutations in two serine and two tyrosine residues (S1291A, Y1292F, S1312A, and Y1387F) in the GluN2A subunit was generated and used as a mouse model to examine the behavioral and physiological significance of those sites. Also, these mutations do not alter the action of PKC on other proteins. Each of the chapters in this dissertation describe the general characterization of the mice, mRNA and protein expression levels of the mutated gene, behavioral phenotypes observed in different behavioral experiments, general activation of hippocampal neurons based on Fos expression and electrophysiological characterization of the *Grin2a*Δ*PKC* mouse hippocampal SC-CA1 synapses using paired pulse facilitation, and theta-burst induced LTP of the synapses in hippocampal

slices. Δ*PKC* mice have specific serines and tyrosines mutated to unphosphorylatable alanines and phenylalanines (S1291A, Y1292F, S1312A, and Y1387F) in the CTD of GluN2A subunit of the NMDARs. They also show a mild spatial memory impairment, and decreased anxiety-related behaviors. Thus, Δ*PKC* mice could be used to study the study the physiological effect of such subtle mutations involved in regulating anxiety, and therapeutic interventions may be designed to target these specific sites involved in modulating emotional behavior.

The key findings from the characterization of the Δ*PKC* mouse is summarized below.

- The expression levels of both the *Grin2a* mRNA and the GluN2A protein in the mutant Δ*PKC* mice were found to be equal to those found in WT mice. There were also no abnormalities found in the brain sections obtained from the Δ*PKC* mice. Overall, the Δ*PKC* mice were indistinguishable from their age-matched WT littermates.
- Δ*PKC* mice exhibited reduced anxiety-like behaviors and may also have a mild spatial memory impairment. Thus, the present study using Δ*PKC* mice may be the only study apart from the YF/YF mice from Yamamato's group that reveals how phosphorylation of specific serines or tyrosines in GluN2A by various kinases could affect the emotional behavior of mice.
- Exposure to novel environment elicited a robust Fos expression in DG, CA3 and CA1 regions of WT mouse hippocampus. However, in mutant mouse hippocampus only the DG showed a mild increase in Fos expression upon placement in the three novel environments, while no change was observed in CA1 or CA3. Thus, the lower Fos expression

in the hippocampus of Δ*PKC* mice was found to be consistent with the anxiolytic-like behavioral phenotype of the Δ*PKC* mice.

- Theta-burst stimulation of the Schaffer collateral-CA1 synapses in the hippocampal slices obtained from the WT and mutant mice, revealed that there was no impairment in LTP. Also, the mutant mice showed no significant differences in input-output curves and paired-pulse facilitation.

Δ*PKC* mice have four mutation sites in the GluN2A subunit of NMDARs, so there is still a question of which of those sites could have contributed to those behaviors. Also, during development the subunit composition of NMDARs switch from predominantly GluN2B to GluN2A-containing receptors. This switch occurs in mice between P15–P60 during the **critical period**, when distinct changes occur in synapses. This might have interfered with the parameters tested in various behavioral experiments. To avoid this issue, adult mice between 4–6 months of age were used in all experiments. Furthermore, all the parameters measured in the behavioral experiments used in this study has been validated for predicting specific memory deficits, or emotional behaviors. NMDAR-dependent form of LTP of synapses are synapse-specific. This is because during LTP induction protocol, glutamate released by the presynaptic neuron activates NMDARs on the postsynaptic membrane. Interestingly, glutamate spillover can also activate extrasynaptic NMDARs. In adult mice, synaptic NMDARs are composed of predominantly GluN2A subunits while the extrasynaptic receptors are made of GluN2B subunits. The differential interaction of these subunits with various kinases (such as Src/Fyn, and PKC), and their significantly different activation/deactivation kinetics may result in nor-

mal hippocampal synaptic plasticity in the mutant. Thus, it may be important to determine the characteristics and kinetics of isolated subunit-specific hippocampal NMDAR currents in ΔPKC.

5.2 Relevance to human pathology

Recent studies have implicated the glutamatergic system in the pathophysiology of a number of anxiety disorders in mammalian brain. In humans, the relatively high prevalence of anxiety disorders among various classes of psychiatric disorders and the complex glutamatergic signaling in the brain makes it difficult to dissect the role of individual NMDAR-mediated signaling in the brain (Cortese and Phan, 2005). Alternative treatments are currently being sought since traditional drugs such as benzodiazepines and serotonin re-uptake inhibitors have been shown to be ineffective in treating certain forms of anxiety due to increasing resistance or due to involvement of multiple signaling pathways (Salzman et al., 1993). Many behavioral testing apparatuses used to determine anxiety-related behaviors in mice were validated by administering benzodiazepines to mice and analyzing their behaviors. After the behavioral testing paradigms were established in mice, the effect of newly developed drugs to treat anxiety disorders could be tested in mice by using the behavioral tests such as elevated plus maze, light dark box emergence and open field exploration (Bailey and Crawley, 2000). In rodents, administration of NMDAR antagonists result in reduction of anxiety levels, and GluN2A subunit has been shown to be involved in regulating anxiety-related behaviors (Boyce-Rustay and Holmes, 2006). While such reports provide a causal link between NMDAR and anxiety-related behaviors in mice, the mechanism for regulation of emotional behavior still remains

to be explored. Activation of NMDARs also lead to influx of calcium into the postsynaptic neuron which further complicates the signaling, since calcium activates a number of kinases and proteins involved neuronal signaling. Using genetically engineered mouse models like Δ*PKC* mice in research can provide insights into how NMDARs can be modulated by specific kinases and how such modulations can result in many behavioral phenotypes.

In conclusion, PKC-mediated serine phosphorylation at S1291/S1312 or tyrosine phosphorylation at Y1312/Y1387 in the GluN2A subunit may play an important role modulating anxiety-related behaviors in an open field test, light dark box emergence test and elevated plus maze test, and may affect spatial working memory in a Y/T maze. The mutants also show region-specific reduction in hippocampal Fos expression compared to WT mice after exposure to novel environments. The Δ*PKC* mice were similar to WT mice in various parameters such as general activity and gross brain morphology. Therefore, understanding the impact of PKC-mediated modulation of NMDA receptors using mouse models could lead to development of new treatments for anxiety-related disorders.

APPENDICES

Appendix A

GENOTYPING PROTOCOL

PROTEINASE K DIGESTION OF TAIL SNIPS

1. Sterilize the scissors with 70% ethanol.
2. Cut about 0.5 cm of the tail sharply in a single snip and place into a clean 1.5 mL micro-centrifuge tube.
   POSSIBLE STOP POINT! - Freeze the tails if planning on extracting DNA the next day. Store the micro-centrifuge tubes at -20°C.
3. Add 500 mL of freshly prepared digestion buffer as per the recipe Table V. (All the chemicals except Proteinase K are stored at room temperature on the shelf beside DNA extraction area. Proteinase K stock (10mg/ml) is stored in -20°C. Vortex once before adding into the tubes with the tail snips.)
4. Incubate the tubes at 55°C overnight in the water bath.

DNA EXTRACTION

1. Prepare two sets of extraction solutions the day before extraction.
   Ex1 - Phenol:Chloroform:isoamyl alcohol - 25:24:1
   Ex2 = Chloroform:isoamyl alcohol - 24:1
2. Label two sets of tubes for each tail snip.
3. To make sure the DNA does not get damaged during the process and to enable easy transfer of organic solvents, use 1000 µL tips cut in the pointed edge using scissors.
4. Remove the tubes from the water bath and move them to the extraction bench.
5. Add 500 µL of Ex1 to each of the tubes and mix the contents by inverting them at least 20 times.
6. Spin the tubes in a micro-centrifuge at top speed for 3 minutes. The liquid in the tube should separate into two layers (aqueous layer on top of organic layer).
7. Using P1000 pipet, transfer the aqueous layer to a new tube. (The aqueous layer might feel viscous!)
8. Extract with Ex2 as above (5-7).
9. For the aqueous layer transfer make sure that that the tip does not touch any solution past the interface between the aqueous and organic phase.

Appendix A (Continued)

10. Add 50 µL of NH_4OAc and 1 mL of 100% ethanol. Invert the tubes 20 times and a white clump/ strand that appears is the DNA!
11. Transfer the DNA to a new tube containing 500 µL 70% ethanol and invert the tube about five times and spin the tubes at top speed for 10 minutes.* Alternately, the tubes can be spun at top speed for 5 minutes and the ethanol could be removed inverting the tubes very carefully. After this add 500 µL 70% ethanol and invert the tube about five times and spin at top speed for an additional 5 minutes at 4°C micro-centrifuge.
12. Remove the residual alcohol either by pipetting or by vacuum aspiration.
13. Air-dry the tubes for about 10 minutes and suspend the DNA in 100 µL sterile water.
14. Incubate the tubes at 50°C for 1 hour and gently re-pipet to dissolve any DNA thoroughly.
15. Run the DNA on an agarose gel to check its presence and integrity.
16. Set up PCR tubes for the extracted DNA.

PCR FOR GENOTYPING

1. Add 1.5 µL template DNA to 48.25 µL of the PCR master mix Table VI.
2. Assemble to tubes in the PCR machine, and start the GRIN2A program.
3. After the initial denaturation step for 3 minutes, press the pause button.
4. Add 0.25 µL Taq polymerase at 80°C.
5. After adding Taq to all the tubes, press the pause again to continue with the PCR cycle.
6. After the PCR cycle is complete, run an agarose gel to check the presence of PCR products.
7. Store the PCR products at 4°C.

RESTRICTION ENZYME DIGEST OF PCR PRODUCTS

1. Add 21 µL of the RE master mix to 10 µL of PCR mixture
2. Allow it to incubate at 37°C overnight.
3. The next day run set up an agarose gel to run 9 µL of restriction digested PCR product per well.
4. Run the gel at 80V for approximately 40 minutes.
5. Post-stain the gel by immersing the gel in 10000X Gel-Red solution. The gel red solution can be reused up to 4 gels.

Appendix A (Continued)

TABLE V: Digestion Buffer

Component	Volume (µL)
1 M Tris HCl (pH 8)	25
10% SDS	25
10 mg/ml Proteinase K	25
0.5 M EDTA (pH 8)	100
dd sterile water	325

TABLE VI: PCR Master Mix

Component	Volume (µL)
dd sterile water	26.25
5X Red juice	10
10X PCR buffer	5
25 mM $MgCl_2$	3
10 mM dNTP mix	2
25 mM primer (each)	1

TABLE VII: RE digest master mix

Component	Volume (µL)
Sterile water	18
Rse buffer	2
RseI enzyme	1

Appendix B

BODY AND BRAIN WEIGHTS OF WT AND Δ*PKC* MICE

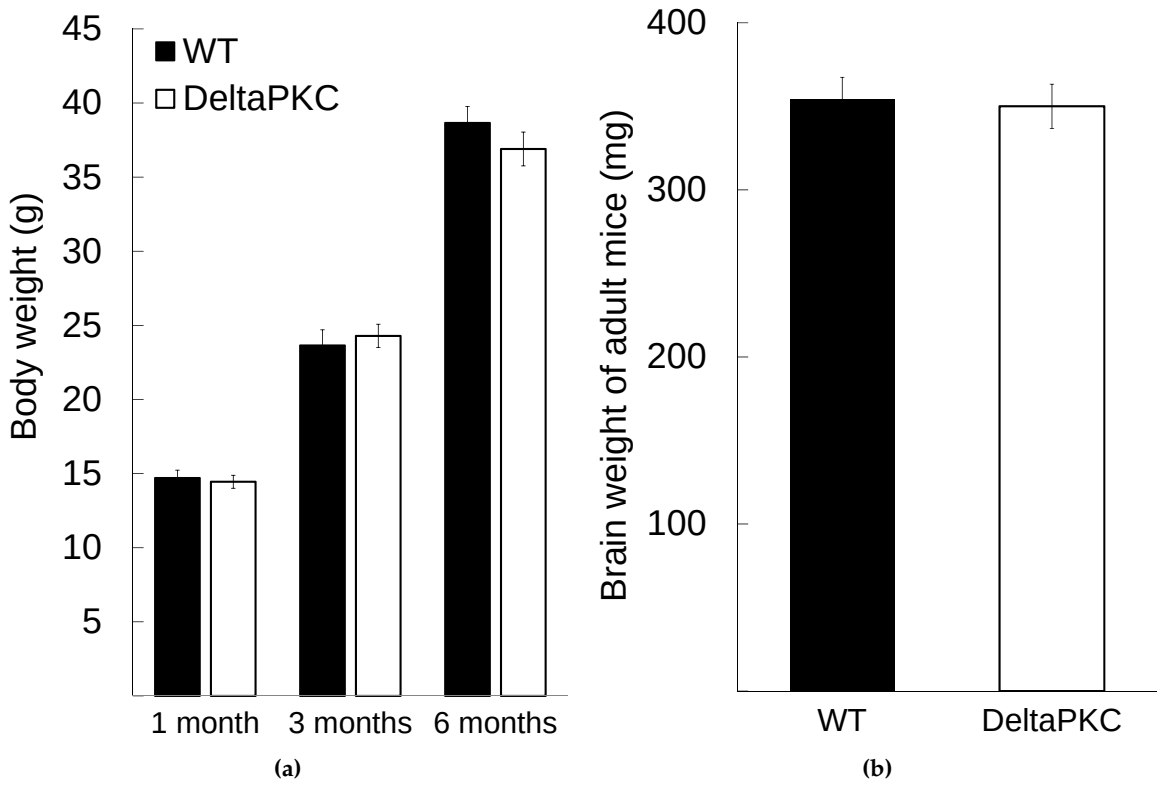

Figure 36: Body and brain weight of Δ*PKC* mice. (a) The body weights of WT and Δ*PKC* were similar through the course of their development to adulthood [1 month: ($F_{1,35}$=0.08,p=.78), 3 months: ($F_{1,35}$=0.27,p=.6), 6 months: ($F_{1,35}$=1.27,p=.27), n=18 in each group.] (b) There was no difference between the brain weights of WT and Δ*PKC* mice ($F_{1,23}$=0.03,p=.82),n=12 in each group). The adult mice were between 4–6 months of age.

Appendix C

BEHAVIORAL EXPERIMENT APPARATUSES

TABLE VIII: Apparatuses used for behavioral phenotyping

Behavior	Apparatus
Spatial working memory	Four-arm maze Y maze T maze
Recognition memory	NOR box
Anxiety	Open field box Light-dark box elevated plus maze
Depression	Forced swim test cylinder

Appendix C (Continued)

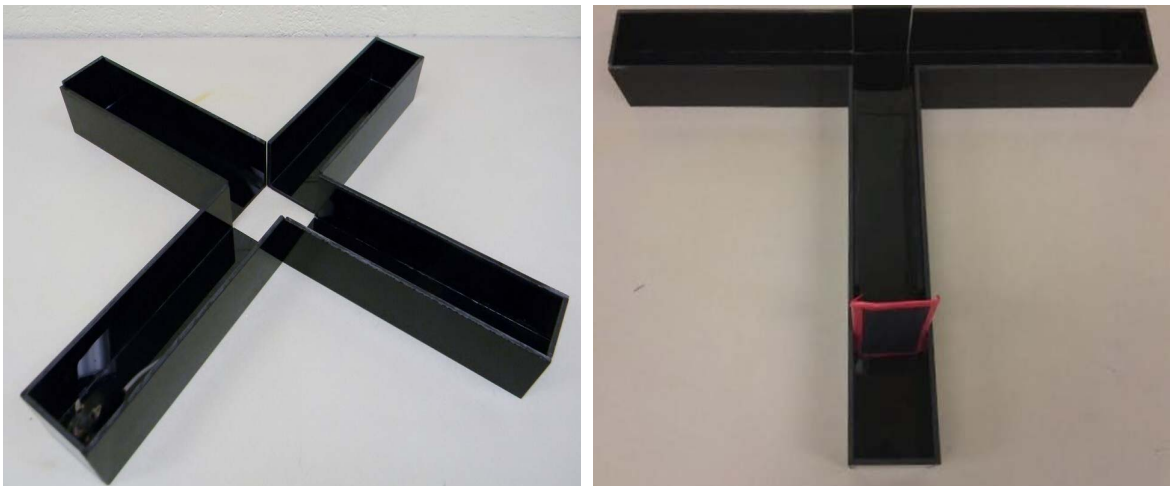

(a) (b)

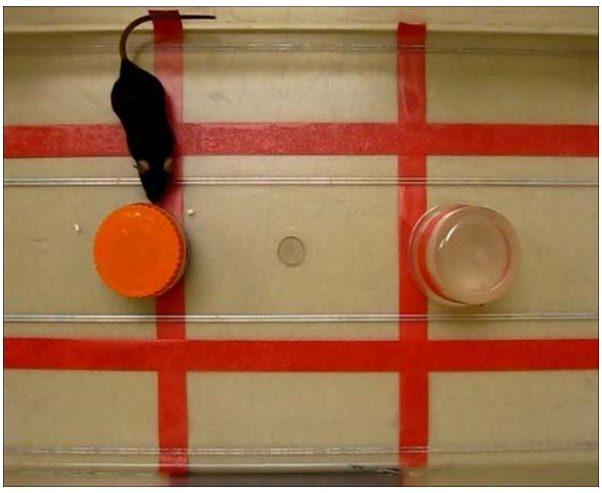

(c)

Figure 37: Apparatuses used for SAB and recognition memory experiments. (a) SAB - Four-arm maze (b) Non-reinforced alternation - T-maze (c) Novel object recognition box

Appendix C (Continued)

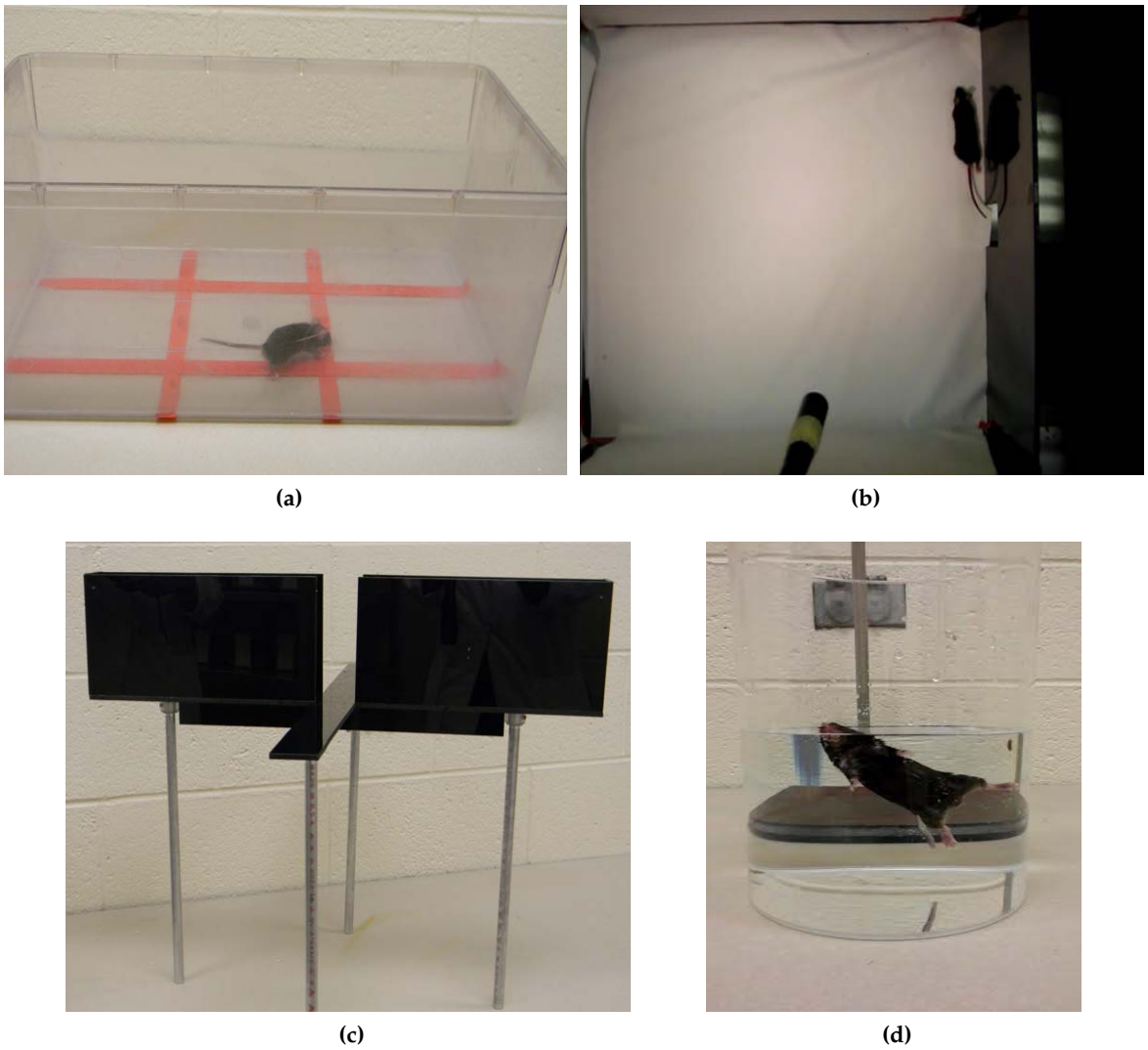

(a) **(b)**

(c) **(d)**

Figure 38: Apparatuses used for anxiety and depression-related behavioral experiments. (a) OF test box (b) LDB emergence test box (c) Elevated plus maze (d) Forced swim test cylinder

Appendix D

ACC PROTOCOL APPROVAL LETTERS

TABLE IX: ACC protocol letters

Approval number	Duration
09-128	10/7/09 to 9/15/12
12-144	10/11/12 to 9/18/15

Appendix D (Continued)

UIC UNIVERSITY OF ILLINOIS AT CHICAGO

Office of Animal Care and Institutional
Biosafety Committee (M/C 672)
Office of the Vice Chancellor for Research
206 Administrative Office Building
1737 West Polk Street
Chicago, Illinois 60612

February 24, 2012

John P. Leonard
Biological Sciences
M/C 067

Dear Dr. Leonard:

The modifications requested in modification indicated below pertaining to your approved protocol indicated below have been reviewed and approved in accordance with the Animal Care Policies of the University of Illinois at Chicago on ***02/21/2012, with following condition.***

Title of Application: Kinase-Resistant NMDA Receptor Mouse Physiology and Behavior

ACC Number: 09-128

Modification Number: ***09-128-05***

Nature of Modification: ***Addition of olfactory learning discrimination and elevated plus maze testing.***

Condition of approval: ***Prior to initiation, PI must review with Dr. Artwohl the procedures for sanitation of equipment from collaborator's laboratory.***

Protocol Approved: ***10/7/2009***

Current Approval Period: ***9/15/11 to 9/15/12.***

Current Funding: ***Portions of this protocol are supported by the funding sources indicated in the table below.***
Number of funding sources: 1

Funding Agency	**Grant Title**			**Portion of Grant Matched**
NIH/NINDS- National Institute of Neurological Disorders and Stroke	*Generation Of Kinase-Resistant NMDA Receptors By Gene-Targeting In The Mouse*			*Matched*
Grant Number	**Current Status**	**UIC PAF NO.**	**Performance Site**	**Grant PI**
R03 NS056321A2	*Funded*	*200704581*	*UIC*	*John P. Leonard*

Phone (312) 996-1972 • Fax (312) 996-9088

Appendix D (Continued)

UIC UNIVERSITY OF ILLINOIS AT CHICAGO

Office of Animal Care and Institutional
Biosafety Committee (OACIB) (M/C 672)
Office of the Vice Chancellor for Research
206 Administrative Office Building
1737 West Polk Street
Chicago, Illinois 60612

9/18/2014

John P. Leonard
Biological Sciences
M/C 067

Dear Dr. Leonard:

The protocol indicated below was reviewed in accordance with the Animal Care Policies and Procedures of the University of Illinois at Chicago and **renewed on 9/18/2014.**

Title of Application:	**Kinase-Resistant NMDA Receptor Mouse Physiology and Behavior**
ACC NO:	**12-144**
Original Protocol Approval:	**10/11/2012 (3 year approval with annual continuation required).**
Current Approval Period:	**9/18/2014 to 9/18/2015**

Currently protocol NOT matched to specific funding source. Modification will need to be submitted prior to Just in time or acceptance of award to match protocol to external funding source. All animal work proposed in the funding application must be covered by an approved protocol.

UIC is the only performance site approved under this protocol.

This institution has Animal Welfare Assurance Number A3460.01 on file with the Office of Laboratory Animal Welfare, NIH. **This letter may only be provided as proof of IACUC approval for those specific funding sources listed above in which all portions of the grant are matched to this ACC protocol.**

Thank you for complying with the Animal Care Policies and Procedures of the UIC.

Sincerely,

Bradley Merrill, PhD
Chair, Animal Care Committee

BM/*kg*
cc: BRL, ACC File

CITED LITERATURE

Akashi, K., Kakizaki, T., Kamiya, H., Fukaya, M., Yamasaki, M., Abe, M., Natsume, R., Watanabe, M., and Sakimura, K.: NMDA receptor GluN2B (GluRε2/NR2B) subunit is crucial for channel function, postsynaptic macromolecular organization, and actin cytoskeleton at hippocampal CA3 synapses. J Neurosci, 29(35):10869–10882, 2009.

Al-Hallaq, R. A., Conrads, T. P., Veenstra, T. D., and Wenthold, R. J.: NMDA di-heteromeric receptor populations and associated proteins in rat hippocampus. J Neurosci, 27:8334–8343, 2007.

Awad, H., Hubert, G. W., Smith, Y., Levey, A. I., and Conn, P. J.: Activation of metabotropic glutamate receptor 5 has direct excitatory effects and potentiates NMDA receptor currents in neurons of the subthalamic nucleus. J Neurosci, 20(21):7871–7879, 2000.

Azevedo, F. A., Carvalho, L. R., Grinberg, L. T., Farfel, J. M., Ferretti, R. E., Leite, R. E., Lent, R., Herculano-Houzel, S., et al.: Equal numbers of neuronal and nonneuronal cells make the human brain an isometrically scaled-up primate brain. J Comp Neurol, 513(5):532–541, 2009.

Bailey, K. R. and Crawley, J. N.: Methods of behavior analysis in neuroscience. CRC Press, 2000.

Bannerman, D. M., Niewoehner, B., Lyon, L., Romberg, C., Schmitt, W. B., Taylor, A., Sanderson, D. J., Cottam, J., Sprengel, R., Seeburg, P. H., et al.: NMDA receptor subunit NR2A is required for rapidly acquired spatial working memory but not incremental spatial reference memory. J Neurosci, 28(14):3623–3630, 2008.

Barbosa, F. F., Santos, J. R., Meurer, Y. S. R., Macêdo, P. T., Ferreira, L. M. S., Pontes, I. M. O., Ribeiro, A. M., and Silva, R. H.: Differential cortical c-Fos and Zif-268 expression after object and spatial memory processing in a standard or episodic-like object recognition task. Front in Behav Neurosci, 7(112):10.3389/fnbeh.2013.00112, 2013.

Barria, A. and Malinow, R.: NMDA receptor subunits control synaptic plasticity by regulating binding to CaMKII. Neuron, 48:289–301, 2005.

Bear, M. F. and Rittenhouse, C. D.: Molecular basis for induction of ocular dominance plasticity. J Neurobiol, 41(1):83–91, 1999.

Benveniste, M., Clements, J., Vyklickỳ, L., and Mayer, M.: A kinetic analysis of the modulation of N-methyl-D-aspartic acid receptors by glycine in mouse cultured hippocampal neurones. J Physiol, 428(1):333–357, 1990.

Berridge, M. J.: Neuronal calcium signaling. Neuron, 21(1):13–26, 1998.

Bevilacqua, L., Doly, S., Kaprio, J., Yuan, Q., Tikkanen, R., Paunio, T., Zhou, Z., Wedenoja, J., Maroteaux, L., Diaz, S., et al.: A population-specific htr2b stop codon predisposes to severe impulsivity. Nature, 468(7327):1061–1066, 2010.

Blair, H. T., Schafe, G. E., Bauer, E. P., Rodrigues, S. M., and LeDoux, J. E.: Synaptic plasticity in the lateral amygdala: A cellular hypothesis of fear conditioning. Learn Memory, 8(5):229–242, 2001.

Bliss, T. V. P. and Lømo, T.: Long-lasting potentiation of synaptic transmission in the dentate area of the anaesthetized rabbit following stimulation of the perforant path. J Physiol, 232:331–356, 1973.

Bliss, T. V. and Collingridge, G. L.: A synaptic model of memory: long-term potentiation in the hippocampus. Nature, 361(6407):31–39, 1993.

Bloodgood, B. L., Giessel, A. J., and Sabatini, B. L.: Biphasic synaptic Ca influx arising from compartmentalized electrical signals in dendritic spines. PLoS Biol, 7(9):2133, 2009.

Bourin, M. and Hascoët, M.: The mouse light/dark box test. Eur J Pharmacol, 463(13):55–65, 2003.

Boyce-Rustay, J. M. and Holmes, A.: Genetic inactivation of NMDA receptor NR2A subunit has anxiolytic and anti-depressant like effects in mice. Neuropsychopharmacol, 31:2405–2415, 2006.

Braithwaite, S. P., Paul, S., Nairn, A. C., and Lombroso, P. J.: Synaptic plasticity: one step at a time. Trends Neurosci, 29(8):452–458, 2006.

Brickley, S. G., Misra, C., Mok, M. H. S., Mishina, M., and Cull-Candy, S. G.: NR2B and NR2D subunits coassemble in cerebellar golgi cells to form a distinct NMDA receptor subtype restricted to extrasynaptic sites. J Neurosci, 23(12):4958–4966, 2003.

Brigman, J. L., Feyder, M., Saksida, L. M., Bussey, T. J., Mishina, M., and Holmes, A.: Impaired discrimination learning in mice lacking the NMDA receptor NR2A subunit. Learn Memory, 15(2):50–54, 2011.

Brigman, J. L., Wright, T., Talani, G., Prasad-Mulcare, S., Jinde, S., Seabold, G. K., Mathur, P., Davis, M. I., Bock, R., Gustin, R. M., et al.: Loss of GluN2B-containing NMDA receptors in Ca1 hippocampus and cortex impairs long-term depression, reduces dendritic spine density, and disrupts learning. J Neurosci, 30(13):4590–4600, 2010.

Broadbent, N. J., Gaskin, S., Squire, L. R., and Clark, R. E.: Object recognition memory and the rodent hippocampus. Learn Memory, 17(1):5–11, 2010.

Chen, B.-S. and Roche, K. W.: Regulation of NMDA receptors by phosphorylation. Neuropharmacol, 53(3):362–368, 2007.

Chen, G., Gharib, T. G., Huang, C.-C., Taylor, J. M. G., Misek, D. E., Kardia, S. L. R., Giordano, T. J., Iannettoni, M. D., Orringer, M. B., Hanash, S. M., and Beer, D. G.: Discordant protein and mRNA expression in lung adenocarcinomas. Mol Cell Prot, 1(4):304–313, 2002.

Choi, U. B., Xiao, S., Wollmuth, L. P., and Bowen, M. E.: Effect of Src kinase phosphorylation on disordered C-terminal domain of N-methyl-D-aspartic acid (NMDA) receptor subunit GluN2B protein. J Biol Chem, 286(34):29904–29912, 2011.

Choi, Y.-B. and Lipton, S. A.: Identification and mechanism of action of two histidine residues underlying high-affinity Zn^{2+} inhibition of the NMDA receptor. Neuron, 23(1):171–180, 1999.

Chu, Y., Fioravante, D., Leitges, M., and Regehr, W. G.: Calcium-dependent PKC isoforms have specialized roles in short-term synaptic plasticity. Neuron, 82:859–871, 2014.

Clayton, K. N.: T-maze acquisition and reversal as a function of intertrial interval. J Comp Physiol Psychol, pages 409–414, 1966.

Collingridge, G. L., Kehl, S. J., and McLennan, H.: Excitatory amino acids in synaptic transmission in the Schaffer collateral-commissural pathway of the rat hippocampus. J Physiol, 334:33–46, 1983.

Cortese, B. M. and Phan, K. L.: The role of glutamate in anxiety and related disorders. CNS spectrums, 10(10):820–830, 2005.

Cousins, S. L., Papadakis, M., Rutter, A. R., and Stephenson, F. A.: Differential interaction of NMDA receptor subtypes with the Post-synaptic Density-95 family of membrane associated guanylate kinase proteins. J Neurochem, 104(4):903–913, 2008.

Crump, F. T., Dillman, K. S., and Craig, A. M.: cAMP-dependent protein kinase mediates activity-regulated synaptic targeting of NMDA receptors. J Neurosci, 21(14):5079–5088, 2001.

Cui, Z., Feng, R., Jacobs, S., Duan, Y., Wang, H., Cao, X., and Tsien, J. Z.: Increased NR2A:NR2B ratio compresses long-term depression range and constrains long-term memory. Sci Rep, 3:doi:10.1038/srep01036, 2012.

Cull-Candy, S., Brickley, S., and Farrant, M.: NMDA receptor subunits: diversity, development and disease. Curr Opin Neurobiol, 11(3):327–335, 2001.

Curtis, D., Phyllis, J., and Watkins, J.: Actions of amino-acids on the isolated hemisected spinal-cord of the toad. Br J Pharmacol Chemother, 16(3):261–283, 1961.

Curtis, D. and Watkins, J.: The excitation and depression of spinal neurones by structurally related amino acids. J Neurochem, 6(2):117–141, 1960.

Dalva, M. B., Takasu, M. A., Lin, M. Z., Shamah, S. M., Hu, L., Gale, N. W., and Greenberg, M. E.: EphB receptors interact with NMDA receptors and regulate excitatory synapse formation. Cell, 103(6):945–956, 2000.

Deacon, R. M. and Rawlins, N. P.: T-maze alternation in the rodent. Nat Protoc, 1:7–12, 2006.

Dingledine, R., Borges, K., Bowie, D., and Traynelis, S.: The glutamate receptor ion channels. Pharmacol Rev, 51(1):7–62, 1999.

Dong, H. and Zhou, H.-X.: Atomistic mechanism for the activation and desensitization of an AMPA-subtype glutamate receptor. Nat Commun, 2:354, 2011.

Dudchenko, P. A.: An overview of the tasks used to test working memory in rodents. Neurosci Biobehav Rev, 28(7):699–709, 2004.

Dunah, A. W., Luo, J., Wang, Y.-H., Yasuda, R. P., and Wolfe, B. B.: Subunit composition of N-methyl-D-aspartate receptors in the central nervous system that contain the NR2D subunit. Mol Pharmacol, 53(3):429–437, 1998.

Dunah, A. W., Yasuda, R. P., , Wang, Y.-h., Luo, J., Dávila-García, M. I., Gbadegesin, M., Vicini, S., and Wolfe, B. B.: Regional and ontogenic expression of the NMDA receptor subunit NR2D protein in rat brain using a subunit-specific antibody. J Neurochem, 67:2335–2345, 1996.

Eisenberger, R., Myers, A. K., Sanders, R., and Shanab, M.: Stimulus control of spontaneous alternation in the rat. J Comp Physiol Psychol, 70(1):136–140, 1970.

Engelhardt, J. v., Doganci, B., Jensen, V., Hvalby, Ø., Göngrich, C., Taylor, A., Barkus, C., Sanderson, D. J., Rawlins, J. N. P., Seeburg, P. H., Bannerman, D. M., and Monyer, H.: Contribution of hippocampal and extra-hippocampal NR2B-containing NMDA receptors to performance on spatial learning tasks. Nat Neurosci, 60:846–860, 2008.

Engin, E. and Treit, D.: The role of hippocampus in anxiety: Intracerebral infusion studies. Beh Pharmacol, 18:365–374, 2007.

Feldman, D. E., Nicoll, R. A., and C, M. R.: Synaptic plasticity at thalamocortical synapses in developing rat somatosensory cortex: LTP, LTD, and silent synapses. Dev Neurobiol, 41(1):92–101, 1999.

Fiering, S., Epner, E., Robinson, K., Zhuang, Y., Telling, A., Hu, M., Martin, D. I., Enver, T., Ley, T. J., and Groudine, M.: Targeted deletion of 5′HS2 of the murine beta-globin LCR reveals that it is not essential for proper regulation of the beta-globin locus. Gen Dev, 9(18):2203–2213, 1995.

Fong, D. K., Rao, A., Crump, F. T., and Craig, A. M.: Rapid synaptic remodeling by Protein Kinase C: reciprocal translocation of NMDA receptors and Calcium/Calmodulin-dependent kinase II. J Neurosci, 22(6):2153–2164, 2002.

Forsythe, I. D. and Westbrook, G. L.: Slow excitatory postsynaptic currents mediated by N-methyl-D-aspartate receptors on cultured mouse central neurones. J Physiol, 396(1):515–533, 1988.

Foster, K. A., McLaughlin, N., Edbauer, D., Phillips, M., Bolton, A., Constantine-Paton, M., and Sheng, M.: Distinct roles of NR2A and NR2B cytoplasmic tails in long-term potentiation. J Neurosci, 30(7):2676–2685, 2010.

Frank, C. A.: How voltage-gated calcium channels gate forms of homeostatic synaptic plasticity. Front Cell Neurosci, 8:doi:10.3389/fncel.2014.00040, 2014.

Furshpan, E. and Potter, D.: Transmission at the giant motor synapses of the crayfish. J Physiol, 145(2):289–325, 1959.

Gardoni, F., Bellone, C., Cattabeni, F., and Di Luca, M.: Protein kinase C activation modulates α-Calmodulin kinase II binding to NR2A subunit of N-methyl-D-aspartate receptor complex. J Biol Chem, 276(10):7609–7613, 2001.

Gerlai, R.: A new continuous alternation task in T-maze detects hippocampal dysfunction in mice: A strain comparison and lesion study. Beh Brain Res, 95(1):91–101, 1998.

Gill, S. S. and Pulido, O. M.: Glutamate receptors in peripheral tissues: Current knowledge, future research, and implications for toxicology. Toxicol Pathol, 29(2):208–213, 2001.

Gill, S. S., Pulido, O. M., Mueller, R. W., and McGuire, P. F.: Molecular and immunological characterization of the ionotropic glutamate receptors in the rat heart. Brain Res Bull, 46:429–435, 1998.

Gill, S. S., Pulido, O. M., Mueller, R. W., and McGuire, P. F.: Potential target sites in peripheral tissues for excitatory neurotransmission and excitotoxicity. Toxicol Pathol, 28:277–284, 2000.

Gillessen, T., Budd, S. L., and Lipton, S. A.: Excitatory amino acid neurotoxicity. In Molecular and Cellular Biology of Neuroprotection in the CNS, pages 3–40. Springer, 2002.

Grant, E. R., Bacskai, B. J., Anegawa, N. J., Pleasure, D. E., and Lynch, D. R.: Opposing contributions of NR1 and NR2 to Protein Kinase C modulation of NMDA receptors. J Neurochem, 71(4):1471–1481, 1998.

Grau, C., Arató, K., Fernández-Fernández, J. M., Valderrama, A., Sindreu, C., Fillat, C., Ferrer, I., de la Luna, S., and Altafaj, X.: DYRK1A-mediated phosphorylation of GluN2A at Ser1048 regulates the surface expression and channel activity of GluN1/GluN2A receptors. Front Cell Neurosci, 8(331):doi:10.3389/fncel.2014.00331, 2014.

Greco, B. and Carli, M.: Reduced attention and increased impulsivity in mice lacking npy y2 receptors: relation to anxiolytic-like phenotype. Beh Brain Res, 169(2):325–334, 2006.

Grover, L. M. and Teyler, T. J.: Activation of NMDA receptors in hippocampal area CA1 by low and high frequency orthodromic stimulation and their contribution to induction of long-term potentiation. Synapse, 16(1):66–75, 1994.

Gygi, S. P., Rochon, Y., Franza, B. R., and Aebersold, R.: Correlation between protein and mrna abundance in yeast. Mol Cell Biol, 19(3):1720–1730, 1999.

Hanson, P. I. and Schulman, H.: Neuronal Ca^{2+}/calmodulin-dependent protein kinases. Annu Rev Biochem, 61:559–601, 1992.

Hawley, R. S. and Mori, C. A.: The human genome: a user's guide. 2010.

Heidinger, V., Manzerra, P., Wang, X. Q., Strasser, U., Yu, S.-P., Choi, D. W., and Behrens, M. M.: Metabotropic glutamate receptor 1-induced upregulation of NMDA receptor current: mediation through the Pyk2/Src-family kinase pathway in cortical neurons. J Neurosci, 22(13):5452–5461, 2002.

Herrera, D. G. and Robertson, H. A.: Activation of c-fos in the brain. Prog Neurobiol, 50:83–107, 2006.

Hsu, M. H.: Domains of the NR2A and NR2B sununits involved in NMDA receptor current modulation by PKC. Doctoral dissertation, University Illinois at Chicago, 1998.

Hughes, R. N.: The value of spontaneous alternation behavior (SAB) as a test of retention in pharmacological investigations of memory. Neurosci Biobehav R, 28(5):497–505, 2004.

Husi, H., Ward, M. A., Choudhary, J. S., Blackstock, W. P., and Grant, S. G.: Proteomic analysis of NMDA receptor–adhesion protein signaling complexes. Nat Neurosci, 3(7):661–669, 2000.

Irvine, E. E., Danhiez, A., Radwanska, K., Nassim, C., Lucchesi, W., Godaux, E., Ris, L., and Giese, K. P.: Properties of contextual memory formed in the absence of αCaMKII autophosphorylation. Mol Brain, 4(8), 2011.

Jaffard, R., Dubois, M., and Galey, D.: Memory of a choice direction in a T maze as measured by spontaneous alternation in mice: Effects of intertrial interval and reward. Behav Process, 6:11–21, 1981.

Johnson, J. W. and Ascher, P.: Voltage-dependent block by intracellular Mg^{2+} of N-methyl-D-aspartate-activated channels. Biophys J, 57(5):1085–1090, 1990.

Johnson, J. and Ascher, P.: Glycine potentiates the NMDA response in cultured mouse brain neurons. Nature, 325:529–531, 1987.

Johnson, J. and Ascher, P.: Equilibrium and kinetic study of glycine action on the N-methyl-D-aspartate receptor in cultured mouse brain neurons. J Physiol, 455(1):339–365, 1992.

Kelso, S., Nelson, T., and Leonard, J.: Protein kinase C-mediated enhancement of NMDA currents by metabotropic glutamate receptors in Xenopus oocytes. J Physiol, 449(1):705–718, 1992.

Kheirbek, M. A., Drew, L. J., Burghardt, N. S., Costantini, D. O., Tannenholz, L., Ahmari, S. E., Zeng, H., Fenton, A. A., Xu, R. H., and Feldon, J.: Differential control of learning and anxiety along the dorsoventral axis of the dentate gyrus. Neuron, 77:955–968, 2013.

Kim, J. H., Liao, D., Lau, L.-F., and Huganair, R. L.: SynGAP: a synaptic RasGAP that associates with the PSD-95/SAP90 protein family. Neuron, 20(4):683–691, 1998.

Kim, M. J., Dunah, A. W., Wang, Y. T., and Sheng, M.: Differential roles of NR2A- and NR2B-containing NMDA receptors in Ras-ERK signaling and AMPA receptor trafficking. Neuron, 46(5):745–760, 2005.

Kim, S.-Y., Jung, Y., Hwang, G.-S., Han, H., and Cho, M.: Phosphorylation alters backbone conformational preferences of serine and threonine peptides. Proteins: Struct, Funct, Bioinf, 79:3155–3165, 2011.

Kinney, J. W., Davis, C. N., Tabarean, I., Conti, B., Bartfai, T., and Behrens, M. M.: A specific role for NR2A-containing NMDA receptors in the maintenance of parvalbumin and GAD67 immunoreactivity in cultured interneurons. J Neurosci, 26(5):1604–1615, 2006.

Kirson, E. D. and Yaari, Y.: Synaptic NMDA receptors in developing mouse hippocampal neurones: functional properties and sensitivity to ifenprodil. J Physiol, 497:437–455, 1996.

Kishimoto, Y., Kawahara, S., Kirino, Y., Kadotani, H., Nakamura, Y., Ikeda, M., and Yoshioka, T.: Conditioned eyeblink response is impaired in mutant mice lacking NMDA receptor subunit NR2A. Neuroreport, 8(17):3717–3721, 1997.

Klein, M., Pieri, I., Uhlmann, F., Pfizenmaier, K., and Eisel, U.: Cloning and characterization of promoter and 5′-UTR of the NMDA receptor subunit epsilon 2: evidence for alternative splicing of 5′-non-coding exon. Gene, 208(2):259–269, 1998.

Kreiss, C., Birder, L. A., Kiss, S., VanBibber, M. M., and Bauer, A. J.: Cox-2 dependent inflammation increases spinal fos expression during rodent postoperative ileus. Gut, 52(4):527–534, 2003.

Krnjević, K. and Phillis, J.: Actions of certain amines on cerebral cortical neurones. Br J Pharmacol Chemother, 20(3):471–490, 1963.

Kumar, A.: Long-term potentiation at CA3–CA1 hippocampal synapses with special emphasis on aging, disease, and stress. Front Ageing Neurosci, 3, 2011.

Kutsuwada, T., Sakimura, K., Manabe, T., Takayama, C., Katakura, N., Kushiya, E., Natsume, R., Watanabe, M., Inoue, Y., Yagi, T., Aizawa, S., Arakawa, M., Takahashi, T., Nakamura, Y., Mori, H., and Mishina, M.: Impairment of suckling response, trigeminal neuronal pattern formation, and hippocampal ltd in NMDA receptor in epsilon 2 subunit mutant mice. Neuron, 16:333–344, 1996.

Labrousse, V. F., Nadjar, A., Joffre, C., Costes, L., Aubert, A., Grégoire, S., Bretillon, L., and Layé, S.: Short-term long chain omega diet protects from neuroinflammatory processes and memory impairment in aged mice. PLoS One, 7(5):doi:10.1371/journal.pone.0036861, 2012.

Lakso, M., Pichel, J. G., Gorman, J. R., Sauer, B., Okamoto, Y., Lee, E., Alt, F. W., and Westphal, H.: Efficient in vivo manipulation of mouse genomic sequences at the zygote stage. Proc Natl Acad Sci USA, 93(12):5860–5865, 1996.

Larkum, M. E., Nevian, T., Sandler, M., Polsky, A., and Schiller, J.: Synaptic integration in tuft dendrites of layer 5 pyramidal neurons: a new unifying principle. Science, 325(5941):756–760, 2009.

Larson, J., Kim, D., Patel, R. C., and Floreani, C.: Olfactory discrimination learning in mice lacking the fragile x mental retardation protein. Neurobiol Learn Mem, 90(1):90–102, 2008.

Larson, J., Lynch, G., Games, D., and Seubert, P.: Alterations in synaptic transmission and long-term potentiation in hippocampal slices from young and aged PDAPP mice. Brain Research, 840(1–2):23–35, 1999.

Larson, J. and Sieprawska, D.: Automated study of simultaneous-cue olfactory discrimination learning in adult mice. Beh Neurosci, 116(4):588, 2002.

Lau, A. and Tymianski, M.: Glutamate receptors, neurotoxicity and neurodegeneration. Pflügers Archiv-Eur J Physiol, 460(2):525–542, 2010.

Lennartz, R.: The role of extramaze cues in spontaneous alternation in a plus-maze. Learn Behav, 36(2):138–144, 2008.

Lester, R., Tong, G., and Jahr, C.: Interactions between the glycine and glutamate binding sites of the NMDA receptor. J Neurosci, 13(3):1088–1096, 1993.

Li, B., Wang, Otsu, Y., Murphy, T. H., and Raymond, L. A.: Developmental decrease in NMDA receptor desensitization associated with shift to synapse and interaction with Postsynaptic Density-95. J Neurosci, 23(35):11244–11254, 2003.

Liao, G.-Y., Wagner, D. A., Hsu, M. H., and Leonard, J. P.: Evidence for direct PKC mediated modulation of NMDA receptor current. Mol Pharmacol, 59(5):960–964, 2001.

Lin, Y., Jover-Mengual, T., Wong, J., Bennett, M. V., and Zukin, R. S.: PSD-95 and PKC converge in regulating NMDA receptor trafficking and gating. Proc Natl Acad Sci USA, 103(52):19902–19907, 2006.

Liu, A., Zhuang, Z., Hoffman, P. W., and Bai, G.: Functional analysis of rat N-methyl-D-aspartate receptor 2A promotor. J Biol Chem, 278(29):26423–26434, 2003.

Loewi, O.: The Ferrier Lecture: on problems connected with the principle of humoral transmission of nervous impulses. Proc R Soc Lond [Biol], 118(809):299–316, 1935.

Logan, S. M., Rivera, F. E., and Leonard, J. P.: Protein kinase C modulation of recombinant NMDA receptor currents: roles for the C-terminal C1 exon and calcium ions. J Neurosci, 19(3):974–986, 1999.

Loos, M., van der Sluis, S., Bochdanovits, Z., Van Zutphen, I., Pattij, T., Stiedl, O., Smit, A., and Spijker, S.: Activity and impulsive action are controlled by different genetic and environmental factors. Genes Brain Behav, 8(8):817–828, 2009.

Lopez-Molina, L., Boddeke, H., and Muller, D.: Blockade of long-term potentiation and of NMDA receptors by the protein kinase C antagonist calphostin C. Naunyn Schmiedebergs Arch Pharmacol, 348:1–6, 1993.

Lozovaya, N. A., Grebenyuk, S. E., Tsintsadze, T. S., Feng, B., Monaghan, D. T., and Krishtal, O. A.: Extrasynaptic NR2B and NR2D subunits of NMDA receptors shape 'superslow' afterburst EPSC in rat hippocampus. J Physiol, 558(2):451–463, 2004.

Lu, W., Xiong, Z., Lei, S., Orser, B., Dudek, E., Browning, M., and MacDonald, J.: G-protein-coupled receptors act via protein kinase C and Src to regulate NMDA receptors. Nature Neurosci, 2(4):331–338, 1999.

Luo, J., Wang, Y.-H., Yasuda, R. P., Dunah, A. W., and Wolfe, B. B.: The majority of N-methyl-D-aspartate receptor complexes in adult rat cerebral cortex contain at least three different subunits (NR1/NR2A/NR2B). Mol Pharmacol, 51:79–86, 1997.

MacDermott, A. B., Mayer, M. L., Westbrook, G. L., Smith, S. J., and Barker, J. L.: Nmda-receptor activation increases cytoplasmic calcium concentration in cultured spinal cord neurones. Nature, 1986.

MacDonald, J. F., Jackson, M. F., and Beazely, M. A.: Hippocampal long-term synaptic plasticity and signal amplification of NMDA receptors. Crit Rev Neurobiol, 18(1–2), 2006.

Mammen, A. L., Kamboj, S., and Huganir, R. L.: Protein phosphorylation of ligand-gated ion channels. Methods Enzymol, 294:353–370, 1999.

Mandolesi, G., Cesa, R., Autuori, E., and Strata, P.: An orphan ionotropic glutamate receptor: The δ2 subunit. Neuroscience, 158(1):67–77, 2009.

Mayadevi, M., Praseeda, M., Kumar, K., and Omkumar, R.: Sequence determinants on the NR2A and NR2B subunits of NMDA receptor responsible for specificity of phosphorylation by CaMKII. Biochim Biophys Acta, 1598:40–45, 2002.

Mayer, M. and Westbrook, G.: Permeation and block of N-methyl-D-aspartic acid receptor channels by divalent cations in mouse cultured central neurones. J Physiol, 394(1):501–527, 1987.

Montag-Salaz, M., Welzl, H., Kuhl, D., Montag, D., and Schachner, M.: Novelty-induced increased expression of immediate-early genes c-fosand arg 3.1 in the mouse brain. J Neurobiol, 38(2):234–246, 1998.

Monyer, H., Burnashev, N., Laurie, D. J., Sakmann, B., and Seeburg, P. H.: Developmental and regional expression in the rat brain and functional properties of four NMDA receptors. J Neurophysiol, 12:529–540, 1994.

Morgan, J. I., Cohen, D. A., Hempstead, J. L., and Curran, T.: Mapping pattersn of c-fos expresssion in the central nervous system after seizure. Science, 237:192–197, 1987.

Morris, R., Anderson, E., Lynch, G., and Baudryl, M.: Selective impairment of learning and blockade of long-term potentiation by an N-methyl-D-aspartate receptor antagonist, AP5. Nature, 319:27, 1986.

Nakazawa, T., Komai, S., Tezuka, T., Hisatsune, C., Umemori, H., Semba, K., Mishina, M., Manabe, T., and Yamamoto, T.: Characterization of Fyn-mediated tyrosine phosphorylation sites on GluRϵ2 (NR2B) subunit of the N-methyl-D-aspartate receptor. J Biol Chem, 276(1):693–699, 2001.

Neithammer, M., Kim, E., and Sheng, M.: Interaction between the C terminus of NMDA receptor subunits and multiple members of the PSD-95 family of membrane-associated guanylate kinase. J Neurosci, 76(7):2157–2163, 1996.

O'Brien, R. J., Lau, L.-F., and Huganir, R. L.: Molecular mechanisms of glutamate receptor clustering at excitatory synapses. Curr Opin Neurobiol, 8:364–369, 1998.

Oliveira, A. M., Hawk, J. D., Abel, T., and Havekes, R.: Post-training reversible inactivation of the hippocampus enhances novel object recognition memory. Learn Memory, 17(3):155–160, 2010.

Olson, E., Arnold, H., Rigby, P., and Wold, B.: Know your neighbors: Three phenotypes in null mutants of the myogenic bHLH gene *MRF4*. Cell, 85(1):1–4, 1996.

Omkumar, R. V., Kiely, M. J., Rosenstein, A. J., Min, K.-T., and Kennedy, M. B.: Identification of a phosphorylation site for Calcium/calmodulin dependent protein kinase II in the NR2B subunit of the N-methyl-D-aspartate receptor. J Biol Chem, 271(49):31670–31678, 1996.

Paoletti, P., Bellone, C., and Zhou, Q.: NMDA receptor subunit diversity: impact on receptor properties, synaptic plasticity and disease. Nat Rev Neurosci, 14(6):383–400, 2013.

Paul, C. A., Beltz, B., and Berger-Sweeney, J.: The Nissl stain: A stain for cell bodies in brain sections. Cold Spring Harb Protoc, 2008(9):pdb.prot4805, 2008.

Perin-Dureau, F., Rachline, J., Neyton, J., and Paoletti, P.: Mapping the binding site of the neuroprotectant ifenprodil on NMDA receptors. J Neurosci, 22(14):5955–5965, 2002.

Pham, C. T. N., MacIvor, D. M., Hug, B. A., Heusel, J. W., and Ley, T. J.: Long-range disruption of gene expression by a selectable marker cassette. Proc Natl Acad Sci USA, 93(23):13090–13095, 1996.

Philpot, B. D., Cho, K. K., and Bear, M. F.: Obligatory role of NR2A for metaplasticity in visual cortex. Neuron, 53(4):495–502, 2007.

Philpot, B. D., Espinosa, J. S., and Bear, M. F.: Evidence for altered NMDA receptor function as a basis for metaplasticity in visual cortex. J Neurosci, 23(13):5583–5588, 2003.

Pinheiro, P. S. and Mulle, C.: Presynaptic glutamate receptors: physiological functions and mechanisms of action. Nat Rev Neurosci, 9:423–436, 2008.

Prut, L. and Belzung, C.: The open field as a paradigm to measure the effects of drugs on anxiety-like behaviors: a review. Eur J Pharmacol, 463(1–3):3–33, 2003.

Prybylowski, K., Chang, K., Sans, N., Kan, L., Vicini, S., and Wenthold, R. J.: The synaptic localization of NR2B-containing NMDA receptors is controlled by interactions with PDZ proteins and AP-2. Neuron, 47(6):845–857, 2005.

Quinlan, E. M., Philpot, B. D., Huganir, R. L., and Bear, M. F.: Rapid, experience-dependent expression of synaptic NMDA receptors in visual cortex in vivo. Nat Neurosci, 2:352–357, 1999.

Radwanska, K., Medvedev, N. I., Pereira, G. S., Engmann, O., Thiede, N., Moraes, M. F. D., Villers, A., Irvine, E. E., Maunganidze, N. S., Pyza, E. M., Ris, L., Szymanska, M., Lipinski, M., Kaczmarek, L., Stewart, M. G., and Giese, K. P.: Mechanism for long-term memory formation when synaptic strengthening is impaired. Proc Natl Acad Sci USA, 108(45):18471–18475, 2011.

Ramfrez-Solis, R., Zheng, H., Whiting, J., Krumlauf, R., and Bradley, A.: Hoxb-4 (Hox-2.6) mutant mice show homeotic transformation of a cervical vertebra and defects in the closure of the sternal rudiments. Cell, 73(2):279–294, 1993.

Richman, C. L., Dember, W. N., and Kim, P.: Spontaneous alternation behavior in animals: A review. Curr Psychol, 5(4):358–391, 1986.

Rio, D. C., Ares, M., Hannon, G. J., and Nilsen, T. W.: Purification of RNA using TRIzol (TRI reagent). Cold Spring Harb Protoc, 2010(6):pdb.prot5439, 2010.

Roberts, A. C., Díez-García, J., Rodriguiz, R. M., López, I. P., Luján, R., Martínez-Turrillas, R., Picó, E., Henson, M. A., Bernardo, D. R., Jarrett, T. M., Clendeninn, D. J., López-Mascaraque, L., Feng, G., Lo, D. C., Wesseling, J. F., Wetsel, W. C., Philpot, B. D., and Pérez-Otaño, I.: Downregulation of NR3A-containing NMDARs is required for synapse maturation and memory consolidation. Neuron, 63(3):342–356, 2009.

Rusakov, D. A. and Kullmann, D. M.: Extrasynaptic glutamate diffusion in the hippocampus: ultrastructural constraints, uptake, and receptor activation. J Neurosci, 18(9):3158–3170, 1998.

Ryan, T. J., Emes, R., Grant, S., and Komiyama, N.: Evolution of NMDA receptor cytoplasmic interaction domains: implications for organisation of synaptic signalling complexes. BMC Neurosci, 9(1):6, 2008.

Ryan, T. J., Kopanitsa, M. V., Indersmitten, T., Nithianantharajah, J., Afinowi, N. O., Pettit, C., Stanford, L. E., Sprengel, R., Saksida, L. M., Bussey, T. J., O'Dell, T. J., Grant, S. G. N., and Komiyama, N. H.: Evolution of GluN2A/B cytoplasmic domains diversified vertebrate synaptic plasticity and behavior. Nat Neurosci, 16:25–32, 2013.

Sakimura, K., Kutsuwada, T., Ito, I., Manabe, T., Takayama, C., Kushiya, E., Yagi, T., Aizawa, S., Inoue, Y., Sugiyama, H., et al.: Reduced hippocampal LTP and spatial learning in mice lacking NMDA receptor ε1 subunit. Nature, (373):151–155, 1995.

Salzman, C., Miyawaki, E. K., le Bars, P., and Kerrihard, T. N.: Neurobiologic basis of anxiety and its treatment. Harv Rev Psychiatry, 1(4):197–206, 1993.

Sanchez-Roige, S., Peña-Oliver, Y., and Stephens, D. N.: Measuring impulsivity in mice: the five-choice serial reaction time task. Psychopharmacol, 219(2):253–270, 2012.

Sanderson, D., McHugh, S., Good, M., Sprengel, R., Seeburg, P., Rawlins, J., and Bannerman, D.: Spatial working memory deficits in GluA1 AMPA receptor subunit knockout mice reflect impaired short-term habituation: Evidence for Wagner's dual-process memory model. Neuropsychologia, 48(8):2303–2315, 2010.

Sanz-Clemente, A., Matta, J. A., Isaac, J. T., and Roche, K. W.: Casein kinase 2 regulates the NR2 subunit composition of synaptic NMDA receptors. Neuron, 67(6):984–996, 2010.

Sarnyai, Z., Sibille, E. L., Pavlides, C., Fenster, R. J., McEwen, B. S., and Tth, M.: Impaired hippocampal-dependent learning and functional abnormalities in the hippocampus in mice lacking serotonin1A receptors. Proc Natl Acad Sci USA, 97(26):14731–14736, 2000.

Sather, W., Johnson, J., Henderson, G., and Ascher, P.: Glycine-insensitive desensitization of NMDA responses in cultured mouse embryonic neurons. Neuron, 4(5):725–731, 1990.

Satoko, H., Hideo, H., Koji, O., Ichio, A., Tsuneo, S., Tetsuya, S., Makoto, H., and Tsuyoshi, M.: In vivo evaluation of cellular activity in a CaMKII heterozygous knockout mice us-

ing manganese-enhanced magnetic resonance imaging (MEMRI). Front Integr Neurosci, 7(00076):doi:10.3389/fnint.2013.00076, 2013.

Scott, D. B., Blanpied, T. A., and Ehlers, M. D.: Coordinated PKA and PKC phosphorylation suppresses RXR-mediated ER retention and regulates the surface delivery of NMDA receptors. Neuropharmacol, 45:5079–5088, 2003.

Scott, D. B., Blanpied, T. A., Swanson, G. T., Zhang, C., and Ehlers, M. D.: An NMDA receptor ER retention signal regulated by phosphorylation and alternative splicing. J Neurosci, 21(9):3063–3072, 2001.

Seeburg, P., Burnashev, N., Köhr, G., Kuner, T., Sprengel, R., and Monyer, H.: The NMDA receptor channel: molecular design of a coincidence detector. Recent Prog Horm Res, 50:19–34, 1995.

Sherrington, C. S.: Lecture I-Introductory-Coordination in the simple reflex. In The Integrative Action of the Nervous System. Yale University Press, 1906.

Simpson, H. B., Neria, Y., Lewis-Fernández, R., and Schneier, F.: Anxiety disorders: Theory, research and clinical perspectives. Cambridge University Press, 2010.

Skeberdis, V. A., Chevaleyre, V., Lau, C. G., Goldberg, J. H., Pettit, D. L., Suadicani, S. O., Lin, Y., Bennett, M. V., Yuste, R., Castillo, P. E., and Zukin, R. S.: Protein kinase A regulates calcium permeability of NMDA receptors. Nat Neurosci, 9(4):501–510, 2006.

Skeberdis, V. A., Lan, J.-y., Zheng, X., Zukin, R. S., and Bennett, M. V.: Insulin promotes rapid delivery of N-methyl-D-aspartate receptors to the cell surface by exocytosis. Proc Natl Acad Sci USA, 98(6):3561–3566, 2001.

Slattery, D. A. and Cryan, J. F.: Using the rat forced swim test to assess antidepressant-like activity in rodents. Nat Protoc, 7(6):1009–1014, 2012.

Sobczyk, A., Scheuss, V., and Svoboda, K.: NMDA receptor subunit-dependent Ca^{2+} signaling in individual hippocampal dendritic spines. J Neurosci, 25(26):6037–6046, 2005.

Sobolevsky, A., Rosconi, M. P., and Gouaux, E.: X-ray structure, symmetry and mechanism of an AMPA-subtype glutamate receptor. Nature, 462:745–756, 2009.

Sprengel, R.: Ionotropic glutamate receptors. In Neuroscience in the 21st Century, ed. D. W. Pfaff, pages 59–80. Springer New York, 2013.

Strack, S. and Colbran, R. J.: Autophosphorylation-dependent targeting of calcium/calmodulin-dependent protein kinase II by the NR2B subunit of the N-methyl-D-aspartate receptor. J Biol Chem, 273(33):20689–20692, 1998.

Sumioka, A.: Auxiliary subunits provide new insights into regulation of AMPA receptor trafficking. J Biochem, 153(4):331–337, 2013.

Sutton, G. and Chandler, L. J.: Activity-dependent NMDA receptor-mediated activation of protein kinase B/Akt in cortical neuronal cultures. J Neurochem, 82(5):1097–1105, 2002.

Tang, Y.-P., Shimizu, E., Dube, G. R., Rampon, C., Kerchner, G. A., Zhuo, M., Liu, G., and Z., T. J.: Genetic enhancement of learning and memory in mice. Nature, 401:63–69, 1999.

Taniguchi, S., Nakazawa, T., Tanimura, A., Kiyama, Y., Tezuka, T., Watabe, A. M., Katayama, N., Yokoyama, K., Inoue, T., Izumi-Nakaseko, H., Kakuta, S., Sudo, K., Iwakura, Y., Umemori, H., Inoue, T., Murphy, N. P., Hashimoto, K., Kano, M., Manabe, T., and Yamamoto, T.: Involvement of NMDAR2A tyrosine phosphorylation in depression-related behaviour. EMBO J, 28(23):3717–3729, 2009.

Thomas, A., Burant, A., Bui, N., Graham, D., Yuva-Paylor, L. A., and Paylor, R.: Marble burying reflects a repetitive and perseverative behavior more than novelty-induced anxiety. Psychopharmacol, 204(2):361–373, 2009.

Tovar, K. R., McGinley, M. J., and Westbrook, G. L.: Triheteromeric NMDA receptors at hippocampal synapses. J Neurosci, 33:9150–9160, 2013.

Traynelis, S. F., Wollmuth, L. P., McBain, C. J., Menniti, F. S., Vance, K. M., Ogden, K. K., Hansen, K. B., Yuan, H., Myers, S. J., and Dingledine, R.: Glutamate receptor ion channels: Structure, regulation, and function. Phamacol Rev, 62(3):405–494, 2010.

VanDongen, A. M. and VanDongen, H. M.: Effects of mRNA untranslated regions on translational efficiency of NMDA receptor subunits. Neurosignals, 13(4):194–206, 2004.

Vicini, S., Wang, J. F., Li, J. H., Zhu, W. J., Wang, Y. H., Luo, J. H., Wolfe, B. B., and Grayson, D. R.: Functional and pharmacological differences between recombinant N-methyl-D-aspartate receptors. J Neurophysiol, 79(2):555–566, 1998.

Walf, A. A. and Frye, C. A.: The use of the elevated plus maze as an assay of anxiety-related behavior in rodents. Nat Protoc, 2:322–328, 2007.

Wallace, D. G., Hines, D. J., Pellis, S. M., and Whishaw, I. Q.: Vestibular information is required for dead reckoning in the rat. J Neurosci, 22(22):10009–10017, 2002.

Wei, F., Wang, G.-D., Kerchner, G. A., Kim, S. J., Xu, H.-M., Chen, Z.-F., and Zhuo, M.: Genetic enhancement of inflammatory pain by forebrain NR2B overexpression. Nat Neurosci, 4:164–169, 2001.

Wenthold, R. J., Yokotani, N., Doi, K., and Wada, K.: Immunochemical characterization of the non-NMDA glutamate receptor using subunit-specific antibodies. Evidence for a hetero-oligomeric structure in rat brain. J Biol Chem, 267:501–507, 1992.

Wenzel, A., Fritschy, J. M., Mohier, H., and Benke, D.: NMDA receptor heterogeneity during postnatal development of the rat brain: differential expression of the NR2A, NR2B, and NR2C subunit proteins. J Neurochem, 62(2):469–478, 1997.

Westphal, R. S., Tavalin, S. J., Lin, J. W., Alto, N. M., Fraser, I. D. C., Langeberg, L. K., Sheng, M., and Scott, J. D.: Regulation of NMDA receptors by an associated phosphatase-kinase signaling complex. Science, 285(5424):93–96, 1999.

Wirtshafter, D. and Sheppard, A.: Role of dopamine D2 receptors in the striatal immediate early gene response to amphetamine in reserpinized rats. Br Res Bull, 62(1):77–83, 2003.

Wirtshafter, D.: Cholinergic involvement in the cortical and hippocampal Fos expression induced in the rat by placement in a novel environment. Brain Res, 1051(12):57–65, 2005.

Wo, Z. G. and Oswald, R. E.: Unraveling the modular design of glutamate-gated ion channels. Trends Neurosci, 18(4):161–168, 1995.

Wyeth, M. S., Pelkey, K. A., Petralia, R. S., Salter, M. W., McInnes, R. R., and McBain, C. J.: Neto auxiliary protein interactions regulate kainate and NMDA receptor subunit localization at mossy fiberCA3 pyramidal cell synapses. J Neurosci, 34(2):622–628, 2014.

Yang, K., Trepanier, C., Sidhu, B., Xie, Y.-F., Li, H., Lei, G., Salter, M. W., Orser, B. A., Nakazawa, T., Yamamoto, T., et al.: Metaplasticity gated through differential regulation of GluN2A versus GluN2B receptors by Src family kinases. EMBO J, 31(4):805–816, 2012.

Yang, M. and Leonard, J. P.: Identification of mouse NMDA receptor subunit NR2A C-terminal tyrosine sites phosphorylated by coexpression with v-Src. J Neurochem, 77(2):580–588, 2001.

Yashiro, K. and Philpot, B. D.: Regulation of NMDA receptor subunit expression and its implications for LTD, LTP, and metaplasticity. Neuropharmacol, 55(7):1081–1094, 2008.

Zhang, W.-N., Bast, T., Xu, Y., and Feldon, J.: Differential control of learning and anxiety along the dorsoventral axis of the dentate gyrus. Beh Br Res, 262:47–56, 2014.

Zhao, M., Adams, J. P., and Dudek, S. M.: Pattern-dependent role of NMDA receptors in action potential generation: consequences on extracellular signal-regulated kinase activation. J Neurosci, 25:7032–7039, 2005.

Zukin, R. S. and Bennett, M. V.: Alternatively spliced isoforms of the NMDARI receptor subunit. Trends Neurosci, 18(7):306–313, 1995.

VITA

Deebika Balu

Department of Biological Sciences,
University of Illinois-Chicago

Email: dbalu2@uic.edu

EDUCATION

Doctor of Philosophy, Biological Sciences (interdisciplinary concentration in Neuroscience), University of Illinois-Chicago, Spring 2015.

Dissertation title:
Behavioral and Physiological Significance of PKC-mediated Phosphorylation of the GluN2A C-terminus.

Doctoral guidance committee:
Drs. J. Leonard (Advisor), S. Alford (Chair), J. Larson, M. Ragozzino, and J. Schmidt.

Master of Science, Clinical Laboratory Sciences, Michigan State University, 2010.

Thesis title:
Study of Sporicidal Properties of Crosslinked Polyelectrolyte Multilayers.

Master's guidance committee:
Drs. S. Cendrowski (Advisor & Chair), S. Kaganove, and D. Thorne.

Master of Science, Chemical Engineering, Michigan State University, 2007.

Thesis title:
Regional Disparities in Expressing Alzheimers Disease Neuropathology: An Inferential Study.

Master's guidance committee:
Drs. C. Chan (Advisor & Chair), P. Walton, and B. Dale.

Bachelor of Technology, Chemical Engineering, Anna University, India, 2005.

RESEARCH EXPERIENCE

- Doctoral student, Biological Sciences, University of Illinois-Chicago, Chicago, IL, August 2010 – Present.
  - Proposed and performed behavioral experiments to characterize $Grin2a\Delta PKC$ mice.
  - Developed novel behavioral protocols for the experiments.
  - Developed a novel method of interpreting spontaneous alternation of mice in mazes.

- ◇ Trained and mentored six undergraduate biology majors, with three students receiving UIC LASURI Grants based on the doctoral research.
- ◇ Maintained and genotyped mice colonies.

◇ Master's student, Clinical Laboratory Sciences, Michigan State University, East Lansing, MI, August 2008 – August 2010.

- ◇ Performed experiments that established polyelectrolyte multi-layered films manufactured by Dendritech Inc. as novel sporicidal coatings.

◇ Research Technician, Department of Neurology and Ophthalmology, Michigan State University, East Lansing, MI, August 2007 – August 2008.

- ◇ Collected data for a R01 grant involving cell culture models for Parkinson's disease.
- ◇ Maintained laboratory animals, coordinated laboratory meetings, and was responsible for experiment supplies.

◇ Master's student, Chemical Engineering, Michigan State University, East Lansing, MI, August 2005 – August 2007.

- ◇ Worked on in-vitro neuronal and astrocyte cell culture models that established regional disparities in pathology of Alzheimer's disease.

HONORS & AWARDS

◇ College of Liberal Arts and Sciences Travel Award, University of Illinois-Chicago (Fall 2012 & 2014).

◇ Departmental research fellowship, Department of Biological Sciences, University of Illinois-Chicago (Summer 2014).

◇ Excellence in undergraduate student mentorship, Department of Biological Sciences, University of Illinois-Chicago (Fall 2012).

◇ Graduate Student Council Travel Award, University of Illinois-Chicago (Fall 2012).

◇ Graduate School Fellowship, Michigan State University (Summer 2008 & 2010).

◇ Department of Chemical Engineering Graduate Student Fellowship, Michigan State University (Fall 2005).

◇ Rank Certificate for 12^{th} rank in Bachelor of Technology in Chemical Engineering, Anna University (2005).

◇ Collegial Award of One of the Best Students in the Department of Chemical Engineering (2005).

RESEARCH PUBLICATIONS

Peer-reviewed publications

- S. Troxell-Smith, M.J. Tutka, J.M. Albergo, *D. Balu*, J.S. Brown, and J.P. Leonard. "Foraging Decisions in Wild Versus Domestic Mus musculus: What does life in the lab select for?" *Applied Animal Behaviour Science*, in review.
- K.R. Bae, H.J. Shim, *D. Balu*, S.R. Kim, and S.W. Yu. "Translocator Protein 18kDa Negatively Regulates Inflammation in Microglia." *J. Neuroimmune Pharmacol.*, 2014.
- S. Patil, *D. Balu*, J. Melrose, and C. Chan. "Brain Region-Specificity of Palmitic Acid-Induced Abnormalities Associate with Alzheimer's Disease." *BMC Res. Notes*, 2008.
- K. Ravikumar, *B. Deebika*, and K. Balu. "Decolorization of Aqueous Dye Solutions by a Novel Absorbent: Application of Statistical Designs and Surface Plots for the Optimization and Regression Analysis." *J. Haz. Mater.*, 2008.

Conference proceedings

- *D. Balu*, J. Larson, J.V. Schmidt, and J. Leonard. "Genetic Mutations in GluN2A Serine and Tyrosine Phosphorylation Sites Controlled by PKC Decrease Anxiety-Related Behaviors in Mice." Society for Neuroscience Meeting, Washington D.C. 2014.
- *D. Balu*, J. Larson, J.V. Schmidt, and J. Leonard. "NMDA Phosphorylation Mutant *Grin2aΔPKC* Mice Show Anxiolytic Behavior." Society for Neuroscience, Chicago Chapter Meeting, Chicago, IL 2014.
- *D. Balu*, J. Schmidt, and J. Leonard. "Impaired Spatial Learning in Mice that have Mutations Affecting Phosphorylation of Serine/Tyrosine Residues in NR2A C-terminus." Society for Neuroscience Meeting, New Orleans, LA 2012.

TEACHING EXPERIENCE

- Teaching Assistant, BIOS 350: General Microbiology, Department of Biological Sciences, University of Illinois-Chicago, Fall 2014.
  - Assisted in teaching related activities.
  - Graded exams.
  - Average enrollment of 220 students.
- Teaching Assistant, BIOS 351: Microbiology Laboratory, Department of Biological Sciences, University of Illinois-Chicago, Fall 2010, Summer 2011, Fall 2012, and Spring 2014.
  - Taught a senior-level laboratory section that involves culturing, staining, and identifying many microorganisms under a bright field microscope.
  - Average enrollment of 24 students.

- ◇ Teaching Assistant, BIOS 223: Cell Biology Laboratory, Department of Biological Sciences, University of Illinois-Chicago, Spring 2013 and Fall 2013.
  - ◇ Taught a laboratory section in which the students gain expertise on basic protein and DNA extraction and fluorescent staining techniques involving a wide range of organisms such as yeast, sea urchins, and termites.
  - ◇ Average enrollment of 20 students.
- ◇ Teaching Assistant, BIOS 433: Animal Physiological Systems, Department of Biological Sciences, University of Illinois-Chicago, Spring 2011.
  - ◇ Taught a senior-level laboratory section in which the students have hands-on experience measuring physiological variables such as heart rate, nerve conduction velocity, respiration rate, spinal cord reflexes, and reaction time.
  - ◇ Average enrollment of 24 students.
- ◇ Teaching Assistant, CHE 804: Foundations in Chemical Engineering, Department of Chemical Engineering, Michigan State University, Spring 2007.
  - ◇ Assisted in teaching related activities.
  - ◇ Graded papers and helped students with assignments.
  - ◇ Average enrollment of 12 students.
- ◇ Teaching Assistant, CHE 433: Process Design and Optimization I, Department of Chemical Engineering, Michigan State University, Fall 2005.
  - ◇ Assisted in teaching related activities.
  - ◇ Graded papers and met with students during office hours.
  - ◇ Average enrollment of 90 students.

PROFESSIONAL WORK

- ◇ Graduate Assistant, Office of Radiation, Chemical and Biological Safety (ORCBS), Michigan State University, East Lansing, MI August 2008 – May 2010.
  - ◇ Assisted in assessing compliance of laboratory spaces on university campus with MI-OSHA safety standards.
  - ◇ Prepared safety inspection reports.
  - ◇ Developed and maintained a digital database for all safety trainings and inspections records for all departments on and off MSU's campus.

SKILLS

Biochemistry and Molecular Biology

- ◇ Isolating primary cultures (neurons and astrocytes) of cortical, hippocampal, and cerebellar tissues, cell line maintenance, Western and Northern Blot, UV-Visible spectroscopy, Fluores-

cence Spectroscopy, Immunochemistry, PCR, Colorimetric Assays, DNA isolation, Mouse Brain tissue extraction, perfusion for c-Fos immunostaining.

Psychology (behavior)

◇ Short term and long term memory, anxiety-related symptoms assessment, behavioral despair in mice using paradigms such as T-maze, novel object recognition and elevated plus maze, forced swim test.

Software and tools

◇ Microsoft Office (Excel, Powerpoint, Word), Polymath, Mathematica, MATLAB, ASPEN, SoftMax.

Others

◇ Lab management, Laboratory Animals Management (including breeding, preparation of Animal Use Forms for research approval), Projects Management, Compliance Standards for Chemical Safety in Laboratories, Genotyping rodents.

AFFILIATIONS

Professional

◇ Associate Member, Sigma Chi Research Society.
◇ Student Member, Society for Neuroscience.
◇ Student Member, Indian Institute of Chemical Engineers.

Other

◇ Board Member, Indian Graduate Student Association (2011–2012).
◇ President, Association for India's Development - UIC Chapter (2011–2012).
◇ Member, Association for India's Development - UIC Chapter.
◇ Member, Urban Sketchers Chicago.